APRIL 2019

M.Sc. in Civil Engineering

SINAN NOORI FAIHAN ALDOORI

REPUBLIC OF TURKEY

GAZİANTEP UNIVERSITY

GRADUATE SCHOOL OF

NATURAL & APPLIED SCIENCES

EXPERIMENTAL STUDY FOR THE CHARACTERISTICS OF FLOW IN SEMICIRCULAR CHANNELS WITH FREE OVERFALL

M. Sc. THESIS

IN

CIVIL ENGINEERING

BY

SINAN NOORI FAIHAN ALDOORI

APRIL 2019

EXPERIMENTAL STUDY FOR THE CHARACTERISTICS OF FLOW IN SEMICIRCULAR CHANNELS WITH FREE OVERFALL

M.Sc. Thesis

in

Civil Engineering

Gaziantep University

Supervisor

Asst. Prof. Dr. Ayşe Yeter Günal

by

Sinan Noori Faihan ALDOORI

April 2019

REPUBLIC OF TURKEY

GAZİANTEP UNIVERSITY

GRADUATE SCHOOL OF NATURAL & APPLIED SCIENCES

CIVIL ENGINEERING

Name of the thesis: Experimental Study for the Characteristics of Flow in Semicircular Channels with Free Overfall

Name of the student: Sinan Noori Faihan ALDOORI

Exam date: 25 / 4 / 2019

Approval of the Graduate School of Natural and Applied Sciences

Prof. Dr. A. Necmeddin YAZICI

Director

I certify that this thesis satisfies all the requirements as a thesis for the degree of Master of Science.

Prof. Dr. Hanifi ÇANAKÇI

Head of Department

This is to certify that we have read this thesis and that in our majority opinion it is fully adequate, in scope and quality, as a thesis for the degree of Master of Science.

Asst. Prof. Dr. Ayşe Yeter GÜNAL

Supervisor

Examining Committee Members	Signature
Asst. Prof. Dr. Ayşe Yeter GÜNAL	……..
Prof. Dr. Mehmet Karpuzcu	…….
Prof. Dr. Aytaç Güven	…….

I hereby declare that all information in this document has been obtained and presented in accordance with academic rules and proper conduct. I also declare that, as required by these rules and conduct, I have fully cited and referenced all material and results that are not original to this work.

Sinan Noori Faihan ALDOORI

ABSTRACT

EXPERIMENTAL STUDY FOR THE CHARACTERISTICS OF FLOW IN SEMICIRCULAR CHANNELS WITH FREE OVERFALL

ALDOORI, Sinan Noori Faihan

M.Sc. Thesis in Civil Engineering

Supervisor: Asst. Prof. Dr. Ayşe Yeter GÜNAL

April 2019

106 pages

In this study, the effects of flow characteristics and size of sediments at different channel slopes on the flow over the edge of the free fall in semicircular channels has been studied. For this purpose, four models of free over fall semicircular channels were constructed and tested in the laboratory channel. These models have a length of (2) m. The longitudinal slope of each model has been changed four times as follows. (S = 0, 1/200, 2/200 and 3/200) or (S = 0, 0.005, 0.01 and 0.015). The roughness was determined by three gradients of sand grains (2 mm, 4.75 mm and 6.33 mm) for each model slope. The laboratory program was divided into sixteen groups, including four groups for smooth surface and twelve groups for coarse surface. Ten different discharges were applied. The final depth relationship with the discharge had been calculated each time for the purpose of studying the hydraulic performance of all tested models. It was found that the Froude number of the experiment varies from (0.13) to (2.22). The discharge values vary in the range of (2 m^3/hr) and (11 m^3/hr). The discharge equation of the semicircular channel had been estimated by using statistical analysis program (SPSS 25).

Keywords: Semicircular channels, End depth ratio, Brink water depth, Critical water depth.

ÖZET

Yarı Dairesel Kanallardaki Serbest Düşüşlü Akış Karakteristiklerinin Deneysel Çalışması

ALDOORI, Sinan Noori Faihan
Yüksek Lisans Tezi, İnşaat Mühendisliği
Tez Yöneticisi: Dr. Öğr. Üyesi Ayşe Yeter GÜNAL
Nisan 2019
106 sayfa

Bu çalışmada, akım karakteristikleri ve kanal tabanındaki pürüzlülük ile sediment dane çapı ve kanal eğiminin, yarı dairesel kanal sonunda oluşan serbest düşüşlü akım üzerine etkileri araştırıldı. Bu amaçla, dört tip yarı dairesel kanal inşa edildi ve bu kanallarda deneyler yapıldı. Bu modellerin uzunluğu (2) m'dir. Her modelin boyuna eğimi aşağıdaki gibi dört kez değiştirildi. (S = 0, 1 / 200, 2 / 200 ve 3/200) veya (S = 0, 0.005, 0.01 ve 0.015). Pürüzlülük, her model eğimi için üç farklı kum dane çapı (2 mm, 4.75 mm ve 6.33 mm) ile belirlendi. Laboratuvar programı, dört pürüzsüz, ve oniki pürüzlü taban yüzeyi olmak üzere onaltı gruba ayrıldı. On farklı debi uygulandı. Tüm modellerin hidrolik performansını incelemek amacıyla, her defasında debi ile son derinlik ilişkisi hesaplandı. Deneylerdeki Froude sayısının (0.13) ile (2.22) arasında değiştiği bulundu. Debi değerleri (2 m^3 / saat) ile (11 m^3 / saat) arasındadır. Yarı dairesel kanalın debi denklemi, istatistiksel analiz programı (SPSS 25) kullanılarak tahmin edildi.

Anahtar Kelimeler: Yarı dairesel kanallar, Uç derinlik oranı, Brink su derinliği, Kritik su derinliği.

To My Family

ACKNOWLEDGEMENTS

In the name of Allah, peace and blessings be upon our Prophet Muhammad (peace and blessings of Allah be upon him), first of all, I thank God for his kindness and generosity and who facilitated my way and helped me to achieve this goal of great meaning and great change in my life and in my scientific career, words cannot express my gratitude to the Creator of the Worlds. Praise be to God.

I would like to express my sincere thanks and deep gratitude to my supervisor Dr. Ayşe Y. Günal for her help and moral, scientific and humanitarian support during the period of my study and while I was writing my thesis. I would also like to extend my thanks to my teacher Prof. Dr. Raad Hoobi Irzooki for his scientific support and help from the beginning until the completion of my thesis writing.

My thanks and my love and my gratitude to my family represented by my beloved wife, which was an example of sacrifice, love and loyalty, and for her patience, tolerance and great effort in order to become a scientific and community status and to be a role model in my country, also my children, my loved ones, who always gave me their love and affection and who was waiting for me to complete my research and thesis writing. I do not forget my parents God save them and my brothers and sister all.

I would like to thank my relatives and friends, especially my cousin Ibrahim Al Doori and his wonderful wife, who helped me during my study and research period. My friends Abu Bakr Sami, Ahmed Abdel Aziz, Louay Assami, Mustafa Dulbahan, Abdullah Al-Hamad and Ibrahim Halil who were more than my brothers and will stay. I ask God to save them all.

TABLE OF CONTENTS

Page

ABSTRACT ..... **vi**

ÖZET ..... **vii**

ACKNOWLEDGEMENTS ..... **viii**

TABLE OF CONTENTS ..... **ix**

LIST OF TABLES ..... **xiii**

LIST OF FIGURES ..... **xiv**

LIST OF SYMBOLS/ABREVIATIONS ..... **xviii**

CHAPTER 1 ..... **1**

INTRODUCTION **1**

1.1 General 1

1.2 Aim of Study 2

1.3 The Study Boundaries 3

CHAPTER 2 ..... **4**

LITERATURE REVIEW **4**

2.1 Introduction 4

2.2 Previous Studies 4

CHAPTER 3 ..... **23**

THEORETICAL FUNDAMENTALS **23**

3.1 Introduction 23

3.2 Free Overfall General Properties 24

3.3 The Momentum Equation Application Between the Final Depth and Critical Depth 25

3.4 The Relationship of Brink Depth with The Channel Discharge 27
3.5 Pressure Coefficient Distribution at The Brink 27
3.6 The Critical Depth in Semicircular Channels 28
3.7 Dimensional Analysis 28
3.7.1 Dimensions and Units 29
3.7.2 Buckingham's Pi Theorem 30
3.7.3 Methods for Determining Π's 30
3.7.4 Determination of Pi Terms 31
3.7.4.1 Method of Repeating Variables 31
3.8 Statistical Analysis 33
3.8.1 Correlation Analysis 33
3.8.1.1 Coefficient of Correlation 33
3.8.1.2 Coefficient of Determination 36
3.8.2 Regression Analysis 36
CHAPTER 4 38
LABORATORY EQUIPMENTS, LABORATORY WORK 38
4.1 Introduction 38
4.2 Laboratory Channel 38
4.2.1 The Main Structure 38
4.2.2 The Inlet and Outlet Tanks 39
4.2.2.1 Tank (1) 39
4.2.2.2 Tank (2) 39
4.2.3 Sedimentation Tank 39

4.2.4 Main Water Tank (Reservoir) 40
4.2.5 The Electrical Pump 43
4.2.6 Electromagnetic Gauge 43
4.2.7 The Point Gauge 44
4.3 Depth Measurements 45
4.3.1 Depth Measurements in Soft Channels 45
4.3.2 Depth Measurements in Rough Channels 46
4.4 Manning Roughness Coefficient 46
4.5 Samples Creating 48
4.5.1 Create Bottom Form 48
4.5.2 Bottom Roughness Creation 48
4.6 The Laboratory Program 52
CHAPTER 5 60
RESULTS AND CALCULATIONS 60
Introduction 60
5.1 Results Analysis 60
5.1.1 Manning Roughness Coefficient Values 60
5.1.2 Variation of ($Q/\sqrt{gD^5}$) with (y_b/D) 62
5.1.3 (y_b/D) Change with (y_c/D) 73
5.1.4 (y_b/y_c) Change with Channel Bed Slope 77
5.1.5 Variation of ($Q/\sqrt{gD^5}$) with (y_b/D) and (S) and (n) 79
5.1.6 Comparison of This Study Results with Previous Studies 82
CHAPTER 6 86

CONCLUSIONS AND RECOMMENDATIONS **86**

6.1 CONCLUSIONS 86

6.2 RECOMMENDATIONS 88

REFERENCES **89**

Appendix (A) **94**

Derivations: 94

A.1 The Momentum Equation 94

A.2 The Critical Depth Equation 96

Appendix (B) **99**

The Laboratory Data for The Current Study 99

LIST OF TABLES

Page

Table 4.1 Details of Experiments on Free Overfall Channel Models During the Laboratory Program 59

Table 5.1 Manning Roughness Coefficient Values 61

Table 5.2 The Constants (a_1) and (b_1) and Determination Coefficient (R^2) Values for Soft and Rough Bottom Channels with different Slopes 73

Table 5.3 The Constant (a_2) and Determination Coefficient (R^2) and Froude No. Groups Values for Soft and Rough Bottom Channels with different Slopes 77

Table 5.4 The Flow Equations Comparison of Different Channels Cross Sections 83

Table 5.4.1 The Flow Equations Comparison of Different Channels Cross Sections……...…….……...84

Table 5.4.2 The Flow Equations Comparison of Different Channels Cross Sections……..…….……...…...85

LIST OF FIGURES

Page

Figure 2.1 Discharge changing with the end depth, (Diskin,1961)..... 6

Figure 2.2 Calibration figure for free overfall in trapezoidal channel, (Keller and Fong, 1989)..... 7

Figure 2.3 Laboratory representation between X_b and X_c (Gupta et al., 1993)…….. 10

Figure 2.4 a) sharp crested weir; b) free overfall, (Anastasiadou-Partheniou and Haztigiannaki, 1995)…..……11

Figure 2.5 Velocity distribution upstream the brink (Ramamurthy et al., 2004a)……..... 13

Figure 2.6 Velocity and pressure distribution at brink with y/y_c, (Ramamurthy et al., 2004a..... 14

Figure 2.7 Flow in inverted semicircular channel..... 15

Figure 2.8 Relationship between relative end water depth ($Y_b = Y_e$) and dimensionless measured discharge (Q_{*me}) and dimensionless calculated discharge (Q_{*cal})..... 21

Figure 2.9 Comparison between the laboratory results and the equation of discharge calculating of the trapezoidal free overfall horizontal channels (Ali,2013)..... 22

Figure 2.10 Comparison between the laboratory results and the equation of discharge calculating of the triangular free overfall horizontal channels (Ali,2013)..... 22

Figure 3.1 Theoretical Control Volume..... 25

Figure 3.2 Scatter Diagram showing Perfect Negative Correlation and Perfect Positive Correlation..... 34

Figure 3.3 Scatter Diagram showing Zero, Weak and Strong Correlation 35

Figure 3.4 The Strength and Direction of the Coefficient of Correlation..... 35

Figure 4.1 Laboratory channel top view 40

Figure 4.2 Laboratory channel front view 41
Figure 4.3 Laboratory channel view (1) 42
Figure 4.4 Laboratory channel view (2) 42
Figure 4.5 Laboratory channel view (3) 43
Figure 4.6 Point gauge view (1) 44
Figure 4.7 Point gauge view (2) 45
Figure 4.8 Depth Measurement in Semicircular Channels with Rough bottom ... 47
Figure 4.9 (a) Semicircular Channel Cross Section 49
Figure 4.9 (b) Semicircular Channel (3D) 49
Figure 4.9 (c) Semicircular Channel (View 1) 50
Figure 4.9 (d) Semicircular Channel (View 2) 50
Figure 4.9 (e) Semicircular Channel (View 3) 51
Figure 4.9 (f) Semicircular Channel (View 4) 51
Figure 4.10 Free Overfall in Semicircular Channels with Smooth Bottom 54
Figure 4.11 Free Overfall in Semicircular Channels with (2 mm) Roughness on Bottom 55
Figure 4.12 Free Overfall in Semicircular Channels with (4.75 mm) Roughness on Bottom 56
Figure 4.13 Free Overfall in Semicircular Channels with (6.33 mm) Roughness on Bottom 57
Figure 4.14 The Roughness Types Used in Laboratory Experiments……...58
Figure 5.1 Manning Roughness Coefficient (n) Values 62
Figure 5.2 The Change of ($\frac{Q}{\sqrt{g\,D^5}}$) with ($\frac{y_b}{D}$) For Soft Bottom Channels (C_0) with Slope ($S_0 = 0$) 63
Figure 5.3 The Change of ($\frac{Q}{\sqrt{g\,D^5}}$) with ($\frac{y_b}{D}$) For Soft Bottom Channels (C_0) with Slope ($S_1 = 0.005$) 63
Figure 5.4 The Change of ($\frac{Q}{\sqrt{g\,D^5}}$) with ($\frac{y_b}{D}$) For Soft Bottom Channels (C_0) with Slope ($S_2 = 0.01$) 64

Figure 5.5 The Change of ($\frac{Q}{\sqrt{g\,D^5}}$) with ($\frac{y_b}{D}$) For Soft Bottom Channels (C_0) with Slope (S_3 = 0.015) 64

Figure 5.6 The Change of ($\frac{Q}{\sqrt{g\,D^5}}$) with ($\frac{y_b}{D}$) For Soft Bottom Channels (C_0) with Different Slopes..... 65

Figure 5.7 The Change of ($\frac{Q}{\sqrt{g\,D^5}}$) with ($\frac{y_b}{D}$) For Rough Bottom Channels (C_1) with Slope (S_0 = 0) 65

Figure 5.8 The Change of ($\frac{Q}{\sqrt{g\,D^5}}$) with ($\frac{y_b}{D}$) For Rough Bottom Channels (C_1) with Slope (S_1 = 0.005) 66

Figure 5.9 The Change of ($\frac{Q}{\sqrt{g\,D^5}}$) with ($\frac{y_b}{D}$) For Rough Bottom Channels (C_1) with Slope (S_2 = 0.01) 66

Figure 5.10 The Change of ($\frac{Q}{\sqrt{g\,D^5}}$) with ($\frac{y_b}{D}$) For Rough Bottom Channels (C_1) with Slope (S_3 = 0.015) 67

Figure 5.11 The Change of ($\frac{Q}{\sqrt{g\,D^5}}$) with ($\frac{y_b}{D}$) For Rough Bottom Channels (C_1) with Different Slopes..... 67

Figure 5.12 The Change of ($\frac{Q}{\sqrt{g\,D^5}}$) with ($\frac{y_b}{D}$) For Rough Bottom Channels (C_2) with Slope (S_0 = 0) 68

Figure 5.13 The Change of ($\frac{Q}{\sqrt{g\,D^5}}$) with ($\frac{y_b}{D}$) For Rough Bottom Channels (C_2) with Slope (S_1 = 0.005) 68

Figure 5.14 The Change of ($\frac{Q}{\sqrt{g\,D^5}}$) with ($\frac{y_b}{D}$) For Rough Bottom Channels (C_2) with Slope (S_2 = 0.01) 69

Figure 5.15 The Change of ($\frac{Q}{\sqrt{g\,D^5}}$) with ($\frac{y_b}{D}$) For Rough Bottom Channels (C_2) with Slope (S_3 = 0.015) 69

Figure 5.16 The Change of ($\frac{Q}{\sqrt{g\,D^5}}$) with ($\frac{y_b}{D}$) For Rough Bottom Channels (C_2) with Different Slopes..... 70

Figure 5.17 The Change of ($\frac{Q}{\sqrt{g\,D^5}}$) with ($\frac{y_b}{D}$) For Rough Bottom Channels (C_3) with Slope ($S_0 = 0$) 70

Figure 5.18 The Change of ($\frac{Q}{\sqrt{g\,D^5}}$) with ($\frac{y_b}{D}$) For Rough Bottom Channels (C_3) with Slope ($S_1 = 0.005$) 71

Figure 5.19 The Change of ($\frac{Q}{\sqrt{g\,D^5}}$) with ($\frac{y_b}{D}$) For Rough Bottom Channels (C_3) with Slope ($S_2 = 0.01$) 71

Figure 5.20 The Change of ($\frac{Q}{\sqrt{g\,D^5}}$) with ($\frac{y_b}{D}$) For Rough Bottom Channels (C_3) with Slope ($S_3 = 0.015$) 72

Figure 5.21 The Change of ($\frac{Q}{\sqrt{g\,D^5}}$) with ($\frac{y_b}{D}$) For Rough Bottom Channels (C_3) with Different Slopes 72

Figure 5.22 The Change of (y_b/D) With (y_c/D) For Soft Bottom Channels (C_0) with Different Slopes 74

Figure 5.23 The Change of (y_b/D) With (y_c/D) For Rough Bottom Channels (C_1) with Different Slopes 75

Figure 5.24 The Change of (y_b/D) With (y_c/D) For Rough Bottom Channels (C_2) with Different Slopes 75

Figure 5.25 The Change of (y_b/D) With (y_c/D) For Rough Bottom Channels (C_3) with Different Slopes 76

Figure 5.26 The Change of (y_b/y_c) With channel bed slope (S) (Constant Roughness and Different Slope) 78

Figure 5.27 The Change of (y_b/y_c) With channel bed slope (S) (Constant Slope and Different Roughness) 78

Figure 5.28 The Observed discharge with The Predicted Discharge for smooth bed channels (S=0 and n=0) 80

Figure 5.29 The Observed discharge with The Predicted Discharge for rough bed channels (S=0 and n=0) 81

Figure 5.30 The Observed discharge with The Predicted Discharge for smooth and rough bed channels (S and n = 0) 82

LIST OF SYMBOLS/ABREVIATIONS

Q	Discharge in (m^3/s)
A	Water flow area in (m^2)
A_w	Wetted area in (m^2)
V	Mean flow velocity in (m/s)
y_n	Normal water depth in channel in (m)
y_b	Brink water depth (downstream water depth) in (m)
y_c	Critical water depth in (m)
EDR	End depth ratio
R_h	Hydraulic radius in (m)
P_w	Wetted perimeter in (m)
D_h	Hydraulic depth in (m)
T	Top width of water in (m)
n	Manning roughness coefficient
F_r	Froude number
F_{rb}	Froude number in term of final depth
y_b/D	Brink depth ratio
y_c/D	Critical depth ratio
S	Channel longitudinal slope
D	Channel Diameter in (m)
g	Acceleration gravity in (m^2/sec)
ρ	Water mass density in (kg/m^3)
μ	Water viscosity in (N/m^2.sec)
R_e	Reynolds number

γ	The specific weight of fluid
K	The pressure coefficient

CHAPTER 1

INTRODUCTION

1.1 General

The open channels are one of the most important conveyance structures that is used to convey water naturally (by gravity) between two places different in elevation and it has an open top, the open channels include rivers, streams and estuaries. The most important characteristic that concern our work as hydraulic engineers is the open channels flow. Open-channel flow can occur also in conduits with a closed top, such as pipes and culverts, provided that the conduit is flowing partially full. For example, the flow in most sanitary and storm sewers has a free surface and is therefore classified as open-channel flow.[1]

The overfall refers to the downstream portion of a channel, horizontal or sloping, terminating abruptly at its lower end. If it is not submerged by the tail water, it is referred to as a free overfall (Rajaratnam et al. 1976). It is further classified as confined free overfall and unconfined free overfall, depending on the situation of the sidewalls. If sidewalls extend beyond the brink, it is a confined free overfall. A vertical drop of a free overfall is a common feature in both artificial and natural channels. Natural drops are formed generally by erosion, while drop structures are built in irrigation and drainage channels as energy reducing devices, especially where the flow is supercritical.[2]

In natural channels the free fall will produced from elevation change or stream bed elevation from high to low elevation because of bed abrasion, and in artificial channels by changing the bed elevation for these channels with energy dissipation produced by these falls. The free fall at downstream channel full of air which is similar to the simplest case when water falls with very small height over crested spillway.[2]

Drops (free falls) are the most common hydraulic structures used in water distribution, and wastewater collection networks like rainwater networks and sewerage networks, and in recent years in stepped spillways, where these structures are used as a slope control structures if there is a need to control channels slope. The simplest case of free over fall is the vertical over fall and the most important property in these structures is the free fall of water with the impact of nappe water of the downstream flow which will create hydraulic jump. [3]

Free fall has an importance in water resources engineering structures which represents a guide point in gradually varied water surface profile calculations and the ability of use in discharge measurements in laboratories in addition to its main purpose to convey water from high to low level places.[3,4]

The free fall use for discharge measurements had been studied during the last years, the brink depth at free fall with discharge relationship had been studied theoretically and experimentally by a lot of researchers and they found the relation between critical depth and brink depth. (Rouse,1936) calculate the end depth ratio for free fall (EDR= $\frac{y_b}{y_c}$), where y_b represent the final depth of water at the edge of water drop and y_c represent the critical depth, in rectangular channels as a prelude to further studies by many researchers to show the effect of the bed slope and the bed roughness of the channel on the relationship between the critical depth and the final depth in the channels of rectangular and semi-trapezoidal and circular and semi-circular and channels with U-shape sections.[3,4]

Due to the importance of free fall (drops) in open channels, the final depth (brink depth) ratio of the free fall in the semi-circular channels was calculated in the current study, with the effect of bed slope and bed roughness of the channel on this ratio. It is known that natural rivers and artificial channels are generally rough, so this study is important in practical engineering applications.

1.2 Aim of Study

The aim of this study is to investigate the hydraulic performance for free over fall in semicircular channels with showing the influence of channel bed roughness and longitudinal slope on brink depth also the relation of this depth with the critical depth.

The results had been presented in a form that is useful in hydraulic structures design which included subcritical flow. The obtained results giving information and details as follow:

1. Finding the relationship between brink depth (edge depth) and critical depth for free overfall in semicircular channels.
2. Finding the relationship between discharge and brink (edge) depth for free overfall in semicircular channels (Rating Curve).
3. Finding the influence of free overfall channel bed roughness on the relationship between brink depth and critical depth.
4. Finding the influence of channel longitudinal slope on the relationship between the brink depth and critical depth.

1.3 The Study Boundaries

1. Using free overfall semicircular channel sample in laboratory channel with length (9 m) and width (0.8 m), this channel sample is (2m) length and (0.5 m) height and (0.775 m) width with semicircular cross section of (0.3 m) diameter made from (8mm) glass.

2. four values for longitudinal slope were used (S= 0, 0.005, 0.01, 0.015).

3. Using three grade types of roughness for sand particles (ds ≤ 2mm, 4.75 mm, 6.33 mm) for each bed slope in addition to (zero) roughness.

4. Froude number for experiments is changing from (0.13) to (2.22).

5. Discharge values for experiments is between (2 m^3/hr) to (11 m^3/hr).

6. Using the natural water in all experiments.

7. The experiments had been done in laboratory temperature.

CHAPTER 2

LITERATURE REVIEW

2.1 Introduction

Many researchers have conducted theoretical and practical studies on free fall channels for the purpose of establishing a relationship between the final depth and the critical depth of flow. Through these relations, free fall channels can be used as a measure of discharge in water resources engineering as well as its main function as a means of transferring flow from high to low elevations.

In the past, the study of flow characteristics has attracted many people to benefit from the free fall channels. In this chapter, the previous studies have been examined in the flow over freefalls, the factors affecting it, and the equations derived in this field.

2.2 Previous Studies

Several attempts have been made to clarify the relationship between the final depth and discharge of free overfall channels by finding the factors affecting the flow, such as the shape of the channel section, the channel slope and the influence of the bottom roughness on the free fall. On the other hand, many researchers have expanded their studies on the rectangular channel with free overfall for being the simplest.

The first to lay the cornerstone for these studies in this area is the researcher (Rouse 1936), where he was the first to conduct laboratory tests on the channels of free fall and pointed to the possibility of using the free fall as a simple source of measurement of discharge without the need for any calibration, he based on experiments carried in a horizontal (confined) mildly sloping channel, the researcher found that the final depth is a constant proportion of the critical depth calculated for the flow. The final depth ratio (EDR) was found to be equal to 0.715 when the Froude number is equal to 1, He pointed out that the final depth ratio (EDR) is different number at the beginning

of the flow, he represented the dimensionless flow results based on the laboratory results of Froude number $1 \leq F_r \leq 20$.[2,5,6,7]

The following equation has been derived to calculate the discharge of a rectangular channel with free overfall:

$$Q = 1.654 b g^{0.5} y_b^{1.5} \quad (2.1)$$

Where: Q = discharge (m^3/sec), b = bed width (m), g = acceleration (m/sec^2), y_b = the flow depth at the end (brink depth) (m)

Delleur et al.,(1956) studied the effect of roughness and slope of the bottom on the final depth of the rectangular channels and found by relying on roughness that the final depth ratio EDR affected by the slope ratio (S / S_c) where S is the bed slope and Sc the critical slope, they also reported the variation of pressure coefficient (k_1) as a function of relative slope but they did not mention the discharge measurement through the relationship of the final depth.[6,8]

Anastasiadou-Partheniou and Haztigiannakis,(1995) mentioned that (Diskin,1961) carried out measurements for a supercritical flow in a trapezoidal flume made of iron sheets treated with a special type of pigments mixed with granules of sand to increase the roughness of the channel, the longitudinal slope of the concrete channel was approximately (1.5 feet per 100 feet), and its base width was (0.41 feet) with side slope equal to (1V:2H). there were 20 flow measurements ranging from (0.579) to (1.692 ft^3/sec). The values of the discharge were found using Fig. (2.1) which shows the comparison of the laboratory results of (Diskin,1961) with the empirical equations of (Anastasiadou-Partheniou and Haztigiannakis,1995).[9]

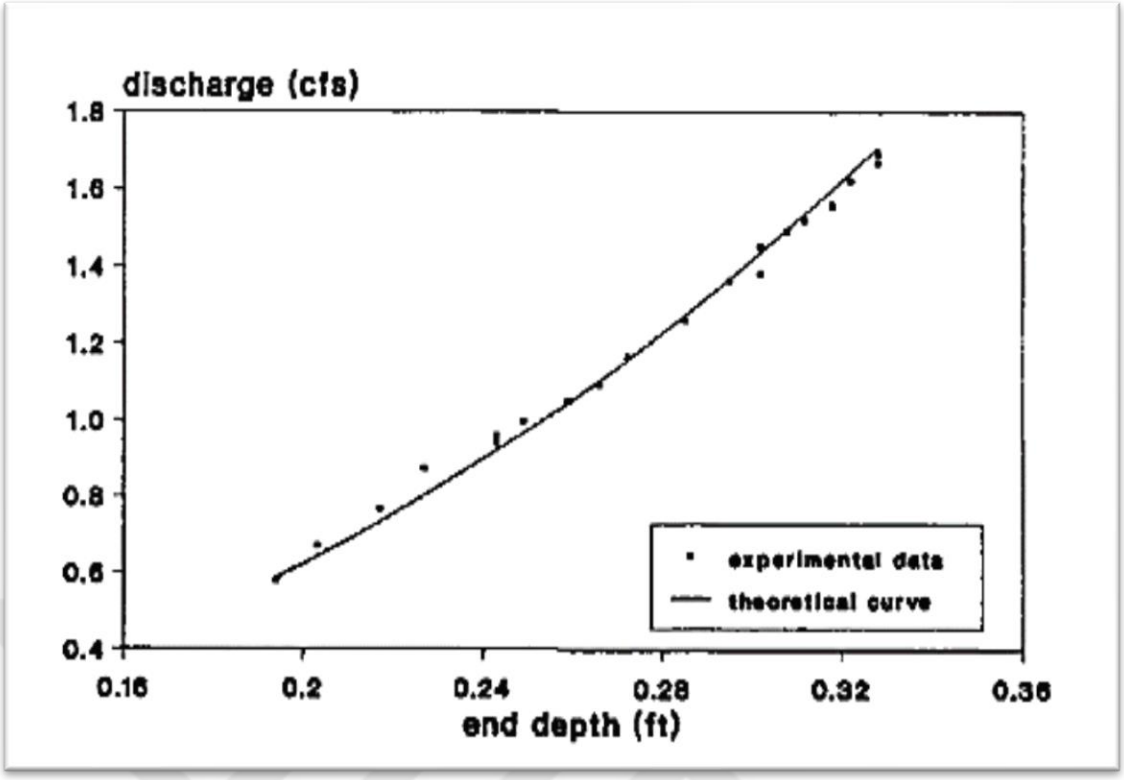

Figure 2.1 Discharge changing with the end depth (Diskin, 1961)

Keller and Fong, (1989) mentioned that (Hamid,1962) had been studied free overfall for trapezoidal channel theoretically and experimentally. He carried out the lab. Work by using horizontal trapezoidal channel with base width (0.322 m) and side slopes (1V:1.712H). He used the momentum equation in all his experiments by assuming the pressure distribution factor equal to zero at the final edge (the brink) and Fig. (2.2) showed the relationship between (my_E/b and EDR) and (my_E/b and Q^2m^3/gb^5) where (m = side slope of the channel).[10]

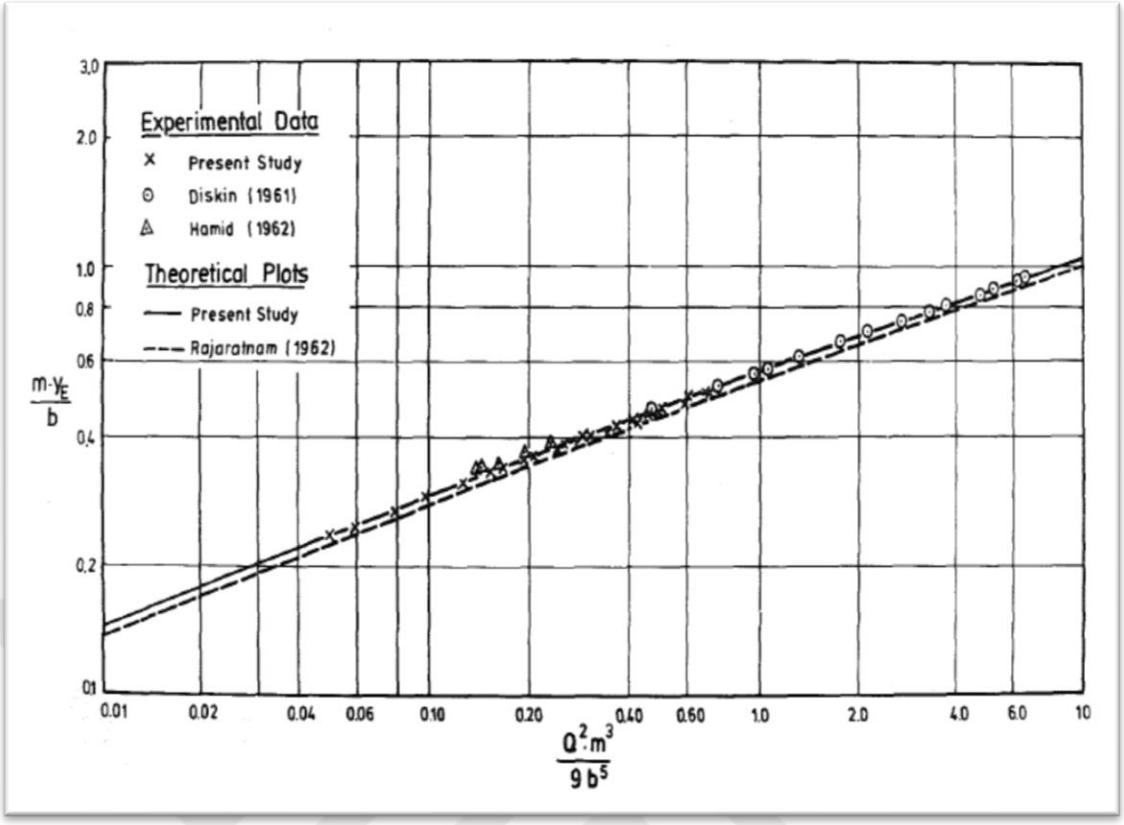

Figure 2.2 Calibration figure for free overfall in trapezoidal channel

(Keller and Fong, 1989)

Rajaratnam et al.,(1976) provided a laboratory study on the channels of free fall on different forms of channel sections: rectangular, triangular and parabolic channels and found that the value of EDR equal to (0.715 and 0.705) for (confined) and (unconfined) rectangular channels respectively, and (0.795) for (unconfined) triangular channels, the results of EDR were compared with the results obtained previously. It was found that the cause of the differences was due to the bottom roughness and the water jet properties, the researcher (Delleur et al.,1956) performed a similar study on a rectangular channel, but for higher roughness values and he performed a high precision curve for relative roughness values (k_s/y_c) less than 0.1, it was found that when the value of (k_s/y_c) is more than 0.1, The value of the EDR will be accurately less than expected and this is due to the effect of roughness.[2,6,11,12]

Rajaratnam et al., (1976) presented a method to solve the curve of (Delleur et al.,1956) by modifying the values of (k_s/y_c) which is higher than 0.1 by the values given to the channel slope, the roughness and the critical depth, and he re-developed the following discharge equations for the different channel shapes:

For (confined) rectangular channels

$$Q = 1.654\ b\ g^{0.5}\ y_b^{1.5} \tag{2.2}$$

For (unconfined) rectangular channels

$$Q = 1.6893\ b\ g^{0.5}\ y_b^{1.5} \tag{2.3}$$

For (unconfined) triangular channels

$$Q = 1.2548\ m\ \ g^{0.5}\ y_b^{2.5} \tag{2.4}$$

Keller and Fong, (1989) studied theoretically and experimentally the free fall of the channels with trapezoidal cross section. The theoretical analysis included the application of the momentum equation to the (Control Volume) at the beginning of the flow through the critical depth and at the end of the flow through the free fall section, Appropriate hypotheses were developed for the pressure distribution factor at the free-fall section, depending on the measurement of the variables in the rectangular and triangular channels, Experiments were conducted using a plastic glass channel with (3m) length and (0.15 m) base width and (1V:1H) side slopes. The bottom inclination to obtain the subcritical flow was (0.00067) in all the discharges used.[9,10,13]

In this study, the two researchers used extensive information related to the final depth and its relation with the pressure coefficient by (Replogle, 1962). A sixth-degree equation was derived, linking the final depth to the critical depth and it needs a lot of iterations to solve it:

$$10X_c^4 + 20X_c^3 + 9X_c^2 - \frac{6}{G_1}(X_c^3 + 3X_c^4 + 3X_c^5 + X_c^6) - K\ G_1\ G_2\ (1 + \ 2X_c) = 0 \tag{2.5}$$

Where:

$$G_1 = X_b + X_b^2 \tag{2.6}$$

$$G_2 = \frac{(3+2X_b)X_b}{(1+X_b)} \tag{2.7}$$

Where: *K*: the pressure coefficient, $X_c = my_c/b$, $X_b = my_b/b$, *m* = side slope, b = channel bed width.

Anastasiadou-Partheniou and Haztigiannakis, (1995) has mentioned that (Terzidis and Anastasiadou-Partheniou, 1990) presented study on the trapezoidal section in the same way for (Keller and Fong, 1989) and using the measurements of both (Replogle, 1962) and (Rajaratnam and Moralidhar, 1964b) where a simple equation has been derived between the final depth and critical depth:

$$X_c = -0.557755 + [0.31109 + 1.5823aX_b(aX_b + 1)]^{0.5} \quad (2.8)$$

Using the value of (a=1.024) for the trapezoidal channels, whose value is less accurate than the measured value by (Replogle), as (a=1.026) for rectangular channels, Equation (2.8) seems easy to solve and suitable in practical applications and in some cases this equation has a higher accuracy than the results of (Keller and Fong, 1989). [9,14]

(Ferro, 1992) has conducted a laboratory study on the free overfall of the rectangular channels, which have different values of the width of the channel and the height of the fall, He made the free overfall wooden channel with length of (6m) and he tested six values of bed width (0.05, 0.1, 0.151, 0.2, 0.251, 0.299) m, and four values for the fall height (0.1043, 0.1533, 0.2041, 0.2071) m.[15] (Ferro, 1992) found that the value of EDR is equal to (0.76) and concluded the relationship between the final depth and critical depth depending on the channel bed width, and presented the following equation:

$$Q = 1.51\ b\ g^{0.5}\ y_b^{1.5} \quad (2.9)$$

Gupta et al., (1993) have analyzed statistically the information for all laboratory experiments and gave a calibration curve, using dimensionless variables to calculate the discharge by knowing the final depth in trapezoidal free overfall channels with smooth bed and by using different values of bed slope, the calibration curve was found between X_b and X_c for the horizontal and positive bottom slope as in Fig. (3.2). They have found that (X_b/X_c) is equal to (0.745) and (0.76) for horizontal and positive slope respectively.[16]

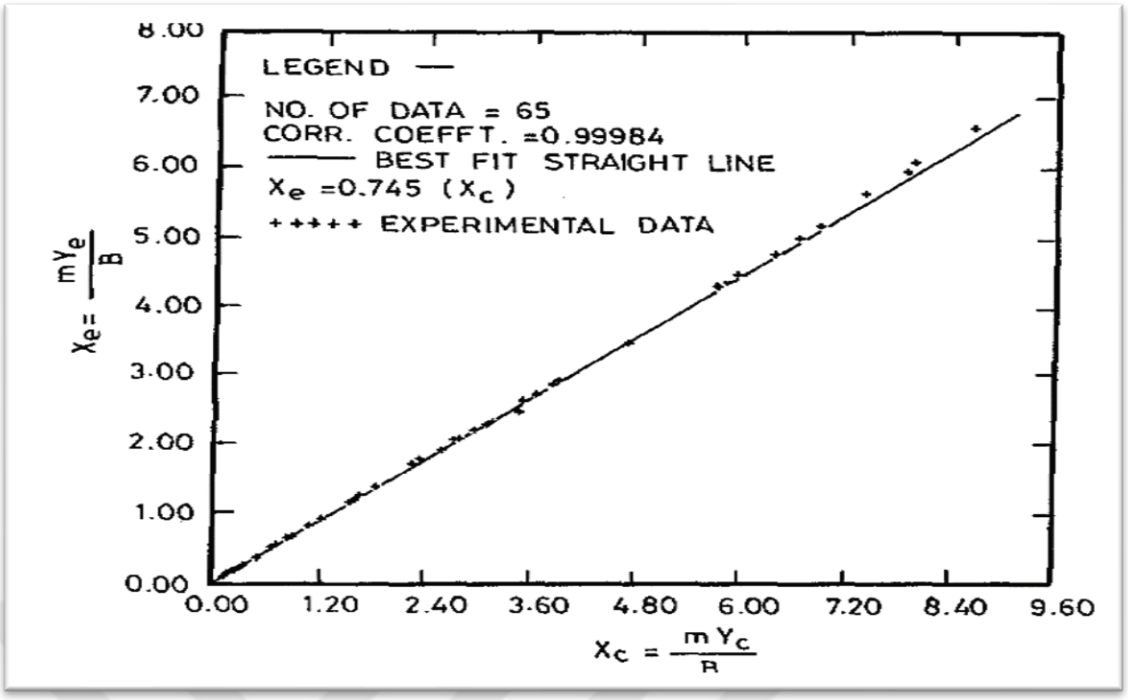

Figure 2.3 Laboratory representation between X_b and X_c (Gupta et al., 1993)

Anastasiadou-Partheniou and Haztigiannakis, (1995) presented a study of flow over free overfall of the trapezoidal channels and was compared with sharp crested weir, considering the flow line and curvature at the end of the flow, as in fig. (2.4).

A general relationship was obtained between the final depth and discharge for both supercritical and subcritical flow conditions, the calculated discharges from the general relationship were compared with laboratory results as well as results obtained from theoretical methods [9]. The following equation was obtained to find the actual value of the discharge over free overfall:

$$Q = C_c\{\frac{2b\sqrt{2g}}{3}\left[E^{\frac{3}{2}} - (E - y_1)^{\frac{3}{2}}\right] - \frac{4m\sqrt{2g}}{15}\left[(3y_1 + 2E)(E - y_1)^{\frac{3}{2}} - 2E^{\frac{5}{2}}\right]\} \qquad (2.10)$$

Where: C_c: Contraction coefficient (A_b/A_1), A_b: The cross-sectional area at the final edge (brink), A_1: The cross-sectional area at section 1, E: Energy, y_1: The flow depth at section 1.

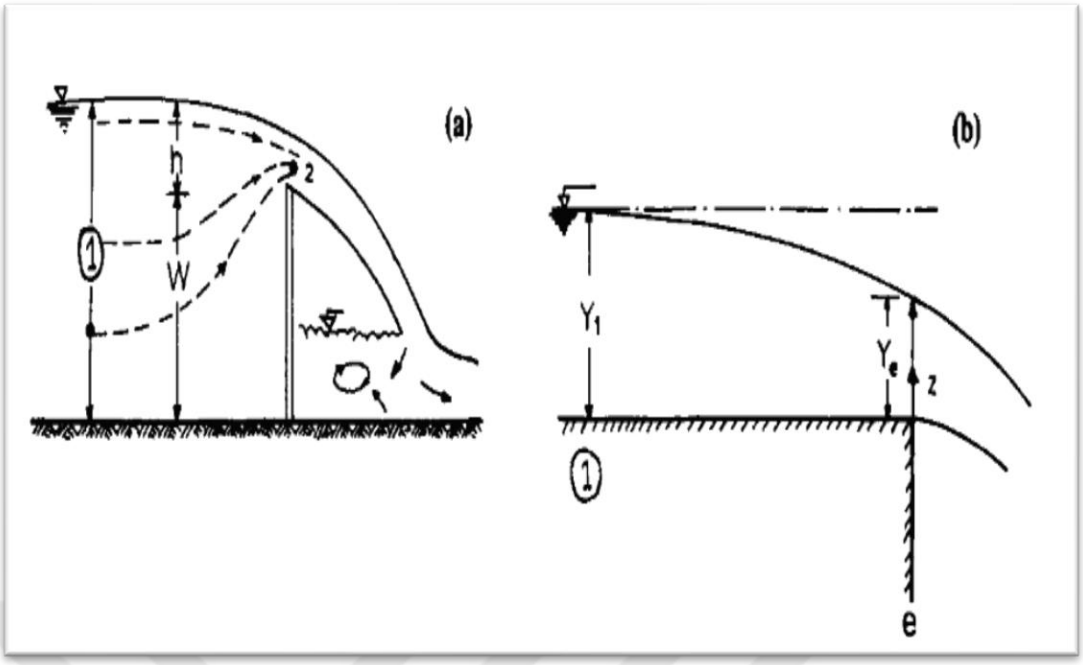

Figure 2.4 a) sharp crested weir; b) free overfall (Anastasiadou-Partheniou and Haztigiannaki, 1995)

Davis et al., (1998) performed a laboratory study on the free overfall of rectangular channels of different values of bottom slope and roughness, carrying out a series of experiments on a confined rectangular laboratory channel with glass sides having (305mm) width and (3.7m) length, the bottom of the laboratory channel is made of iron with Manning roughness coefficient equal to (0.0099) to represent the soft bottom, the rough bottom was represented by adding the sand to obtain a bottom roughness equal to (0.0147), while for the channel slope was chosen as follows (0.033, 0.02, 0.01, 0.0033) respectively.[12]

The relationship between the critical depth at the upstream and the final depth was studied and found to be affected by the slope of the channel and the roughness of the bottom of the channel, the highest effect of roughness was found at the extreme slope. Two equations were used to denote the value of EDR and calculate the channel's discharges and compare it with the measured values. The first equation requires the knowledge of the slope of the channel only, and the second equation requires knowledge of the values of both the slope of the channel and the roughness of the bottom to calculate channel discharge; The accuracy of the two equations was tested and it was found that the equation that requires the slope and the roughness of the channel have the best accuracy in the calculation of the discharge. Therefore, in case

of bottom roughness and slope availability, it is preferable to use the second equation in the calculation of discharge because it gives more accuracy. The equations are as follows:

For smooth bed channels

$$\frac{y_b}{y_c} = 134.84\,S^2 - 12.66\,S + 0.778 \qquad (2.11)$$

For rough bed channels

$$\frac{y_b}{y_c} = 0.846 - 0.219\,\sqrt{\frac{S}{n}} \qquad (2.12)$$

Where: n = Manning roughness coefficient.

Ferro, (1999) represented the free overfall by using a sharp crested weir, he found the theoretical relationship between the final depth and discharge for the two cases subcritical and supercritical flow for rectangular and triangular channels, he compared the laboratory results with the expected theoretical relations of discharge for each section of the channel. He obtained a value of (EDR) equal to (0.715) for rectangular channels.[5,6,17] The following equation was found for subcritical flow for rectangular channels:

$$Q = 1.6542\,b\,g^{0.5}\,y_b^{1.5} \qquad (2.13)$$

Where: b = the width of rectangular channel.

Ahmed, (2003) studied the theoretical method (quasi) of finding the final depth ratio (EDR) and the relationship of discharge to the final depth of both flow conditions subcritical and supercritical flow for the channels of rectangular horizontal slope, the pressure distribution coefficient of the final depth was found, and it was found in this study that the final depth ratio (EDR) was (0.78) and (0.758) for the confined and non-confined channels respectively.[18]

Mohammed et al., (2011) mentioned that (Ahmed, 2005) made a similar study on the free overfall of inverted semicircular channel with a sharp-crested weir, to find the discharge by measuring the final depth only. the final depth ratio in most cases was fixed to an average value of (0.713).[19,20]

Ramamurthy et al., (2004) presented a laboratory study to give the flow velocity, pressure charge and surface shape of the flow above the free overfall of the trapezoidal channels. Experiments have been made by using trapezoidal channel with (7 m) length and (127 mm) base width and (1V:1H) side slopes, he used the volume of fluid (VOF) turbulence model to obtain characteristics of three-dimensional open channel flows involving free surfaces. He showed the experimental and the predicted distributions of the axial velocity in the plane of channel symmetry at three sections (x/y_c= −0.15, −0.61; and −1.23) upstream of the brink as shown in Fig. (2.5).[13]

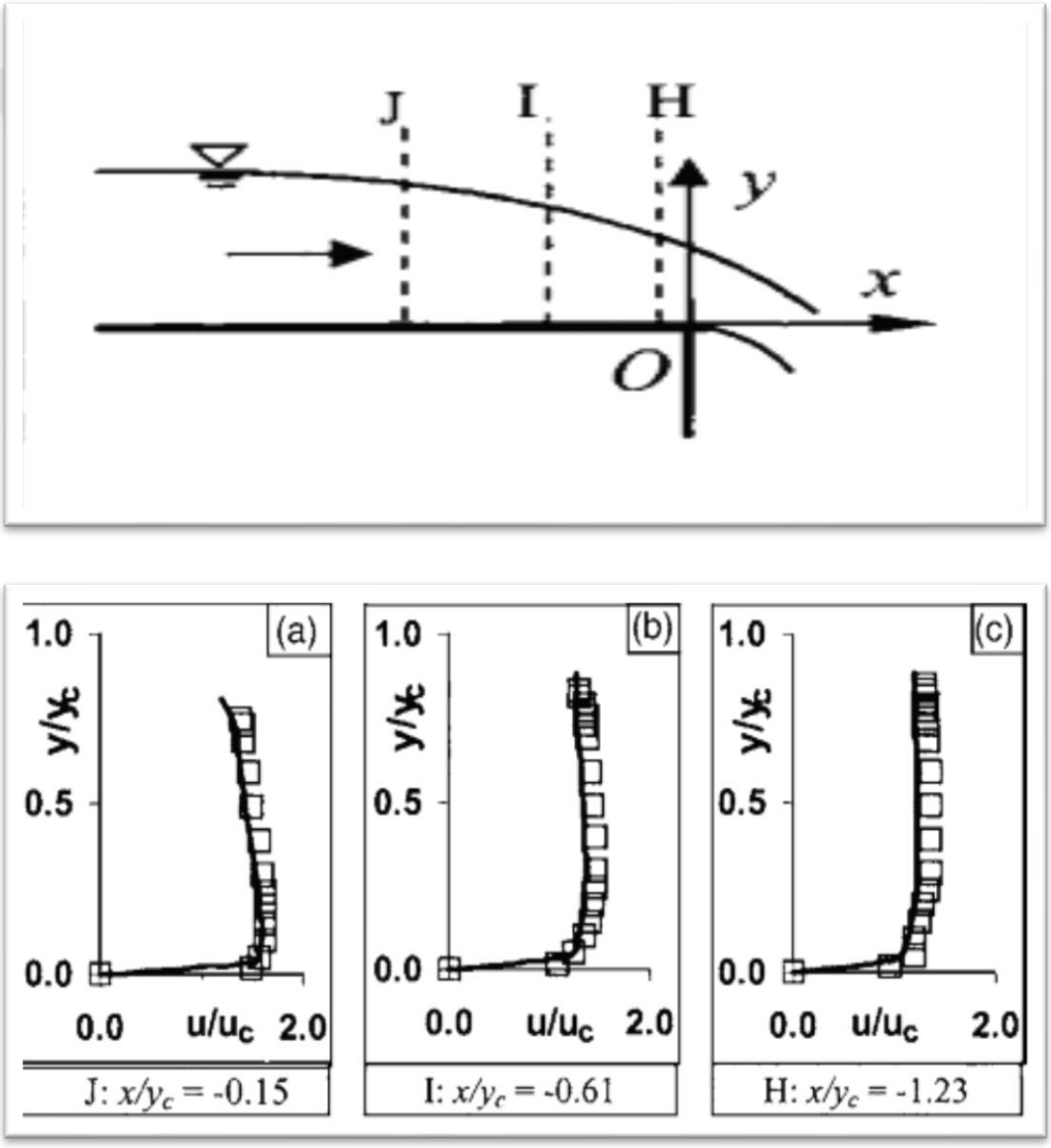

Figure 2.5 Velocity distribution upstream the brink (Ramamurthy et al., 2004a)

Also, he found the distributions of the axial velocity at the end depth sections A, B, C, and D and the distribution of the non-dimensional vertical pressure head ($\boldsymbol{p}/\boldsymbol{\gamma y_c}$) at those various sections close to the brink with y /y_c as in fig. (2.6).

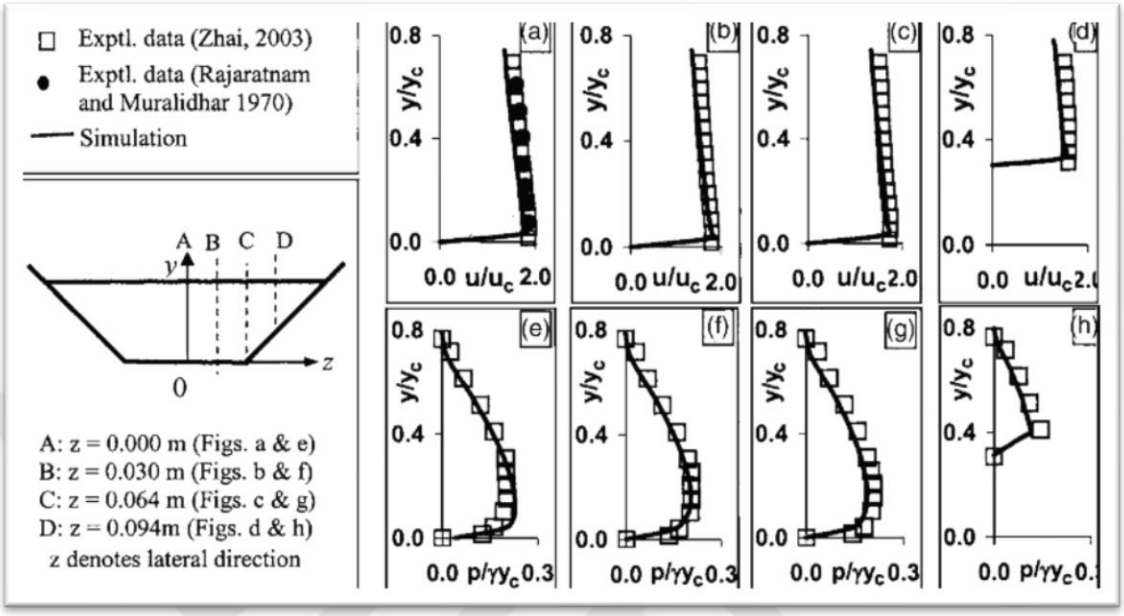

Figure 2.6 Velocity and pressure distribution at brink with y/y_c

(Ramamurthy et al., 2004a)

Dey, (1998, 1999, 2001, 2002, 2003 and 2005) conducted a theoretical study on different channel cross sections: circular, rectangular, inverted semicircular, and channels with U-shape, [5,21] He relied on three cases in all his theoretical analysis methods to find the value of EDR:

First case: He used the momentum equation which depends on (Boussinesq) approximations in circular and inverted semicircular channels as in fig. (2.7) where it needs to find the pressure coefficient in the laboratory, The final depth relationship in the case of subcritical flow had been found about (0.75) for the critical depth ratio of the diameter (y_c/d) is higher than (0.82) in circular channels and approximately (0.705) for the critical depth ratio of the diameter (y_c/d) is higher than (0.420) for the inverted semicircular channels in case of horizontal channel.[11,19,20,22]

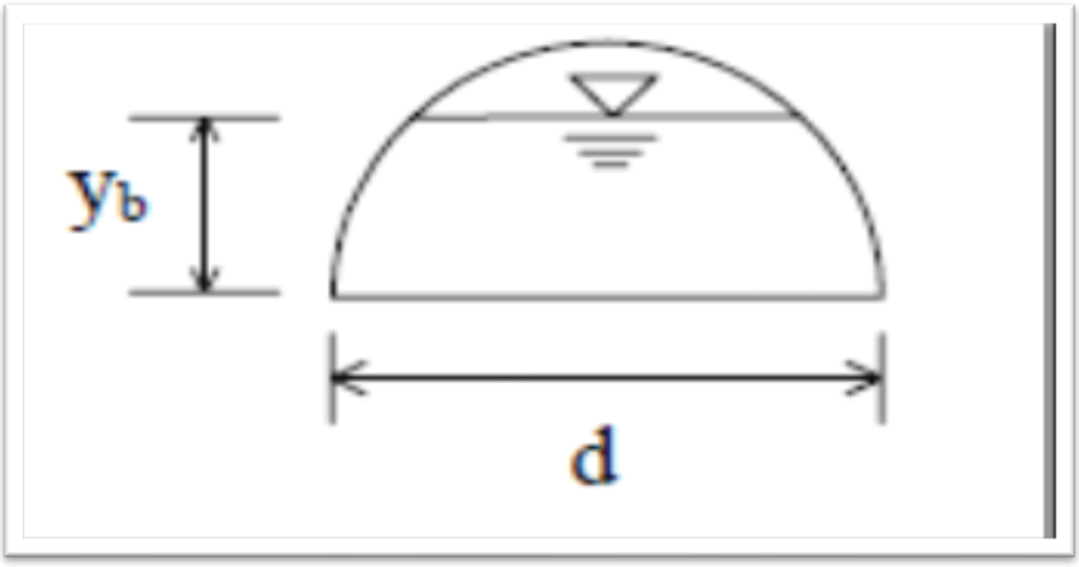

Figure 2.7 Flow in inverted semicircular channel

Second case: He calculated the flow over free overfall by using a sharp-crested weir and found that most of the values of (EDR) are linearly changed from (0.72) to (0.74) for the critical depth diameter ratio more than (0.86) in the horizontal circular channels and more than (0.754) for the dimensionless critical depth ratio of (0.5) in U-shape cross section channels.[5,19,23]

Third case: He used the modified energy equation which depends on (Boussinesq) approximations in inverted semicircular channels where it needs to find the value of the pressure coefficient in the laboratory, He found that the value of (EDR) is approximately (0.695) for the critical depth diameter ratio up to a value higher than (0.4) in inverted semicircular channels.[4]

Beirami et al., (2006) provided a theoretical study based on the theory of the free vortex to predict the distribution of pressure at the edge and the pressure coefficient of the free overfall channels with horizontal slope and for different cross sections. He found that the end depth ratio (EDR) by using the momentum equation for rectangular, triangular and exponential cross sections equal to (0.7016), (0.8051), (0.7641) respectively.[11] He used experimental results and theoretical results of other researchers, the results were investigated for rectangular, triangular, exponential and inverted triangular channels (A-shape) and inverted semicircular and circular channels, [11] The theory was well presented compared to the experiments and he pointed out through his study that (Anderson, 1967) and (Murty, 1994) found that the final depth

ratio equal to (0.694) and (0.705) for rectangular channels and (0.762) and (0.795) for triangular and (0.735) and (0.758) for exponential channels respectively, (Ali and Sykes, 1972) and (Ahmed, 2002) mentioned that the final depth ratio of triangular channels is (0.798) and (0.802) respectively and compared the discharge equation of the triangular channels that they found with the equations of other researchers and it was as follows:

Anderson,1967 equation

$$Q = 1.395\ g^{0.5}\ my_b^{2.5} \quad (2.14)$$

Ali and Sykes,1972 equation

$$Q = 1.243\ g^{0.5}\ my_b^{2.5} \quad (2.15)$$

Murty,1994 equation

$$Q = 1.2548\ g^{0.5}\ my_b^{2.5} \quad (2.16)$$

Ahmed,2002 equation

$$Q = 1.2276\ g^{0.5}\ my_b^{2.5} \quad (2.17)$$

Beirami et al.,2006 equation

$$Q = 1.2158\ g^{0.5}\ my_b^{2.5} \quad (2.18)$$

Gue et al., (2008) presented a study of laboratory experiments and numerical analysis of results to test the effect of bottom roughness (using square slices) and the effect of channel slope on flow over free overfall in rectangular channel, the wooden channel was (0.4 m) depth and (0.4 m) width and (8.4 m) length, and slides with a square-shaped section having a dimensions of (6 mm X 6mm) and fixed horizontally and placed along the length of the channel with varying distances between the center of a slice and another, the values suggested in the study for the different variables were as follows: the ratio of distance between the center of a slide and another to the height of the slide (L/h) is equal to: (3, 6, 9, 18, infinity) and the bottom slope values (0, 1/400, 1/105, 1/150, 1/200) with a change in discharge ranging from (0.011 m^3/s) to (0.036 m^3/s) for each group of roughness and slope, as laboratory measurements showed a good correlation with the computational results.[24]

The results indicated that the distances between the slides is a factor affecting the final depth ratio (EDR), where this value decreases with the increase of (L/h), the relatively small distances between the two slices caused the vortices to form within these spaces, so the discharge flow is reduced in the channel during these distances and a small flow is transmitted at the end of the flow.[24]

Tigrek et al., (2008) studied the effect of the bed slope and two roughness factors (0.0099) and (0.0147) on the properties of the subcritical, critical and supercritical flow of free overfall in a rectangular channels which was (1 m) width and (12.06 m) length for the purpose of finding and clarifying the relationship between the final depth and the normal depth and the slope of the channel bottom and discharge and roughness, they tested the channel for a soft bottom that included nine values of inclination ranging from (0.0003) and (0.0385),The study included eighty-two experiments of a soft bottom, nineteen experiment for subcritical flow, and sixty-three experiments of supercritical flow.[2,6]

The same was for the rough bed, the tests were conducted on eight values of inclination ranging from (0.0008) to (0.0394), and the tests included forty-eight experiments, twenty-five of them was for the condition of subcritical flow.[2,6] They found the following:

1. The ratio between the final depth and critical depth (EDR) is independent of the slope of the channel for (subcritical flow) case and affected by the slope of the channel for (supercritical flow) case.
2. If the bottom slope is constant, the (EDR) will increase with increasing roughness.
3. The effect of roughness on (EDR) increases with increasing slope.
4. The final depth ratio (EDR) in the case of subcritical flow is depends on the Froude number (U/S) while its value is reduced with the Froude number increasing at the upstream of the supercritical flow case of both soft and rough bed conditions.[2]

In other words, the relationship between the brink depth to critical depth ratio (y_b/y_c) shows different characteristics between subcritical and supercritical flow, [2,6] the ratio is constant in the case of subcritical flow and variable in the case of supercritical flow as shown in the following empirical equations:

For subcritical and critical flow:

$$\frac{y_b}{y_c} = 0.683 \qquad \text{Fr} \leq 1 \tag{2.19}$$

For supercritical flow:

$$\frac{y_b}{y_c} = 0.773 - 0.018\ \frac{\sqrt{S_0}}{n} \qquad \text{Fr} > 1 \tag{2.20}$$

5. The following equation was found to calculate the flow rate in case of knowing the values of final depth, roughness and channel bottom slope only:

For subcritical and critical flow:

$$q = 5.55\ y_b^{3/2} \qquad \text{Fr} \leq 1 \tag{2.21a}$$

For supercritical flow:

$$q = \left(\frac{1}{0.361 - 0.00841\sqrt{S_0}/n}\right)^{\frac{3}{2}}\ y_b^{3/2} \qquad \text{Fr} > 1 \tag{2.21b}$$

Where: q = discharge per unit width.

Mohammed et al., (2011) and others investigated the effect of roughness and slope by using different types of gravel for bottom roughness in the laboratory and three values of the slope of free overfall (0, 1/100, 1/200). The laboratory study included the use of a metal rectangular channel with glass sides and with (300 mm) width and (10 m) length.[6] He concluded the equation of end depth ratio (EDR) for different types of roughness as follow :

$$EDR = K_2 + K_3\left(\left(\lambda/y_c\right) S\right)^{1/2} \tag{2.22}$$

K_2 and K_3 are coefficients and they were different for each gravel distribution on the bottom of the channel and slope.[6] The results showed that the effect of the relationship between the depth of the edge and the critical depth in the case of the full roughness (20 * 30) cm^2 for (6 mm) gravel is higher in case of steep slope. The researcher concluded six relationships to calculate the (EDR) according to the case of slope and roughness and these relationships had been compared with (Davis et. al.,1998) and (Tigrek et. al.,2008) to ensure their validity and utility.[25]

The researcher Ibrahim S. S., (2012) conducted a laboratory study on the free overfall of the trapezoidal channels, which has different values of the longitudinal channel slope and roughness models, she made three channels models made of plastic glass with (3.7 m) length and (10 cm) bed width, and she chose three values for the side slope (m = 0.268, 0.577, 1) and four values for the longitudinal slope of the bed (S = 0, 1/50, 1/100, 1/300), [26] She found that the value of (EDR) is equal to (0.729) for the trapezoidal free overfall section with smooth horizontal bed, [26] and she concluded relationships between the final depth and drainage of soft and rough channels and for horizontal and slope bottom cases by the following equations:

For smooth bed channels with different slopes:

$$\frac{Qm^{1.5}}{\sqrt{gb^5}} = 6.514\ (\frac{my_b}{b})^{1.71}\ (S)^{0.182} \qquad (2.23)$$

For smooth horizontal bed channels:

$$\frac{Qm^{1.5}}{\sqrt{gb^5}} = 2.239\ (\frac{my_b}{b})^{1.702} \qquad (2.24)$$

I.M.H.Rashwan, (2012) presented a mathematical and experimental study to evaluate the efficiency of the free overfall as a discharge measuring tool for low flow in circular open channels having horizontal, mild and adverse slopes.[19] He used laboratory flume with (14.25 m) length, (1m) width and (1m) height divided to three parts.[19] The testing channel is circular pipe with (4m) length,(0.25m) internal diameter and (5mm) thickness has inserted into the second part of flume by using upstream and downstream wall with thickness 13 mm. The pipe is horizontal and its bottom is rest at 0.25 from flume bottom. The momentum equation, continuity equation and Froude number equation had been used to find a relation between end depth (y_b) and critical depth (y_c) and he found that the value of (EDR) equal to (0.73).[19] He used two methods to calculate the discharge :

1. For horizontal smooth circular channel:

First case: calculate the discharge using equations as follow:

$$\frac{A_{*c}^2}{2\sqrt{H_a - H_a^2}}\left(\frac{A_{*c}}{A_{*b}} - 1\right) - \frac{8}{15}H_a^{2.5}\left(1 - \frac{H_a}{4}\right) = \frac{A_{*b}}{2}\left(1 - H_e - \frac{5}{16H_e}\right) - \frac{5}{12}\left(1 - \frac{1}{2H_e}\right)(H_e(1 - H_e))^{1.5} \quad (2.25)$$

$$A_{*b} = \frac{20\,H_a^{1.5}\,(1-\frac{H_a}{4}-\frac{4}{25}H_a^2)^3}{9\left(1-\frac{H_a}{4}\right)\sqrt{1-H_a} + 3\,(1-\frac{H_a}{4}-\frac{4}{25}H_a^2)^2} \quad (2.26)$$

$$\frac{Q_{*me}}{Q_{*cal}} = -1.834(H_e) + 1.2347 \quad (2.27)$$

These three equations are used to predict dimensionless critical depth from dimensionless brink water depth and then predict the discharge form the following equation:

$$Q_* = \sqrt{\frac{32\,(H_a^{1.5}(1-\frac{H_a}{4}-\frac{4}{25}H_a^2))^3}{\sqrt[3]{(H_a - H_a^2)}}} \quad (2.28)$$

Where: H_a: relative water depth at the critical section (y_c/D), D: diameter of the circular channel, H_e: relative water depth at the end of channel (y_b/D), A_*: dimensionless water area.

Second case: calculate the discharge using fig. (2.8) as follow:

Estimation of discharge directly by knowing relative water depth at the end of channel (H_e) from fig. (2.8).

2. For mild and adverse circular channel:

By knowing the brink water depth (y_b), equations (2.28) and (2.29) gives accurate discharge:

$$\frac{A_{*c}^2}{2\sqrt{H_a - H_a^2}}\left(\frac{A_{*c}}{A_{*b}-1}\right) - \frac{8}{15}H_a^{2.5}\left(1 - \frac{H_a}{4}\right) = \frac{A_{*b}}{2}\left(1 - H_e - \frac{5}{16H_e}\right) - \frac{5}{12}\left(1 - \frac{1}{2H_e}\right)(H_e(1 - H_e))^{1.5} + \frac{(2\,A_{*c} + A_{*b} - 3\,A_{*n})}{3}\;L\,S \quad (2.29)$$

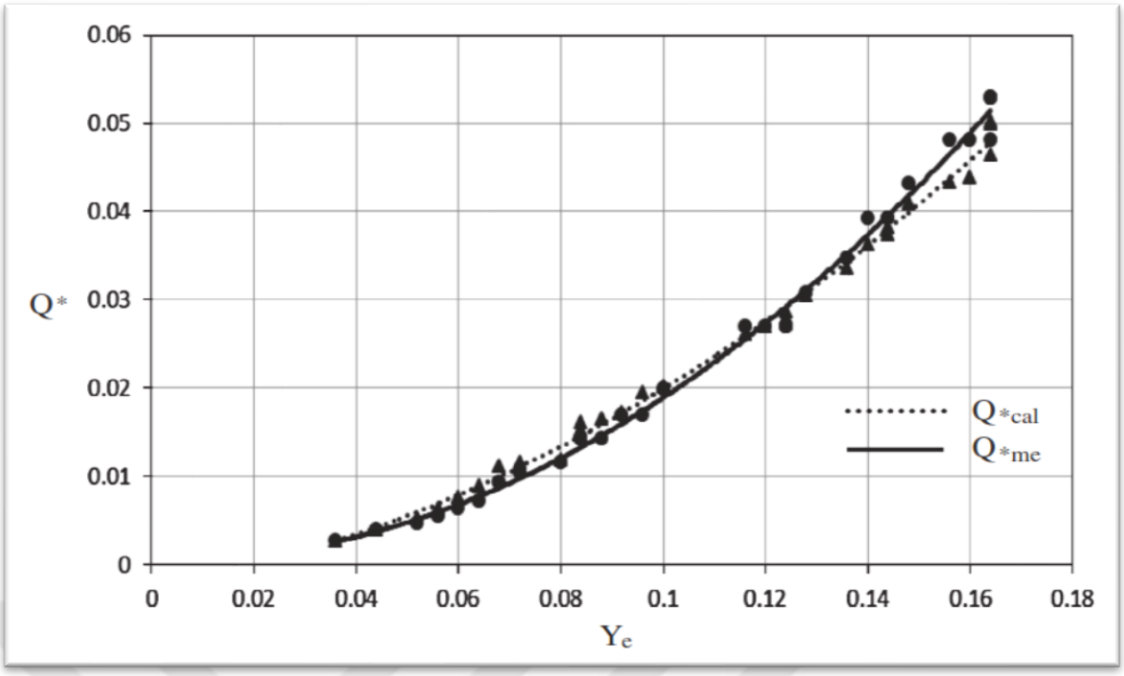

Figure 2.8 Relationship between relative end water depth ($Y_b = Y_e$) and dimensionless measured discharge (Q_{*me}) and dimensionless calculated discharge (Q_{*cal})

Ali, (2013) presented a theoretical study on the channels of free overfall with trapezoidal and triangular cross sections and having horizontal soft bed. He derived two equations to calculate the discharge in subcritical flow condition and the equations were validated by applying them to the results of previous laboratory studies, as shown in Fig. (2.9) and (2.10).[25,27]

The literature in this chapter shows the importance of studying the subject of free overfall in the channels, and since most of the studies on this subject focused on rectangular and trapezoidal channels, in addition to the focus was on changing the slope of the channel and its bed roughness and their impact on the ratio of the final depth and discharge and was not focused on side slopes.in this study we focused on the free overfall in semicircular channels taking into account the effect of channel bed longitudinal slope and bed roughness on the final depth ratio and discharge in these channels and their effect on the calculations of the final depth at the end of channel.

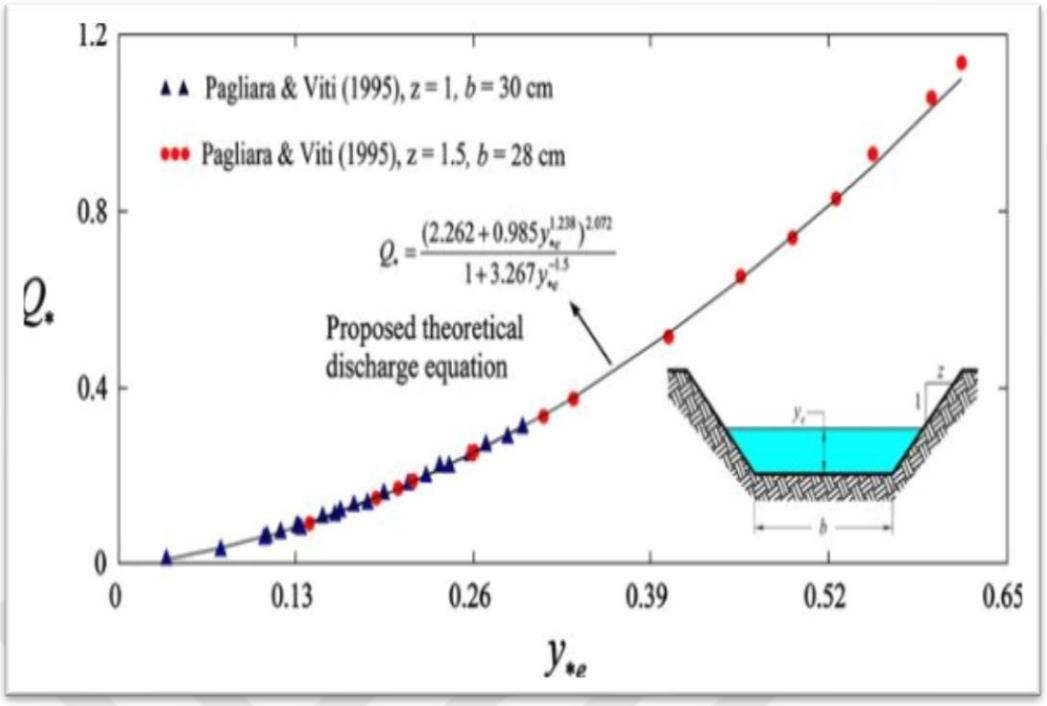

Figure 2.9 Comparison between the laboratory results and the equation of discharge calculating of the trapezoidal free overfall horizontal channels (Ali, 2013)

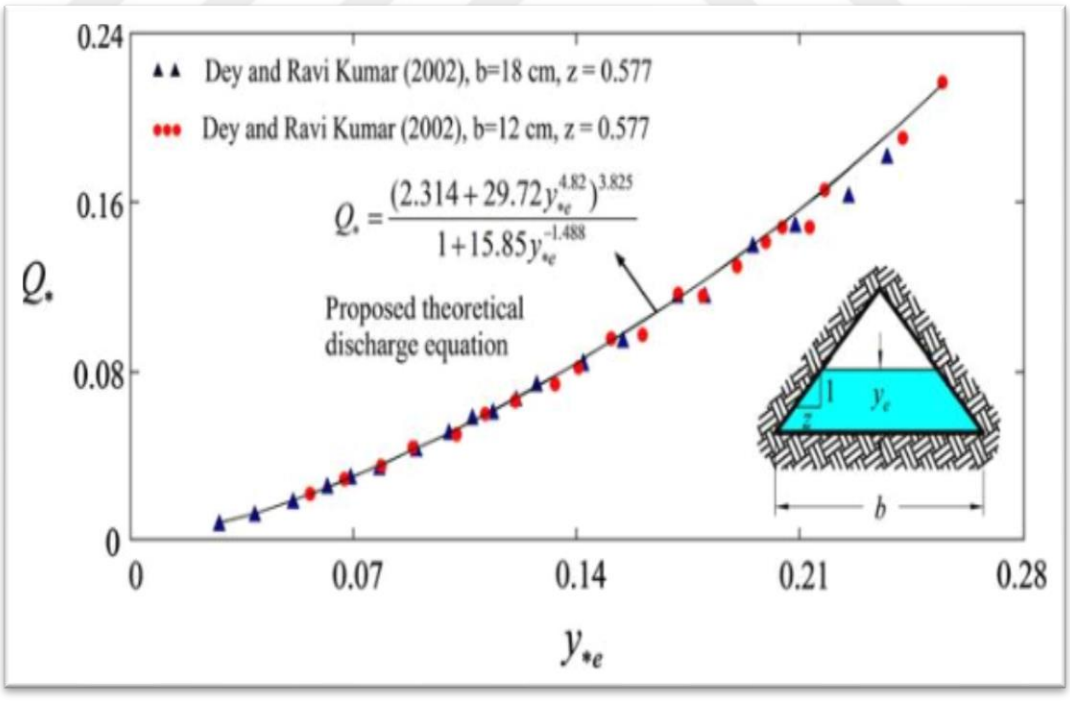

Figure 2.10 Comparison between the laboratory results and the equation of discharge calculating of the triangular free overfall horizontal channels (Ali, 2013)

CHAPTER 3

THEORETICAL FUNDAMENTALS

3.1 Introduction

Analytical attempts have been made by many investigators in the past for computation of end depth, among them most of the approaches are based on application of momentum equation with some assumptions which the majority of these studies have been undertaken by Rajaratnam and Muralidhar and few are based on energy consideration and water surface profile at the end section. The numerical solution of two-dimensional flows for an ideal fluid has also been attempted adopting various finite element techniques. To obtain three-dimensional flow characteristics VOF (Volume of Fluid) model has also been applied. Boussinesq approximation, Free-vortex approach, Weir (without crest) flow approach, Potential flow approach and Empirical approach are some of theory which was used to solve the free overfall theory in channels with different cross sections for both sub. & supercritical approaching flow.[6,25]

The analysis of these studies concluded that the EDR depends on the flow conditions (plane, three-dimensional) and the channel shape affecting the pressure distribution in the brink section, and on approach channel slope and roughness.[8]

In this chapter, the theoretical considerations and the fundamentals of the study of free overfall in the semicircular channels were presented based on what was mentioned in the previous studies, and hypotheses were developed before analyzing the laboratory data of the four study cases. Most theoretical considerations adopted hypotheses to facilitate the complexities of laboratory work to obtain the results of the effect of bottom slope and roughness on flow measurements in the semicircular channels above the free overfall, dimensional analysis of the affecting factors on the study was carried out, the relationship between the depth of the end and the flow rate had been derived based on the momentum equation.

3.2 Free Overfall General Properties

The free overfall is a specific condition or situation in which there is a separation in the flow occurs where the water leaves the bottom of the channel and moves into the air, generating free jet. This condition is generated by the presence of a sharp edge at the end of the channel flow section or water flow path as in Fig. (3.1)

When the flow reaches the free overfall, the mean velocity of the flow is increased and there is a strong vertical curvature in the flow profile and the flow is gradually changed. This phenomenon provides the possibility of using the free overfall to measure discharge in all flow systems (subcritical and supercritical). The water jet is influenced by the force of gravity in the accelerated flow, where there is a strong change of pressure from the state of the hydrostatic distribution along the approach to the free overfall. At the end section, the pressure above and below the water jet is atmospheric pressure, and within the flow section the pressure is not atmospheric pressure.With the atmospheric pressure above and below the water jet, the shape of the water surface is parabola. In the sections upstream of the flow, the curvature of the surface of the water decreases gradually (Wilkinson,1973) and in control section upstream of the flow, the distribution of pressure is hydrostatic. As a result of this, the depth of the water gradually decreases from the control section upstream of the flow towards the control section at the end of the flow with minimum depth (y_b) occurs at the brink, and called the brink depth.

In critical flow, the critical section shall be formed if it is necessary or required for the flow to move to the state of supecritical flow. The critical depth (y_c) based on hydrostatic pressure distribution generate in a specific place between the beginning and the end of the flow. The free overfall works as a controlling section and has a unique relationship with the depth of the end and discharge, for this reason it is used as a tool to measure the discharge for channels of different cross sections. The ratio of end depth to critical depth (EDR) enables us to predict discharge and study erosion near the free overfall at the end. In the case of steep slopes, where the flow in the front is a supercritical flow, flow discharge is a function of the final depth, channel slope and roughness. [4,6,14,18,25,28]

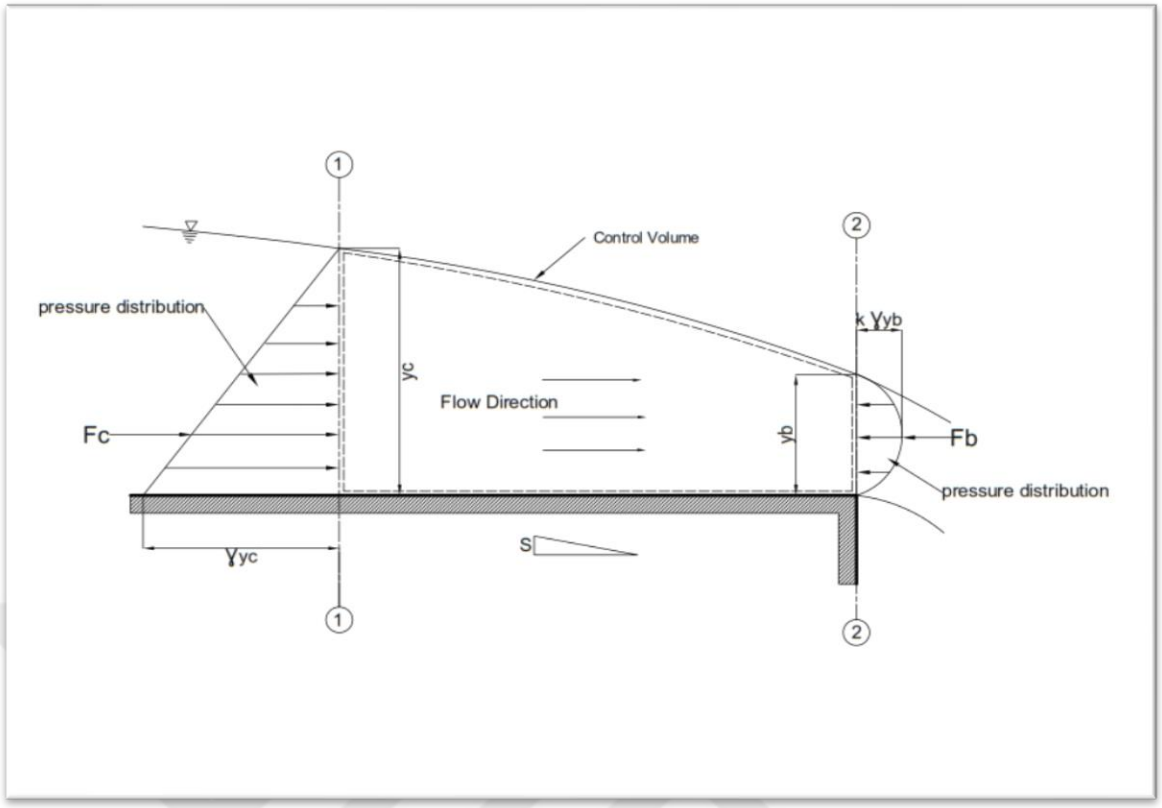

Figure 3.1 Theoretical Control Volume

3.3 The Momentum Equation Application Between the Final Depth and Critical Depth

The following assumptions are used in the momentum equation application:

1. The channel slope is hydraulically mild and sufficiently small that the weight component of the water within the control volume resolved down the slope can be neglected.

2. The pressure distribution at the section of critical depth (the upstream boundary of the control volume) is hydrostatic.

3. The pressure distribution at the end section is a quadratic parabola with a peak pressure head of (ky) where (k) is the pressure factor and (y) the depth. This assumption follows from measurements of the pressure distribution at the overfall of non-trapezoidal channels by Fathy and Shaarawi (1954) and Replogle (1962). In fact, these measurements showed a slightly skewed parabolic shape for the pressure

distribution. However, Fong (1982) has shown that the error involved in assuming a quadratic parabolic shape is negligible.

4. The momentum coefficient, β, has the value of unity. The validity of this assumption has been demonstrated by Replogle (1962).

5. Shear forces arising from contact of the moving water with the channel boundaries are negligible. This assumption follows from the short length of the control volume and the large differential between the pressure forces at the upstream and downstream ends of the control volume.

Since the shear forces (5) and the weight component (1) act in opposite directions, even if not entirely negligible, they tend to cancel each other out.[10]

By using the previous assumptions and applying the momentum equation on the control volume between section (1) and (2) as in Fig. (3.1), we obtain:

$$m_{in} - m_{out} = \frac{dm_{cv}}{dt} \tag{3.1}$$

$$Q\ \rho\ (V_b - V_c) = F_c - F_b \tag{3.2}$$

Where:

Q: is the discharge, ρ: the mass density of fluid, V: the mean velocity, F: the pressure force, c and b are the critical and brink (end) section respectively.

Substituting the pressure forces F_c and F_b in equation (3.2) we obtain:

$$F_c = \gamma(A\bar{y}_c)_c \tag{3.3}$$

$$F_b = K\gamma(A\bar{y}_b)_b \tag{3.4}$$

Where:

K: the pressure coefficient, γ: the specific weight of fluid, A: the cross-sectional area, $\bar{y}$: the depth from the water surface to the centroid of cross-sectional area.

By substituting equations (3.3) and (3.4) in equation (3.2) and by using ($V = {}^{Q}/_{A}$) and ($\gamma = \rho g$) and re-arranging equation (3.2), see appendix A, we obtain:

$$\frac{Q^2}{g}\left[\frac{1}{A_b} - \frac{1}{A_c}\right] = (A\bar{y})_c - K(A\bar{y})_b \tag{3.5}$$

Where: g: gravity acceleration.

3.4 The Relationship of Brink Depth with The Channel Discharge

Theoretical and laboratory investigations showed a relationship between the flow rate and depth at the channel's free overfall. Therefore, free overfall can be used as a device for measuring discharge in addition to its main function. The relationship between discharge and critical depth can be written as follows:

$$\frac{Q^2}{g} = \frac{A_c^3}{T_c} \tag{3.6}$$

T_c: the top width of water.

Substituting equation (3.6) in equation (3.5) and re-arranging it, see appendix A, we obtain:

$$\frac{A_c}{T_c}\left[\frac{A_c^2}{A_b} - A_c\right] = (A\bar{y})_c - K(A\bar{y})_b \tag{3.7}$$

3.5 Pressure Coefficient Distribution at The Brink

The coefficient of pressure distribution (K) can be calculated by using equation (3.7), where the beginning of the final depth pressure coefficient was found through (Replogle,1962) investigations, and as indicated by (Keller and Fong,1989), for both the triangular and rectangular channels. According to (Replogle) investigations, the pressure coefficient values (K_{equiv}) for the triangular (90^o) and rectangular channels (K_t = 0.175) and (K_t = 0.215) respectively, [10] where:

$$K = \frac{4}{3} K_{equiv} \tag{3.8}$$

(Beirami et al.,2006) mentioned that the pressure coefficient for rectangular, triangular and exponential channels is (K = 0.3033, 0.3558, 0.3366).[11] An equation has been derived to find the pressure coefficient for the semicircular channels as shown in Appendix (A).

3.6 The Critical Depth in Semicircular Channels

Critical depth represents the water depth at critical flow, the state in which the flow is divided into two types: supercritical flow and subcritical flow, the state of critical flow through the channel is related to several important conditions:

1. The specific energy and specific forces should be minimal for the flowing discharge.
2. Froude number should be equal to one.
3. The discharge should be the highest value at the critical flow of the given specific energy.
4. The velocity head should be equal to half the hydraulic depth of the low slope channel.
5. The flow is unstable at critical condition.

The critical depth depends on the rate of discharge and the geometry of the channel. [29] Equation (3.6) represents a general form of the critical flow state. In the semicircular channels, the values of the variables (A) and (T) are as follows:

$$A_c = A_w = \pi r^2 \frac{2\Theta}{360} - (r^2 \, Sin\, \Theta \, Cos\, \Theta) \quad (3.9)$$

$$T_c = \mathrm{T} = 2\ \mathrm{r}\ \mathrm{Sin}\ \Theta \quad (3.10)$$

When substituting these variables in Froude no. equation and for the critical flow state and after re-arranging it as in Appendix (A), the following equation is produced:

$$y_c = \mathrm{r}\,(1 - \mathrm{Cos}\,\Theta) \quad (3.11)$$

In our case of study, the critical depth values for different discharge situations were found using the above equation.

3.7 Dimensional Analysis

The dimensional analysis is a mathematical method used to create a functional relationship between a number of physical variables (dependent and non-dependent variables) and reduce them to the lowest number of variables or non-dimensional relations, [30,31] It is particularly useful for:

1. Presenting and interpreting experimental data.

2. Attacking problems not amenable to a direct theoretical solution.
3. Checking equations.
4. Establishing the relative importance of particular physical phenomena.
5. Physical modelling.
6. Reduction in variables:

   $F = (C_1, C_2, \ldots, C_n) = 0$, C_i= dimensional variables

   $f = \Pi_1, \Pi_2, \ldots, \Pi_{r<n} = 0$, Π_i = non-dimensional parameters
7. Helps in understanding physics.
8. Useful in data analysis and modeling.
9. Fundamental to concepts of similarity and model testing.

3.7.1 Dimensions and Units

Dimension is a measure or a tool used to describe the physical quantity. **Unit** is a mean or a way to assign a number to that quantity. The main systems of units are:

1. C.G.S. system [centimeter (cm); gram (g) and second (s)].
2. F.P.S system [foot; pound; second].
3. M.K.S. system [meter; kilogram; second].
4. S.I. (system of international).

In 1971 the international Bureau of weight and measures held its meeting and decided a system of units. Which is known as the international system of units.[30,31,32,33] The Scottish physicist and philosopher (Maxwell) used the following letters:

(F) for force, (M) for mass, (L) for length, (T) for time and (θ) for temperature, the dimensions are named on the results of multiplying these letters and they raised to the power. Maxwell believes the importance of these dimensions in the presence of similarities between different branches of physics such as mechanics, electricity and heat. These dimensions have acquired more physical and mathematical significance than their philosophical significance. The unit quantifies concludes from the definitions, links and physical laws. For example, according to Newton's law, force is ($F = ma$), the mass multiply by acceleration and the sum of the mass unit multiply by the acceleration unit $[M]X\left[\frac{L}{T^2}\right]$, we obtain the unit of force $\left[\frac{ML}{T^2}\right]$, as well as write $[MLT^{-2}]$. There is no evidence that two different systems of dimensions need to be used, such as the mass system $[M]$ and the force system$[F]$.[33] Dimensional

homogeneity is a useful tool for checking formulae. For this reason, it is useful when analyzing a physical problem to retain algebraic symbols for as long as possible, only substituting numbers right at the end.

3.7.2 Buckingham's Pi Theorem

Experienced practitioners can do dimensional analysis by inspection. However, the formal tool which they are unconsciously using is Buckingham's Pi Theorem.

"If an equation or problem involves **n dimensional variables**, it can be reduced to a relation between only **r dimensionless variables** or **Π's**.

The **reduction, m = n − r**, equals the maximum number of variables that do not form a pi among themselves and is always **less than or equal to the number of dimensions** describing the variables." this is called the (Buckingham pi theorem).[30,31,33] where :

n = Number of dimensional variables.

m = Minimum number of dimensions to describe the variables.

r = n − m = Number of non-dimensional variables.

3.7.3 Methods for Determining Π's

1. Functional relationship method

a. Inspection (Intuition) method.

b. Exponent method (Also called as the method of repeating variables).

c. Step-by-step method.

2. Non-dimensionalize governing differential equations (GDE's) and initial (IC) and boundary (BC) conditions.

3.7.4 Determination of Pi Terms

3.7.4.1 Method of Repeating Variables

1. List all the variables that are involved in the problem. Geometry of the system (such as pipe diameter), Fluid properties (ρ, μ) External effects (driving pressure, V) It is important that all variables be independent.
2. Express each of the variables in terms of basic dimensions. (choose suitable system of dimensions (MLT) or (FLT)).

   $F = ma = MLT^{-2}$

   $M = \frac{F}{LT^{-2}}$ so: $\rho = ML^{-3} = FL^{-4}T^{2}$
3. Determine the required member of pi terms. Buckingham pi theorem:

   n: variables.

   m: reference dimensions (M, L, T, or θ).

   n – m: independent dimensionless groups.
4. Select a number of repeating variables, where the number required is equal to the number of reference dimensions.

Notes:

a. Each repeating variable must be dimensionally independent of the others.

b. Do not choose the dependent variable (e.g., Δp) as one of the repeating variables.

5. Form a pi form by multiplying one of the nonrepeating variables by the product of the repeating variables, each raised to an exponent that will make the combination dimensionless. like:

   u_i, $u^a{}_1$, $u^b{}_2$, $u^c{}_3$, where:

   u_i: non-repeating variable.

   $u^a{}_1$, $u^b{}_2$, $u^c{}_3$: repeating variables.
6. Repeat Step 5 for each of the remaining non-repeating variables.
7. Check all the resulting pi terms to make sure they are dimensionless.
8. Express the final form as a relationship among the pi terms, and think about what it means.

   $\Pi_1 = \phi(\Pi_2, \Pi_3, \ldots . \Pi_{n-m})$

the dimensional analysis had been Performed by using the (Buckingham's Pi-theory) for the purpose of demonstrating the real correlation between the variables**.**

The variables used in the dimensional analysis were chosen to represent the cases of the laboratory experiments. Therefore, the variables for the discharge of the semicircular channel with free overfall are expected to be the function of the following variables:

$$Q = f(V, D, y_b, \rho, \mu, g, S, n) \tag{3.12}$$

Where: Q: the mean discharge (L^3T^{-1}), V: the flow mean velocity (LT^{-1}), y_b: the depth of flow at the end of the channel (brink) (L), D: the channel diameter (L), μ: the water viscosity ($ML^{-1}T^{-1}$), ρ: the mass density of water ($M\ L^{-3}$), g: the gravity acceleration (LT^{-2}), S: longitudinal slope of the channel, n: The Manning roughness coefficient of channel bed ($L^{-1/3}$ T).

(n) was assumed as a dimensionless, according to (Chow,1959). After the order of equation (3.12) becomes as follows:

$$f_1(Q, V, D, y_b, \rho, \mu, g, S, n) = constat \tag{3.13}$$

Using the Buckingham theory and choosing (V, D and ρ) as frequent variables, equation (3.13) becomes as follows:

$$f_2\left(\frac{Q}{V\,D^2}, \frac{y_b}{D}, \frac{\mu}{\rho\,VD}, \frac{gD}{V^2}, S, n\right) = constant \tag{3.14}$$

Where

$$R_e = \frac{\rho VD}{\mu} \tag{3.15}$$

R_e: Reynolds number

equation (3.14) can be written as follow:

$$f_3\left(\frac{Q}{V\,D^2}, \frac{y_b}{D}, R_e, \frac{gD}{V^2}, S, n\right) = 0 \tag{3.16}$$

According to (Chow,1959), the flow in the channels is disturbed and the viscosity strength is relatively weak for the internal forces. Therefore, the current flow assumption in the current study does not depend on Reynold's number. It can be

ignored, Re-ordering equation (3.16) and using mathematical operations for obtaining new dimensionless parameters, yields:

$$\frac{Q}{\sqrt{g\,D^5}} = f_4\left(\frac{y_b}{D}, S, n\right) \tag{3.17}$$

3.8 Statistical Analysis

For the purpose of understanding the correlation between data or information and how to distribute it and to create a relationship between variables, statistical analysis of the data obtained in the field or laboratory is used. Based on the results of the statistical analysis, decisions or judgments are made regarding a particular case. The information or data obtained is generally classified into two types:

1.Dependent Variable: The variable that is being predicted or estimated.

2.Independent Variable: A variable that is provides the basis for estimation.it is the predictor variable.

Among the methods of statistical analysis:

3.8.1 Correlation Analysis

Correlation analysis is a group of techniques used to measure the strength of the association between two variables. The usual first step is to plot the data in a scatter diagram. **Scatter diagram** is a chart that portrays the relationship between two variables. To develop this diagram, we need to draw two axes horizontal and vertical and scale the dependent variable on the vertical or (y-axis), and the independent variable on the horizontal or (x-axis). Note that while there appears to be a positive relationship between the two variables, all the points do not fall on a straight line. The strength and direction of this relationship between two variables will measure by determining the coefficient of correlation.[34,35]

3.8.1.1 Coefficient of Correlation

The coefficient of correlation describes the strength of the relationship between two sets of interval-scaled or ratio-scaled variables. Designated (r), it is often referred to as Pearson's (r). It can assume any value from (- 1.00) to (+ 1.00) inclusive. A correlation coefficient of (- 1.00) or (+1.00) indicates perfect correlation. A computed value of

(+1.00) reveals that the independent variable (X) and the dependent variable (Y) are perfectly related in a positive linear way. The same way if a computed value of (-1.00) reveals that the independent variable (X) and the dependent variable (Y) are perfectly related in a negative linear way. The scatter diagram would appear as in fig. (3.2) if the relationship between the two sets of data were linear and perfect.[34,35]

If there is no relationship between the two sets of variables, Person's (r) will be zero and the relationship will be quite weak. Fig. (3.3) and Fig. (3.4) showing zero, weak and strong correlation and the strength and direction of the coefficient of correlation respectively. The strength of the correlation does not depend on the direction (either + or -). To determine the numerical value of the coefficient of correlation, we use the following formula. The formula for (r) is:

$$r = \frac{n(\sum XY) - (\sum X)(\sum Y)}{\sqrt{[n(\sum X^2) - (\sum X)^2][n(\sum Y^2) - (\sum Y)^2]}} \qquad (3.18)$$

Where: n: the number of paired observations, ($\sum$ X): is the X variable summed, ($\sum$ Y): is the Y variable summed, ($\sum$ X^2): is the X variable squared and the squares summed, ($\sum$ $X)^2$: is the X variable summed and the sum squared, ($\sum$ Y^2): is the Y variable squared and the squares summed, ($\sum$ $Y)^2$: is the Y variable summed and the sum squared ,$\sum$ XY: is the sum of the products of X and Y.

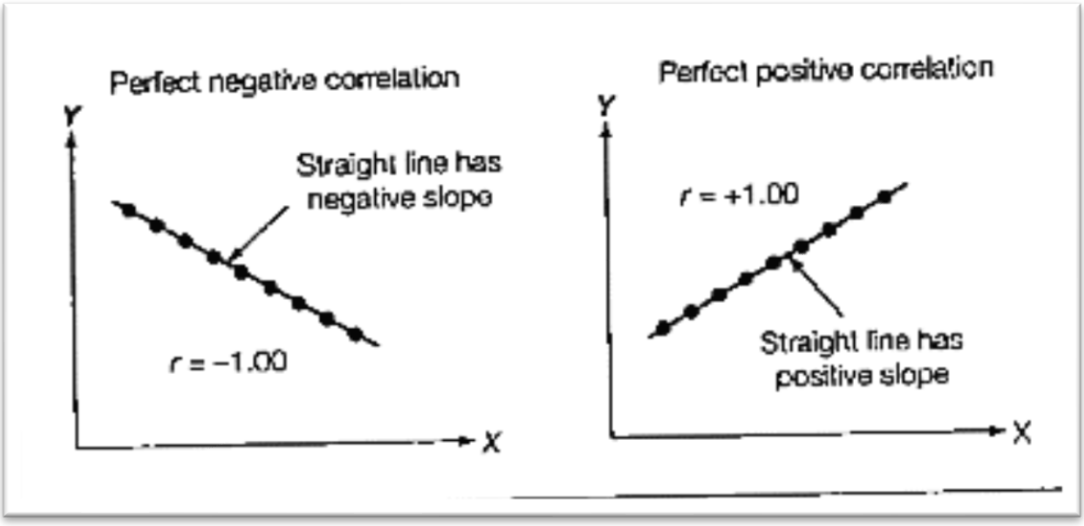

Figure 3.2 Scatter Diagram showing Perfect Negative Correlation and Perfect Positive Correlation

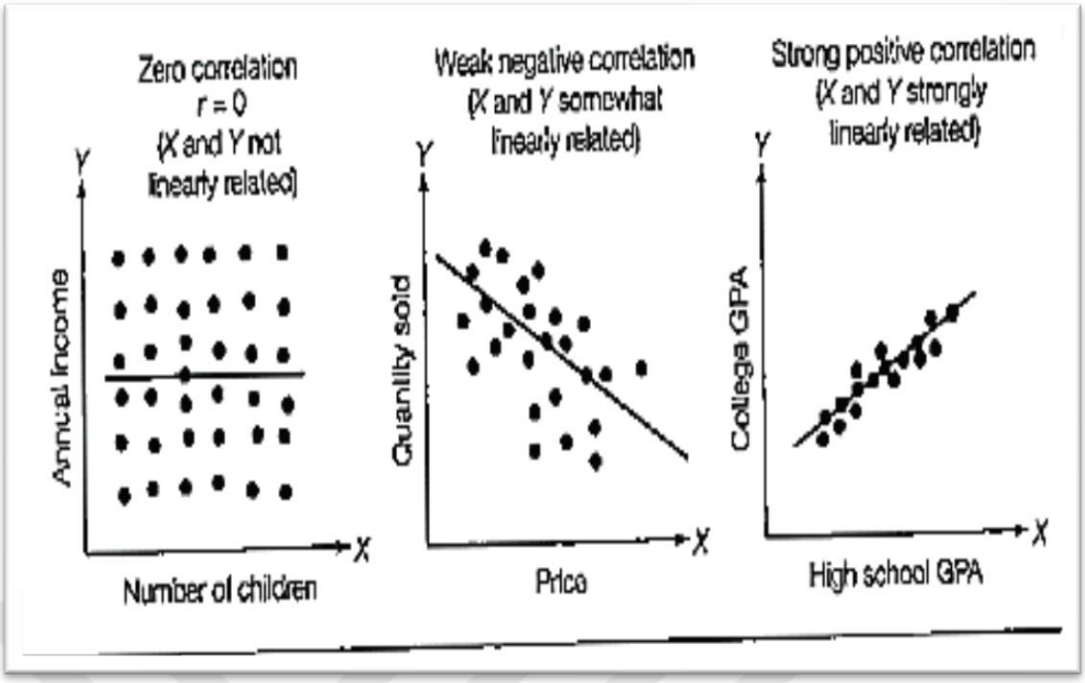

Figure 3.3 Scatter Diagram showing Zero, Weak and Strong Correlation

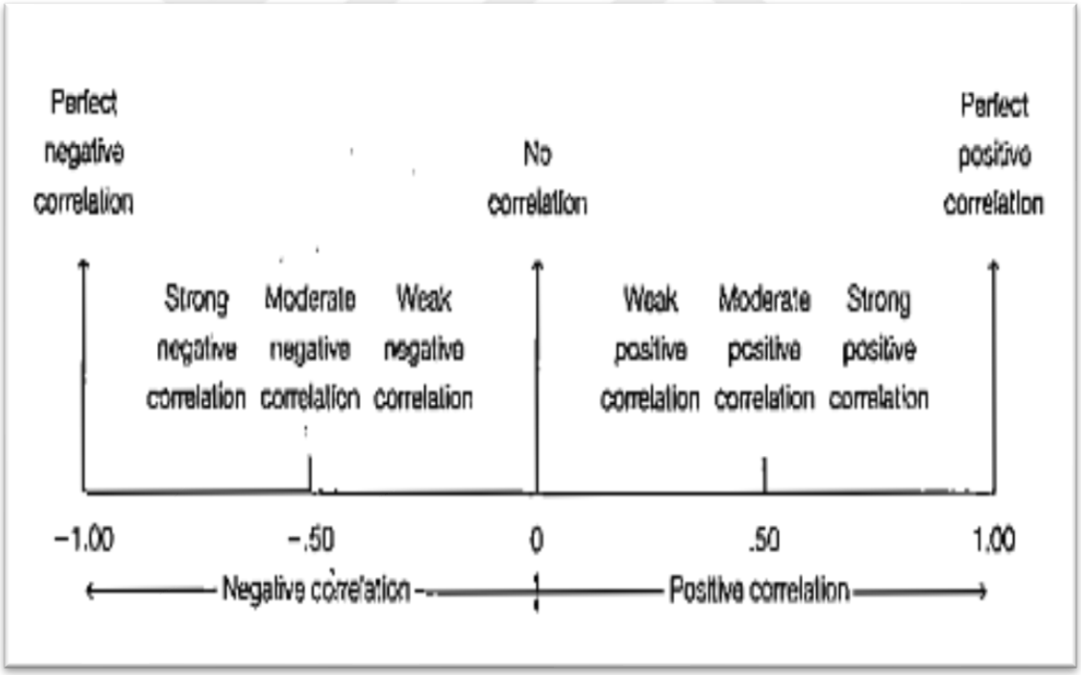

Figure 3.4 The Strength and Direction of The Coefficient of Correlation

3.8.1.2 Coefficient of Determination

Coefficient of determination is the proportion of the total variation in the dependent variable (Y) that is explained, or accounted for, by the variation in the independent variable (X). It is computed by squaring the coefficient of correlation and denoted by (R^2).

3.8.2 Regression Analysis

Regression analysis is a statistical tool that constructs a statistical model to estimate the relationship between one quantitative variable or several quantitative variables, which is the independent variables, so that it produces a statistical equation showing the relationship between the variables. This equation can be used to determine the type of relationship between variables and estimate the dependent variable using other variables. When the relationship in the statistical model is between one dependent variable and one independent variable, this model is the simplest regression model called the linear or simple model (Simple Linear Regression). When the independent variables are more than one quantitative variable, the model is called the multiple regression model. [34,35]

The general form of the regression equation is:

$$\acute{Y} = a + bX \tag{3.19}$$

Where: $\acute{Y}$: is the predicted value of the (Y) variable for a selected (X) value, a: is the Y-intercept.it is the estimated value of (Y) when (X = 0). another way to put it is: (a) is the estimated value of (Y) when the regression line crosses the Y-axis when (X) is zero, b: is the slope of the line, or the average change in $\acute{Y}$ for each change of one unit (either increase or decrease) in the independent variable (X), X: is any value of the independent variable that is selected.

The formulas for (b) and (a) are:

$$b = \frac{n(\sum XY) - (\sum X)(\sum Y)}{n(\sum X^2) - (\sum X)^2} \quad \text{(Slope of Regression line)} \tag{3.20}$$

$$a = \frac{\sum Y}{n} - b\,\frac{\sum X}{n} \quad \text{(Y-axis intercept)} \tag{3.21}$$

X: is a value of the independent variable, Y: is a value of the dependent variable, n: is the number of items in the sample. We can do the statistical analysis by using equations or by using programs like (Excel) or (SPSS).

CHAPTER 4

LABORATORY EQUIPMENTS, LABORATORY WORK

4.1 Introduction

This chapter includes a detailed presentation of laboratory experiments, laboratory work, specifications and characteristics of the free overfall of the semi-circular channels used in this study. Laboratory experiments were carried out in the Hydraulics Laboratory of the Civil Engineering Department of Gaziantep University, Laboratory work was carried out to demonstrate the impact of roughness and bottom slope of different models of the channel. Laboratory work was divided into a series of experiments for each model used, the following paragraphs describe the equipment's, laboratory models used and descriptions of laboratory work.

4.2 Laboratory Channel

The main laboratory channel used in the experiments is a rectangular channel consisting of several parts connected to each other to be an integrated system gives the form and properties necessary for laboratory experiments, figures (4.1), (4.2), (4.3), (4.4), (4.5) illustrate the laboratory channel used, below is a detailed presentation of each part of the channel:

4.2.1 The Main Structure

The structure of the channel consists of an iron base with a width of (0.8 m) and two walls of transparent glass thickness of (1 cm). These walls are installed with iron supports at (95 cm) between one and the other. At the top of the wall, along the length of the channel, there is an iron threshold in the shape of a letter (L), which is fixed by welding to the iron supports on which the transparent walls are placed. These two iron thresholds are used to obtain walls strength and straightening of the channel. It can also be used as a pouch to facilitate the operation of the point gauge.

The length of the channel is (9 m) and a depth of (1 m) and connected at the beginning and end with two tanks. also, there are two iron gates at the beginning and the end of the channel, they can be moved to the top and bottom and they are with dimensions (0.8 m width, 1m depth) for the purpose of controlling the strength of water and calm before entering the channel also maintain a fixed level of water in the channel. A model of semicircular free overfalls channel have been built and tested in the laboratory flume. This model had (2 m length and 0.775 m width with 0.50 m height with semicircular cross section of 0.15 m radius (half of plastic pipe)). The free overfall channel having bottom and side walls made of transparent (8mm) glass, with three supports inside to carry and support the channel section. The main flume is horizontal, so during the experiments three pieces of glass with (10 mm) thickness used to get the desired slope value for each set of experiments.

4.2.2 The Inlet and Outlet Tanks

4.2.2.1 Tank (1)

It is an iron tank with dimensions of (length 1.3m, depth 1.5 m and width 0.8 m) receiving the water from the electric pump with a tube measuring (53.5 cm) and then enters the channel for the purpose of conducting the necessary tests. This tank contains a water discharge valve.

4.2.2.2 Tank (2)

It is an iron tank with a dimension of (length 1.3m, depth 1.5 m and width 0.8 m) works on the collection of water out of the channel after the end of the experiments and then drain it through two drainage tubes measuring (67 cm) to the drainage trench by a main hole with dimensions of (0.5 m length, 0.5 m width and 0.6 m depth).

4.2.3 Sedimentation Tank

It is an underground concrete tank with a dimension of (1.6 m length,1.6 m width and 1 m depth) connected to the main channel by a discharge trench and receives water from tank (2) and transfers it to the main reservoir. This tank collects the water from the channel and depositing the existing sediment or which comes with the water because it contains on a filter in the exit hole of the water to the main reservoir.

4.2.4 Main Water Tank (Reservoir)

It is a large underground concrete tank containing the water needed for experiments, water is stored in it from the main city network and the water is drawn from it by an electric pump.

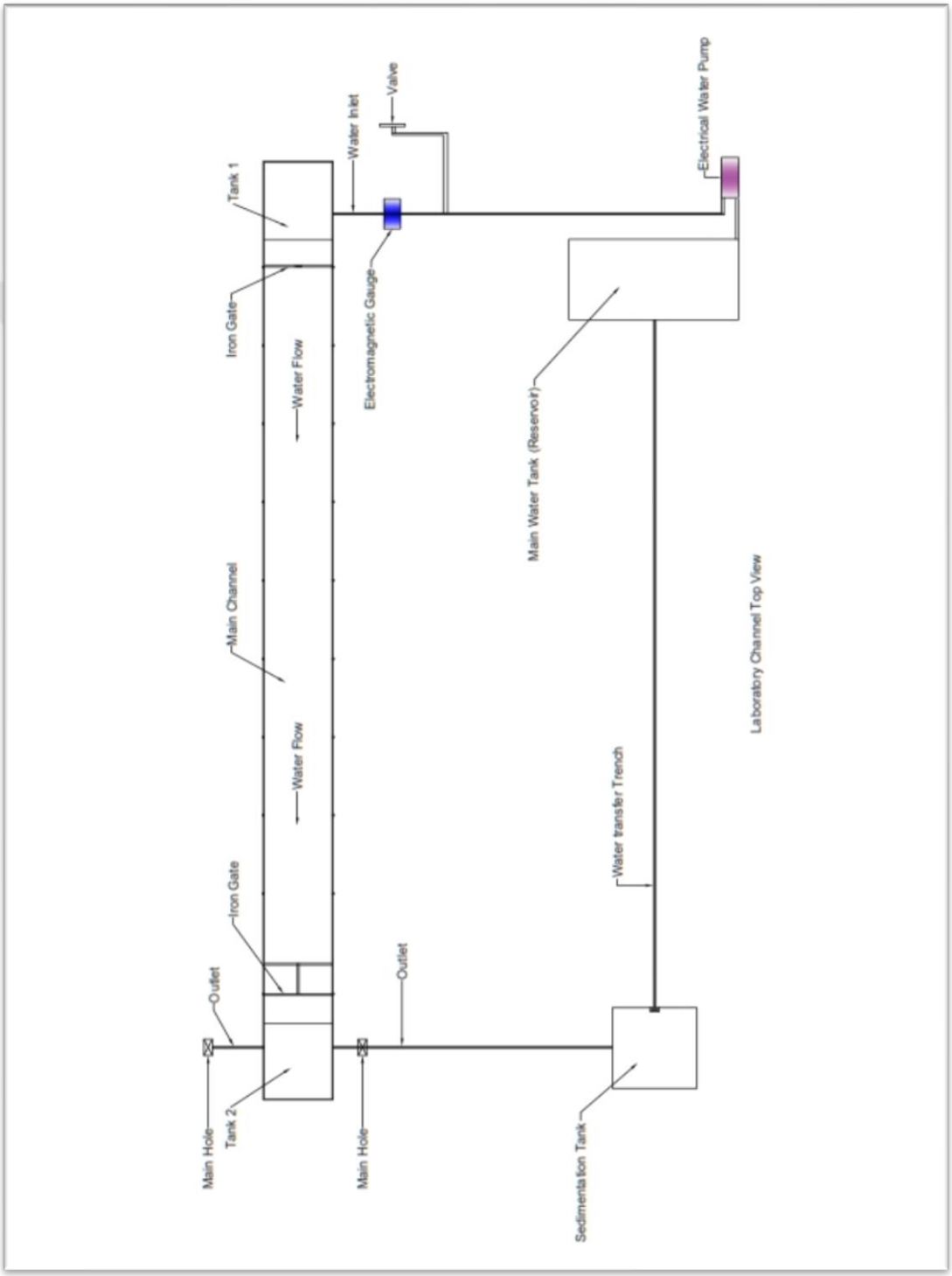

Figure 4.1 Laboratory channel top view

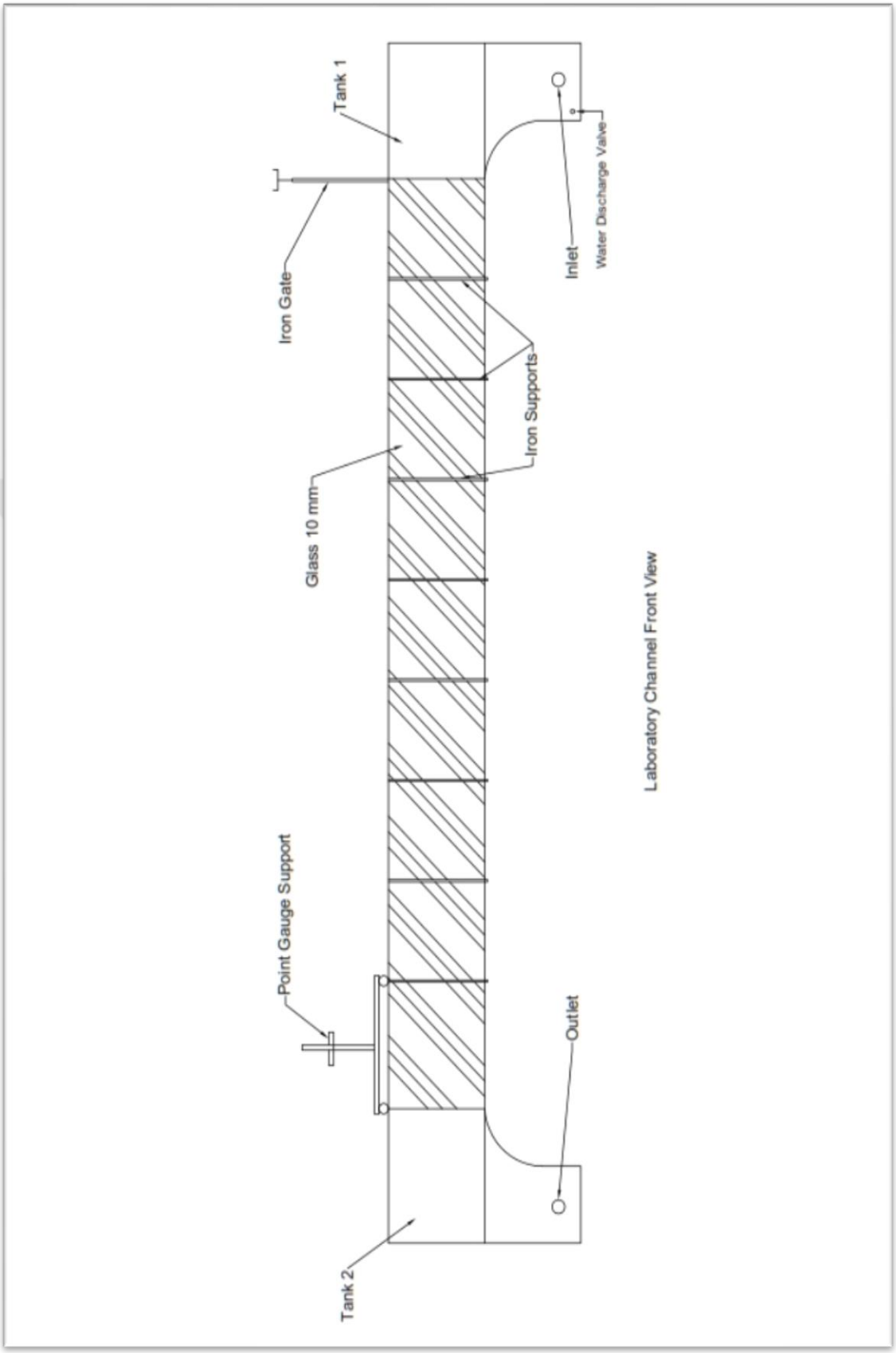

Figure 4.2 Laboratory channel front view

Figure 4.3 Laboratory channel view (1)

Figure 4.4 Laboratory channel view (2)

Figure 4.5 Laboratory channel view (3)

4.2.5 The Electrical Pump

A three-phase electrical water pump type (WAT) with the following specifications:

(Q = 350 m^3/hr, H = 14 m, P = 18.5 KW, n = 1450 rpm, TP: SNT 150 ~ 250)

Works to pull up water from the main water tank by a (70 cm) tube and pumping water to the channel with a (53.5 cm) tube.

4.2.6 Electromagnetic Gauge

The system contains a valve to control the amount of water to be used in the channel as needed, where the quantity passed by the discharge meter is read which is called (Electromagnetic gauge), this device reads the amount of discharge passing by units (m^3/hr) and is a very accurate electronic device.

4.2.7 The Point Gauge

An accurate electronic device to measure the amount of water passing through the channel having measuring accuracy of (0.10 mm), measuring the water height in the channel by a pointed metal needle by touching the surface of the water and the reading is determined by a metal lever in the right side of the device and then read the level required in (mm or inch) units, as in figures (4.6) and (4.7).

Figure 4.6 Point gauge view (1)

Figure 4.7 Point gauge view (2)

4.3 Depth Measurements

The water depth of the channel was measured during the laboratory experiments using the point gauge device. The depth was measured according to the type of bottom of the channel. The depth measurement in the channels can be divided into two types:

4.3.1 Depth Measurements in Soft Channels

The flow of water is regular through the bottom of the soft channels at the edge of the end, so the bottom level is taken directly as a reference to measure the depth of flow in the channel.

4.3.2 Depth Measurements in Rough Channels

The flow along the rough bottom is in fact irregular, as the depth constantly changes with the flow direction. For the purpose of bringing the flow state of such channels to the regular flow state, a regular elevation level is selected for the bottom of the channel.

(Schlichting,1937) presented his vision regarding the geometric level of the bottom, as all the roughness models were melted into a smooth surface and the level of that surface was used as a true measurement, [36] (Gordienko, 1967) concluded that the designed depth is higher than the depth above the top of the rough surface but smaller than the calculated depth of the lower bottom of the channel structure ($y_e < y < y_e + h$). In his experiments on the coarse channels with scattered regular roughness and with (L/h >1.414), [37] the design depth of the channel was as follows:

$$y = y_e + h - \frac{2\,h^3}{L^2} \qquad (4.1)$$

Where: y_e: The depth of flow measured from the top of the roughness elements, h: Roughness elements height, L: Longitudinal distance from center to center of roughness elements.

In the present study, the depth of flow was measured as in the fig.(4.8).[38] The geometric average of the bottom level was calculated as a true level to measure the normal depths at the front side of the edge place:

$$y = \frac{y_e+(y_e+h)}{2} = y_e + \frac{h}{2} \qquad (4.2)$$

4.4 Manning Roughness Coefficient

One of the biggest problems facing the hydraulic engineer is the calculation of the roughness coefficient for the calculations of the subsequent designs of the drainage quantity of the channel or river. The data for roughness is usually few or not available, especially in flood situations. Therefore, it is the hydraulic engineer work to estimate the roughness values of the river or the water stream or the channel and use it in the discharge calculations, which is used as a base in the calculations of other designs. The values of the Manning roughness coefficient adopted in this study are one of the main variables that are included in the calculations as they were completed on the basis of importance of the impact of the roughness on the flow behavior.

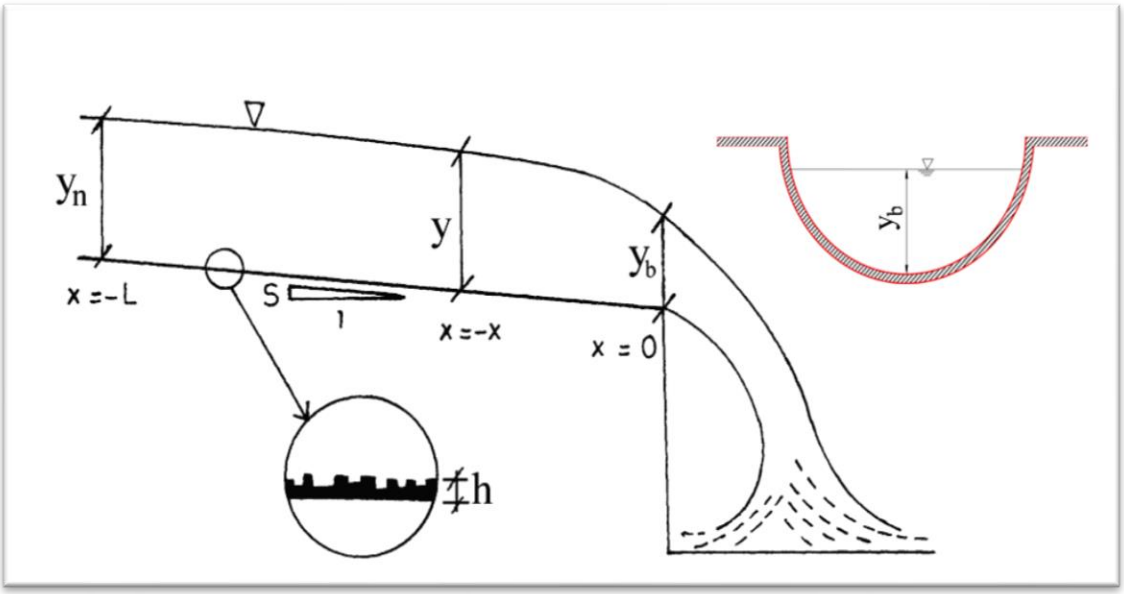

Figure 4.8 Depth Measurement in Semicircular Channels with Rough bottom

The Manning equation were used for the purpose of evaluating the correct values of the manning roughness coefficient based on the models of the roughness of the bottom, as follows:

$$V = \frac{k}{n} R^{2/3} S^{1/2} \tag{4.3}$$

Where: k: coefficient = 1 (if the equation (4.3) in SI units), k = 1.49 (if the equation (4.3) in English units)

the mean velocity in equation (4.3) can be found by using the continuity equation as follow:

$$Q = VA \tag{4.4}$$

By substituting equation (4.3) in equation (4.4) and re-arranging it we concluding:

$$n = \frac{kR^{2/3} S^{1/2} A}{Q} \tag{4.5}$$

Where: n: Manning roughness coefficient, Q: the discharge in (m^3/sec), V: the velocity in (m/sec), R: the hydraulic radius in (m). ($R = \frac{A}{P_w}$), A: the flow cross sectional area in (m^2), P_w: the wetted perimeter in (m), S: the slope of energy gradient line, where it taken parallel to the bottom of the channel at regular flow.

4.5 Samples Creating

A semicircular channel model was created for the free overfall and it had been used in the operational section of the rectangular laboratory channel, the channel model was designed with a dimension of (lemgth:2m, width:0.775m and height:0.5m). This model was manufactured using transparent glass thickness of (8 mm) and the parts of the model were connected using silicone as adhesive and to avoid any leakage of water during work. The use of transparent glass in the manufacturing of the channel model helped to provide visual vision. Gravel gradients were used as roughness models, steps to create the model can be summarized as follows:

4.5.1 Create Bottom Form

The bottom of the semicircular canal was made using a plastic tube of (30 cm) smooth from inside. This tube was cut into two equal halves. One of these halves was then used to simulate the shape of the semicircular channel and was connected to the transparent glass structure by using the silicon. The plastic pipe was installed parallel to the structure of the laboratory channel and at a height of (35 cm) from the bottom of the main canal structure to ensure that the free vertical fall at the end of the model will happen. Three transparent glass supports have been used and they putted at one third of the length of the test channel for each one to ensure the support and strength of the plastic pipe.as shown in fig. (4.9).

4.5.2 Bottom Roughness Creation

Three gradients of gravel were used to form the bottom roughness for each slope of the channel. In addition, the surface of the channel was used in its natural condition, without adding any roughness to the walls of the channel. That is, four types of roughness were used in this study.

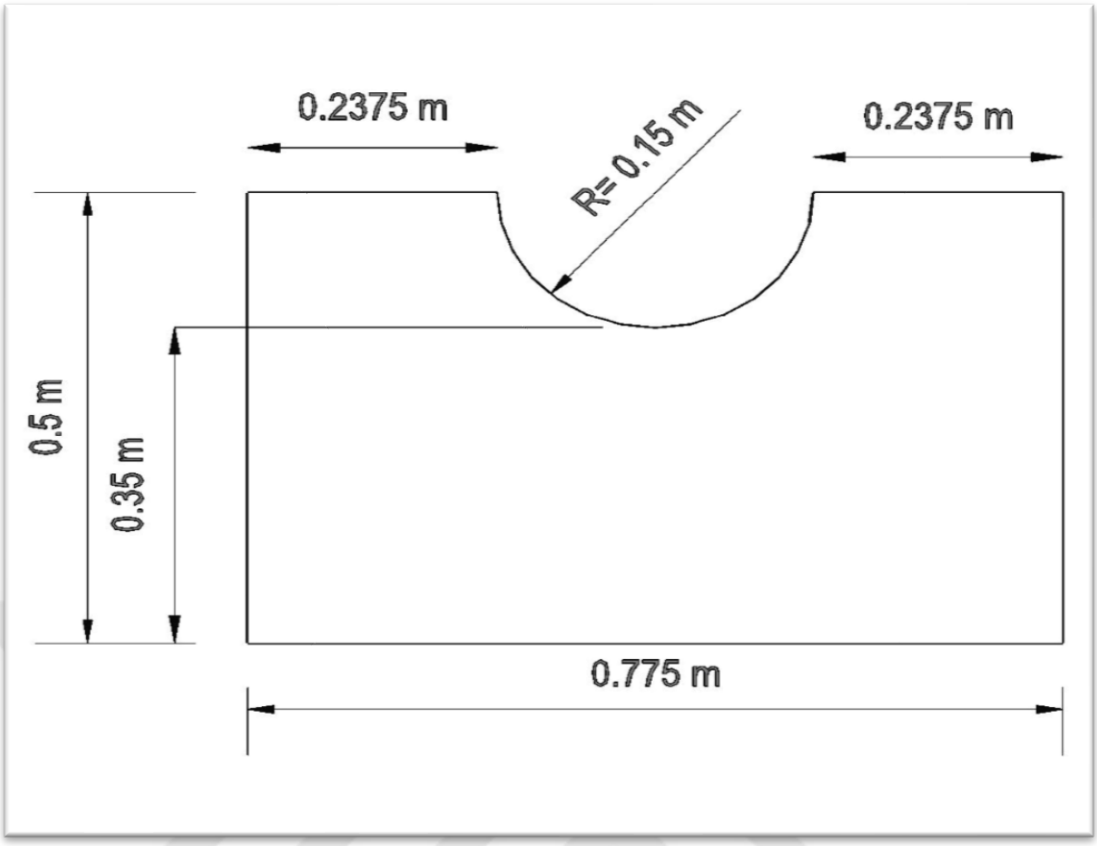

Figure 4.9 (a) Semicircular Channel Cross Section

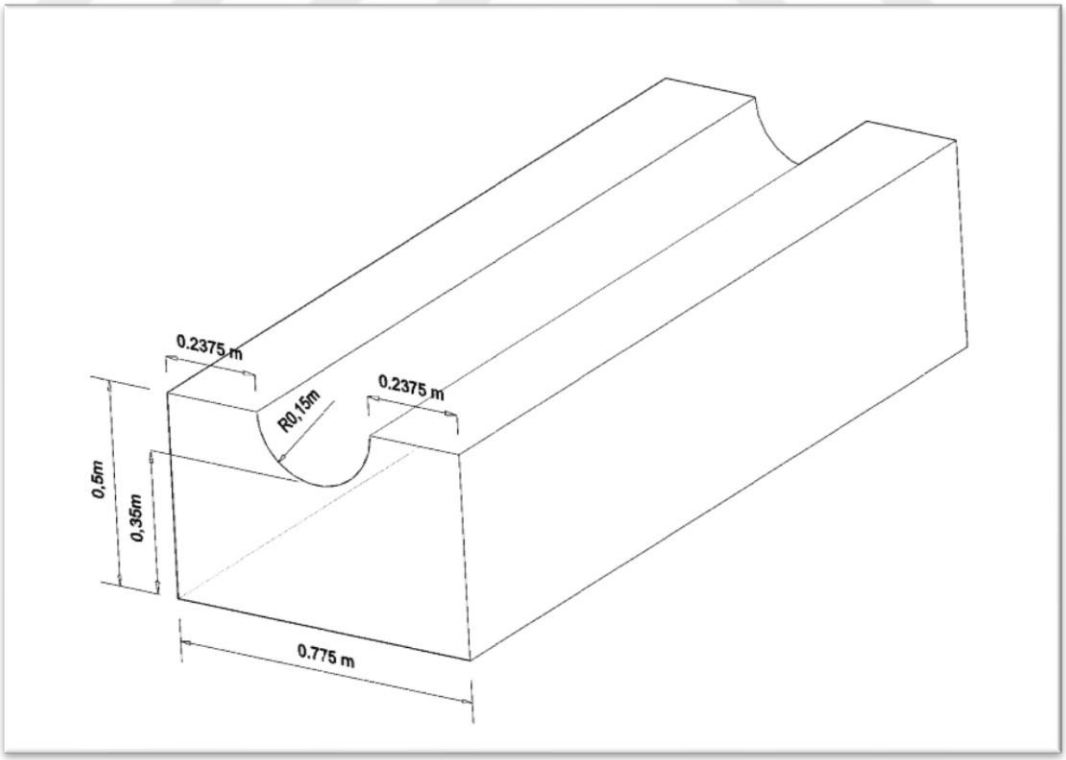

Figure 4.9 (b) Semicircular Channel (3D)

Figure 4.9 (c) Semicircular Channel (View 1)

Figure 4.9 (d) Semicircular Channel (View 2)

Figure 4.9 (e) Semicircular Channel (View 3)

Figure 4.9 (f) Semicircular Channel (View 4)

4.6 The Laboratory Program

In the present study, each experiment has a range of values for the depth of the edge, the normal depth and the discharge. The discharge has been measured directly by using the electromagnetic gauge instrument. Also, the depth of the edge was measured directly by using the point gauge instrument because the points and procedures were clear. However, because of the difficulty of finding the normal depth points, the data were collected for a number of points along the center of the bottom of the free fall channel and we take the average of it. The slope of the bottom and roughness of the channel had been changed during experiments.

The work and experiments of each model can be summarized by the following steps:

1. The longitudinal slope of the laboratory channel has been adjusted to zero. (S=0)
2. A semicircular channel was used with a zero-longitudinal slope and a soft bottom. The point gauge instrument was then adjusted to the bottom of the channel and zeroed to be a bottom reading of zero. Then, ten different discharges were carried out by controlling the valve next to the discharge measuring device (electromagnetic gauge) until the desired discharge value was reached. The depth values were recorded at the edge of the free over fall and the normal depth values of the water by recording a number of points along the center line of the channel bottom. For each experiment, the pump is operated for sufficient time to obtain stability for flow and then readings are taken.
3. The longitudinal slope of the bottom of the channel was changed three times using transparent glass pieces, each one (1 cm) thickness, placed below the channel, and then replaced by the following slope, two pieces are used, readings are taken and after the experiment done the slope is replaced and three pieces are placed down the channel and so on for each case, the same previous steps were repeated in the calculations of (Q, y_n, y_b) for each slope.
4. For the last slope used in previous experiments, the roughness of the bottom of the channel is changed. Gravel granules are used with ($d_s \geq 2$ mm) diameter. This represent the remaining size of gravel on the sieve of (2 mm) in size and the transition from (2.75 mm) sieve and this roughness is fixed using adhesive

paper to cover the bottom of the entire channel from start to finish. The roughness is then installed on the adhesive paper using adhesive material. Experiments are then carried out and steps (1 and 2) are repeated but in descending order, the channel slope changed from (S = 3/200) to (S = 0).

5. Two other types of roughness were used for the bottom of the channel using gravel granules with diameters of ($d_s \geq 4.75$ mm) and ($d_s \geq 6.33$ mm) and the previous steps are then repeated.
6. The total number of experiments conducted was (160) experiment.

Figs. (4.10), (4.11), (4.12), and (4.13) shows samples of soft and rough bottom experiments and fig. (4.14) show the roughness models used in the current study. The details of the laboratory work are presented in table (4.1).

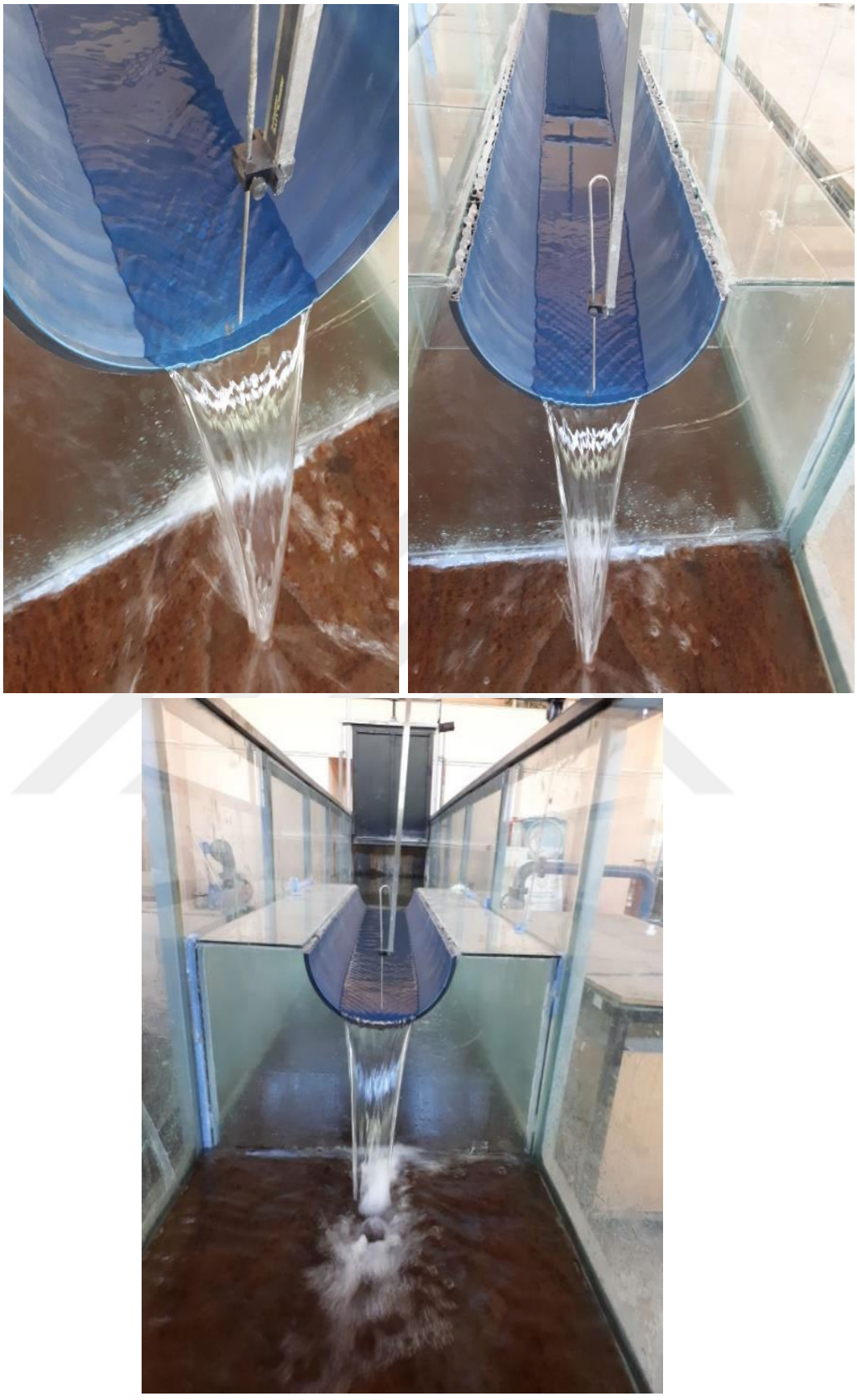

Figure 4.10 Free Overfall in Semicircular Channels with Smooth Bottom

Figure 4.11 Free Overfall in Semicircular Channels with (2 mm) Roughness on Bottom

Figure 4.12 Free Overfall in Semicircular Channels with (4.75 mm) Roughness on Bottom

Figure 4.13 Free Overfall in Semicircular Channels with (6.33 mm) Roughness on Bottom

Figure 4.14 The Roughness Types Used in Laboratory Experiments

Table 4.1 Details of Experiments on Free Overfall Channel Models During the Laboratory Program

No.	Bottom Slope (S)	Surface Condition	Roughness Diameter (mm) Size of Granules	Number of Experiments
1	0	Smooth	0	10
2	1/200	Smooth	0	10
3	2/200	Smooth	0	10
4	3/200	Smooth	0	10
5	0	Rough	2	10
6	1/200	Rough	2	10
7	2/200	Rough	2	10
8	3/200	Rough	2	10
9	0	Rough	4.75	10
10	1/200	Rough	4.75	10
11	2/200	Rough	4.75	10
12	3/200	Rough	4.75	10
13	0	Rough	6.33	10
14	1/200	Rough	6.33	10
15	2/200	Rough	6.33	10
16	3/200	Rough	6.33	10
Summation				160

CHAPTER 5

RESULTS AND CALCULATIONS

Introduction

The results of the laboratory program for the four models of free overfall semi-circular channels were analyzed by analyzing the details in this chapter, the different effects of the factors on the discharge measurement and the final depth ratio, and presented the various empirical equations to predict the discharge and by using limitations for the depth of the edge and the bottom slope of the soft bottom channels, while the coarse channels also included the bottom roughness, experimental results were represented and a common relationship was found and compared with the results of other researchers.

5.1 Results Analysis

The results of the semicircular free overfall channel shown in Appendix (B) were analyzed as found in the dimensional analysis of paragraph (3.7).

5.1.1 Manning Roughness Coefficient Values

The values of normal depth and discharge were found in each experiment, and then the values of Manning roughness coefficient were calculated using equation (4.5), where the only unknown in this equation is (n). A single mean value of (n) coefficient for each roughness model and different bottom slopes was found and classified in table (5.1). During the calculations we used the following formulas for the semicircular channel as follow:

$$A = \pi r^2 \frac{2\theta}{360} - \left(\frac{1}{2}(2X)(H)\right) \quad (5.1)$$

$$X = r\ sin\theta \quad (5.1.1)$$

$$H = r - y_n \quad (5.1.2)$$

$$Cos\ \Theta = \frac{H}{r} \quad (5.1.3)$$

$$P_w = 2\pi\, r\, \frac{2\Theta}{360} \quad (5.2)$$

$$R_h = \frac{A}{P_w} \quad (5.3)$$

y_n: normal water depth. (m), r: channel radius. (m)

see Appendix (A) for variables details.

The rate of change of Manning roughness coefficient (n) values was represented with the size of the gravel granules used as roughness for the channel (for particles diameters, $d_s \geq 2$ mm, 4.75 mm, 6.33 mm) as in Fig. (5.1).

Table 5.1 Manning Roughness Coefficient Values

Particles Size (mm)	**Channel Sample**					**Average (n)**
	C	**S_0**	**S_1**	**S_2**	**S_3**	
0	C_0	0	0.00871	0.009403	0.01011	0.007056
2	C_1	0	0.022001	0.026454	0.024507	0.01824
4.75	C_2	0	0.028441	0.032643	0.035982	0.024266
6.33	C_3	0	0.036681	0.042296	0.045866	0.031211

Where: C: semicircular channel sample according to roughness (C_0: with zero roughness, C_1: with 2 mm roughness, C_2: with 4.75 mm roughness, C_3: with 6.33 mm roughness), S: semicircular channel slope (S_0: zero slope, S_1: 1/200 slope, S_2: 2/200 slope, S_3:3/200 slope), n: roughness values for smooth and rough bed channels.

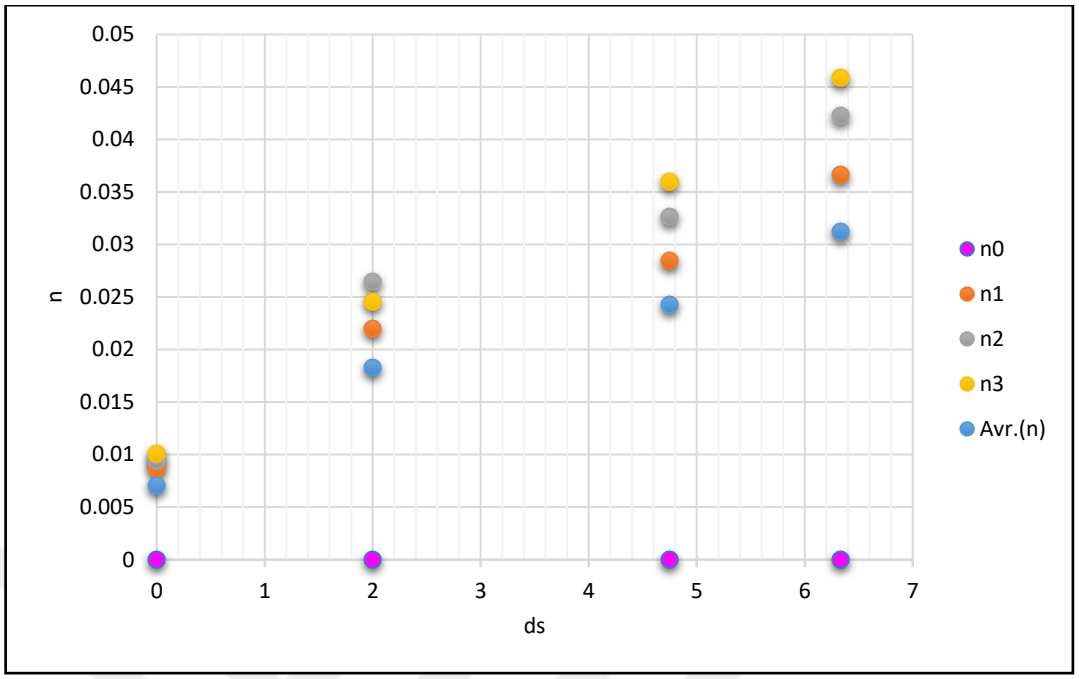

Figure 5.1 Manning Roughness Coefficient (n) Values

This figure showed the importance of understanding that the highest roughness appeared in the grain size (6.33 mm) of the forth model, where the value of Manning roughness coefficient (n) = 0.045866.

It is noted that the impact of roughness increases with the size of granules, and this is what many researchers and scientists are reached, such as (Ibrahim 2012), where they noticed that there are vortices between models of roughness.

5.1.2 Variation of ($\frac{Q}{\sqrt{g\,D^5}}$) with ($\frac{y_b}{D}$)

The variation of ($\frac{Q}{\sqrt{g\,D^5}}$) which represent the flow Froude No. in term of the final depth (F_{rb}) with ($\frac{y_b}{D}$) was studied for the channels of different slopes (0, 1/200, 2/200 and 3/200). The obtained results plotted in figures (5.2 to 5.21) and the relationship between the two variables is a simple power equation of the form:

$$\left(\frac{Q}{\sqrt{g\,D^5}}\right) = a_1\left(\frac{y_b}{D}\right)^{b_1} \qquad (5.4)$$

Where: a_1 and b_1 are constants.

From these figures we observe that the values of ($\frac{Q}{\sqrt{g\,D^5}}$) increase with the increase of ($\frac{y_b}{D}$) values. The values of the constants (a_1) and (b_1) and the corresponding values of the determination coefficient (R^2) had been found and arranged in table (5.2).

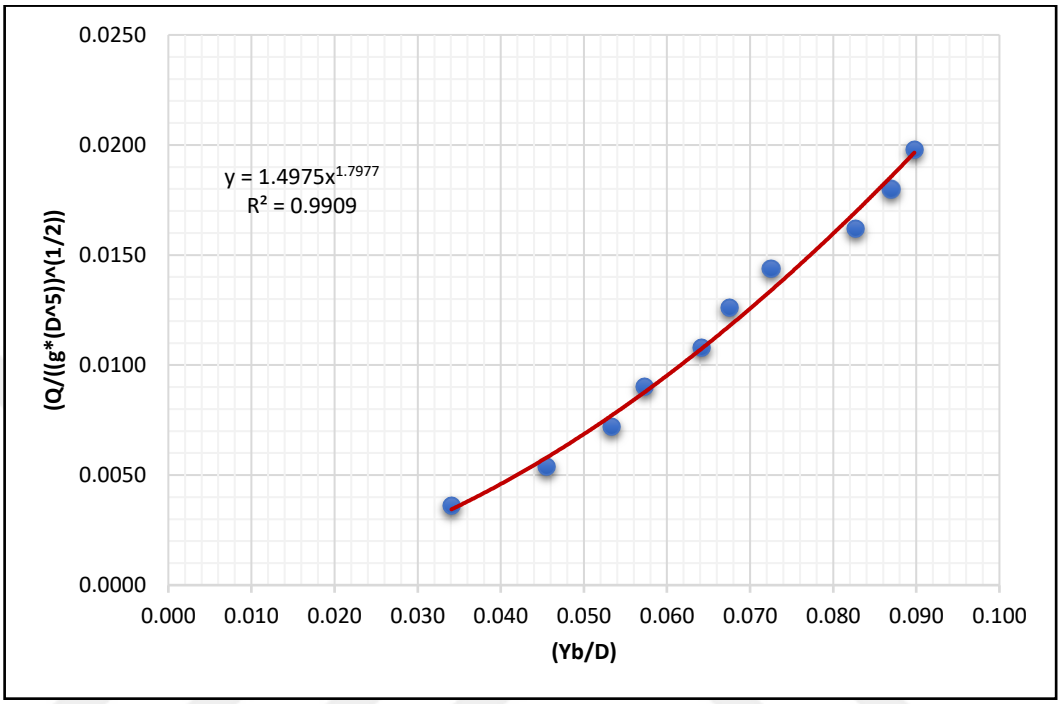

Figure 5.2 The Change of ($\frac{Q}{\sqrt{g\,D^5}}$) with ($\frac{y_b}{D}$) For Soft Bottom Channels (C_0) with Slope (S_0 = 0)

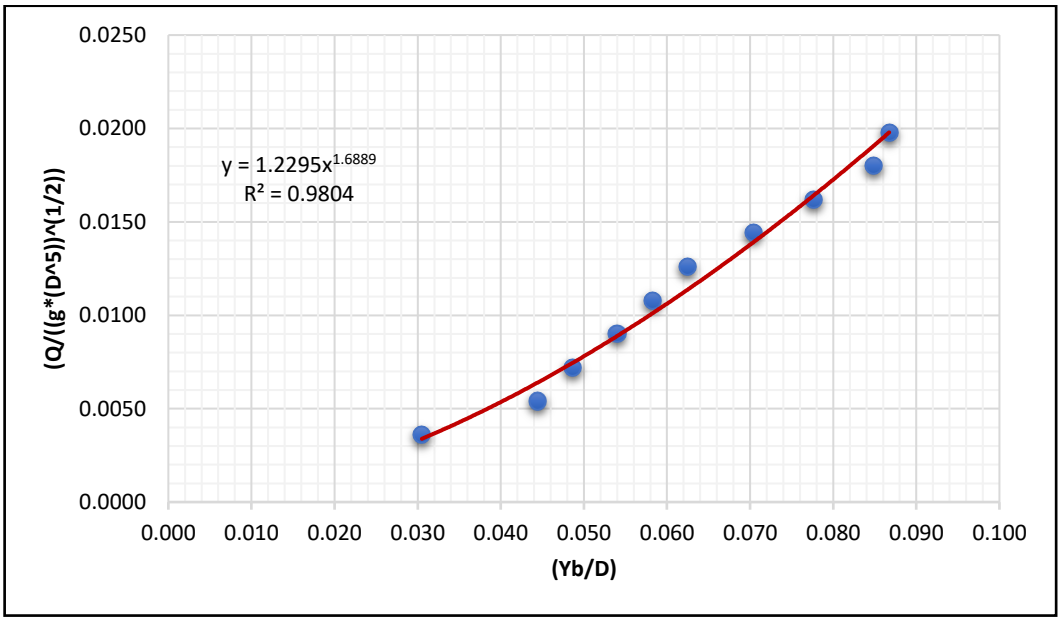

Figure 5.3 The Change of ($\frac{Q}{\sqrt{g\,D^5}}$) with ($\frac{y_b}{D}$) For Soft Bottom Channels (C_0) with Slope (S_1 = 0.005)

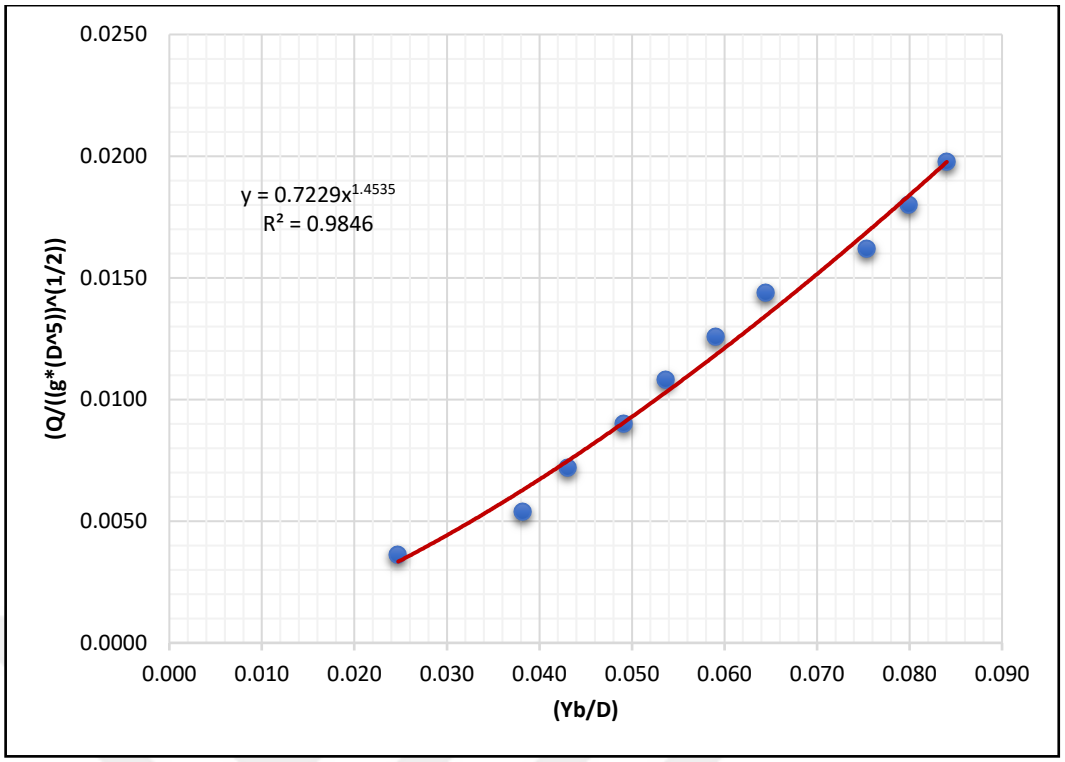

Figure 5.4 The Change of ($\frac{Q}{\sqrt{g\ D^5}}$) with ($\frac{y_b}{D}$) For Soft Bottom Channels (C_0) with Slope (S_2 = 0.01)

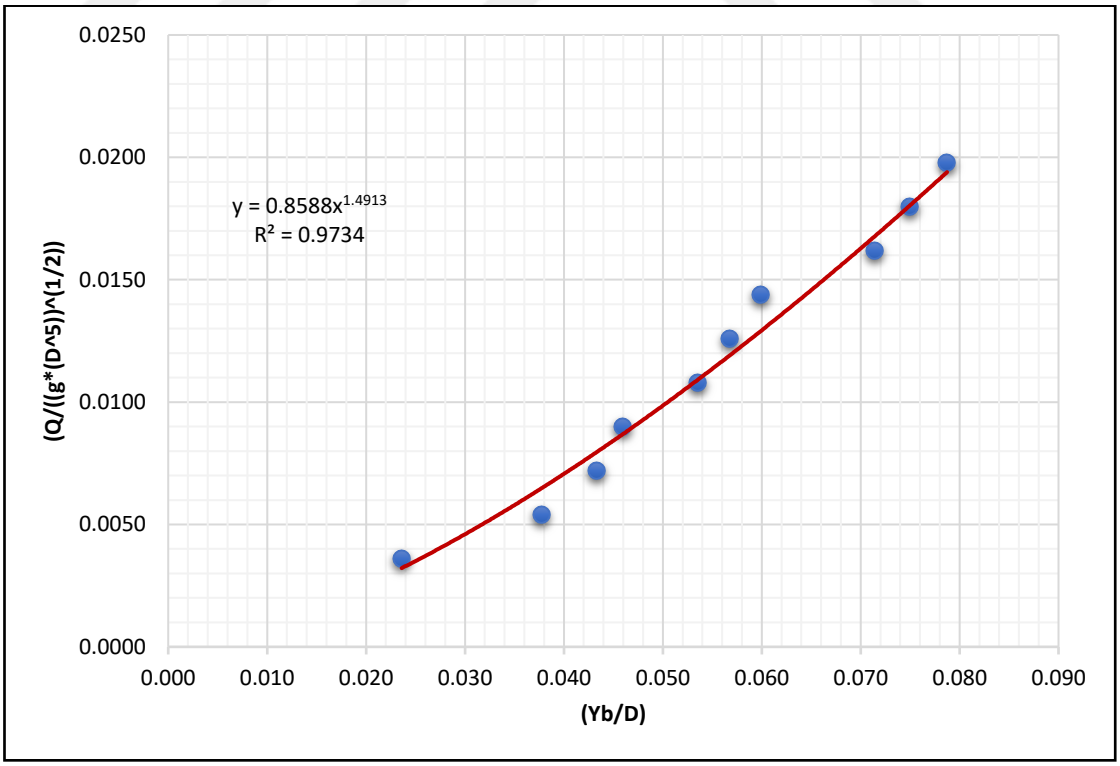

Figure 5.5 The Change of ($\frac{Q}{\sqrt{g\ D^5}}$) with ($\frac{y_b}{D}$) For Soft Bottom Channels (C_0) with Slope (S_3 = 0.015)

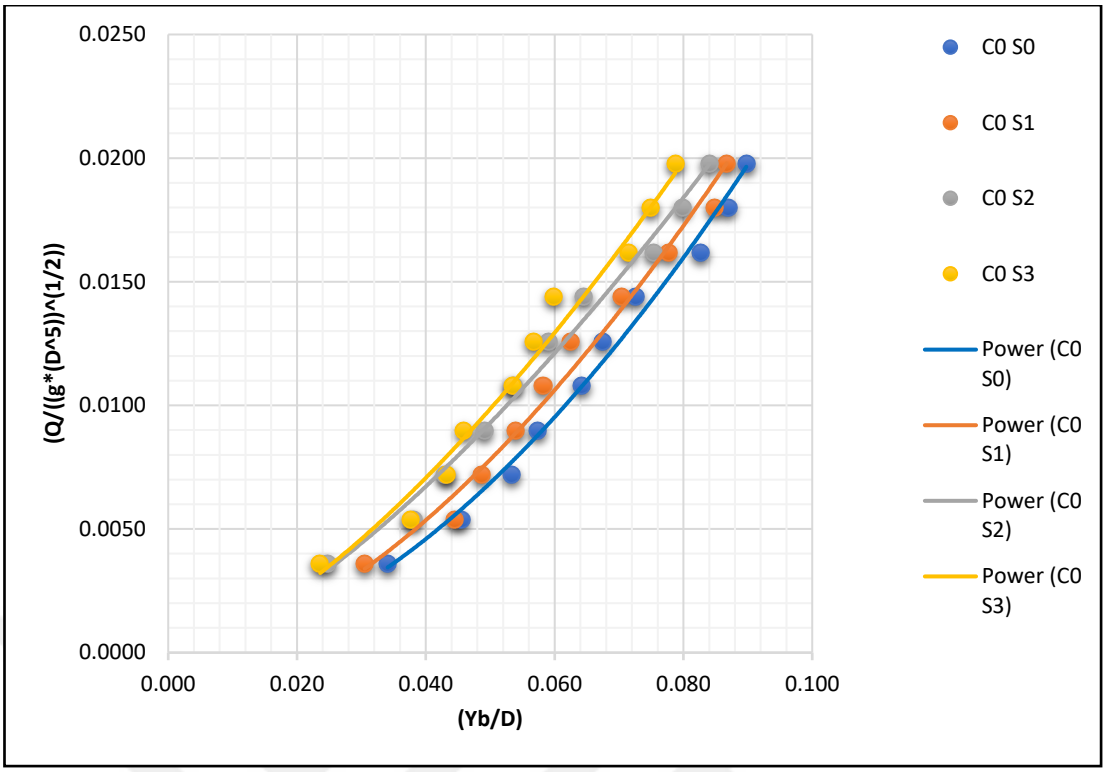

Figure 5.6 The Change of ($\frac{Q}{\sqrt{g\,D^5}}$) with ($\frac{y_b}{D}$) For Soft Bottom Channels (C_0) with Different Slopes

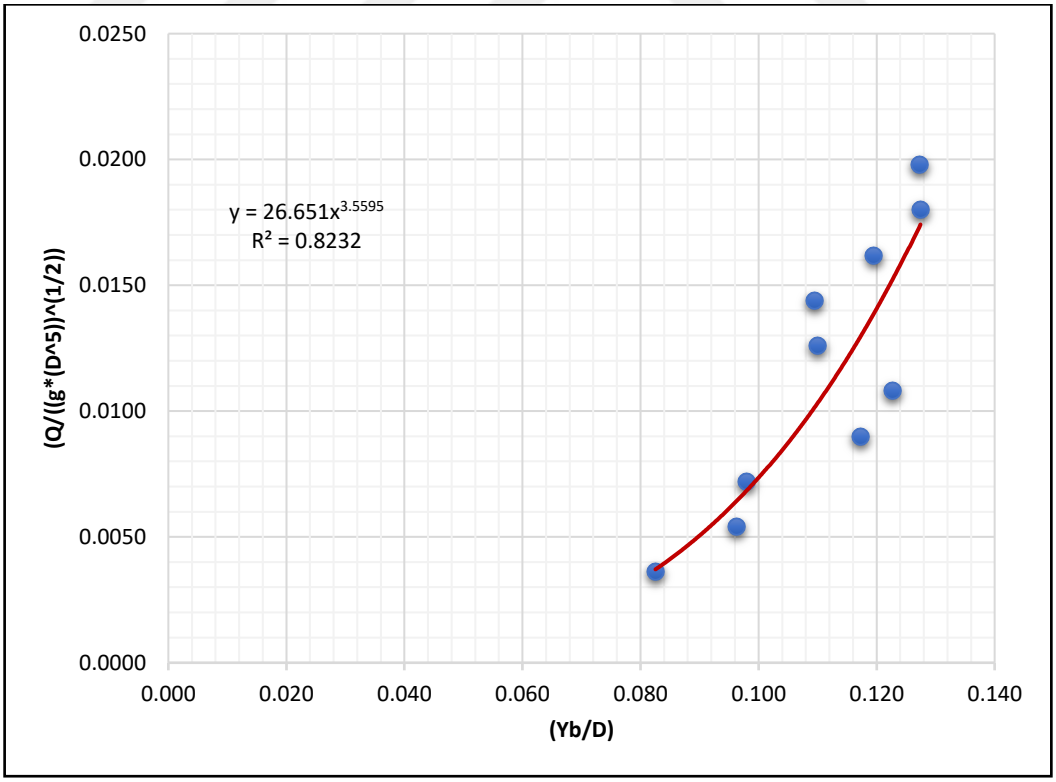

Figure 5.7 The Change of ($\frac{Q}{\sqrt{g\,D^5}}$) with ($\frac{y_b}{D}$) For Rough Bottom Channels (C_1) with Slope ($S_0 = 0$)

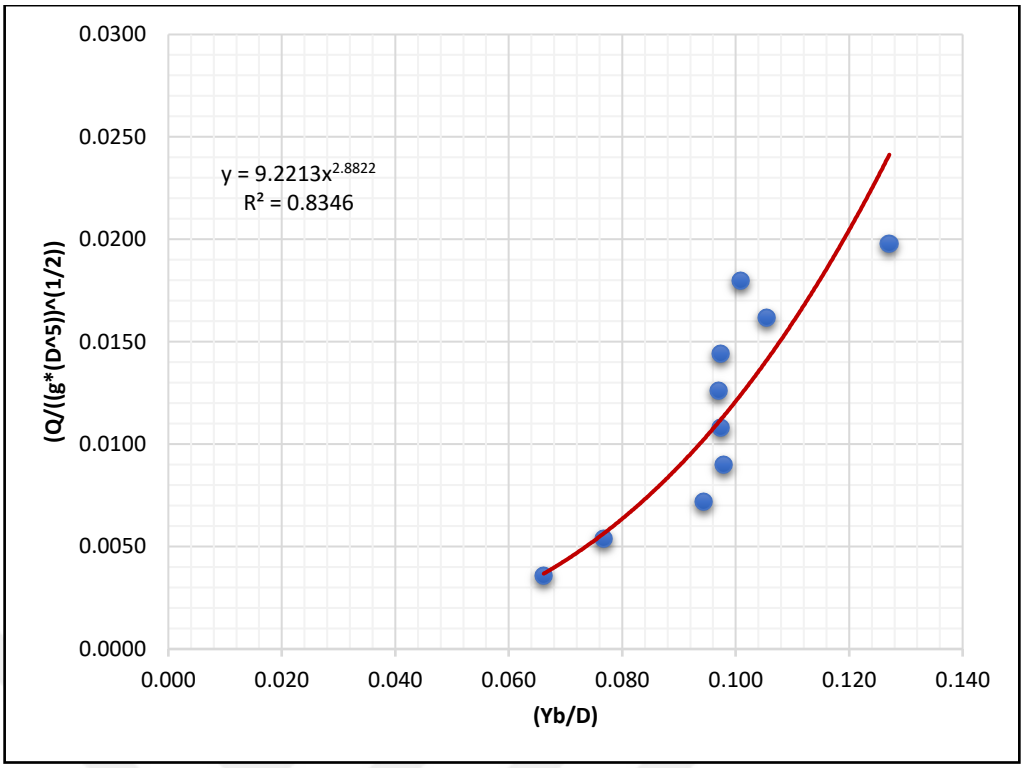

Figure 5.8 The Change of ($\frac{Q}{\sqrt{g\,D^5}}$) with ($\frac{y_b}{D}$) For Rough Bottom Channels (C_1) with Slope (S_1 = 0.005)

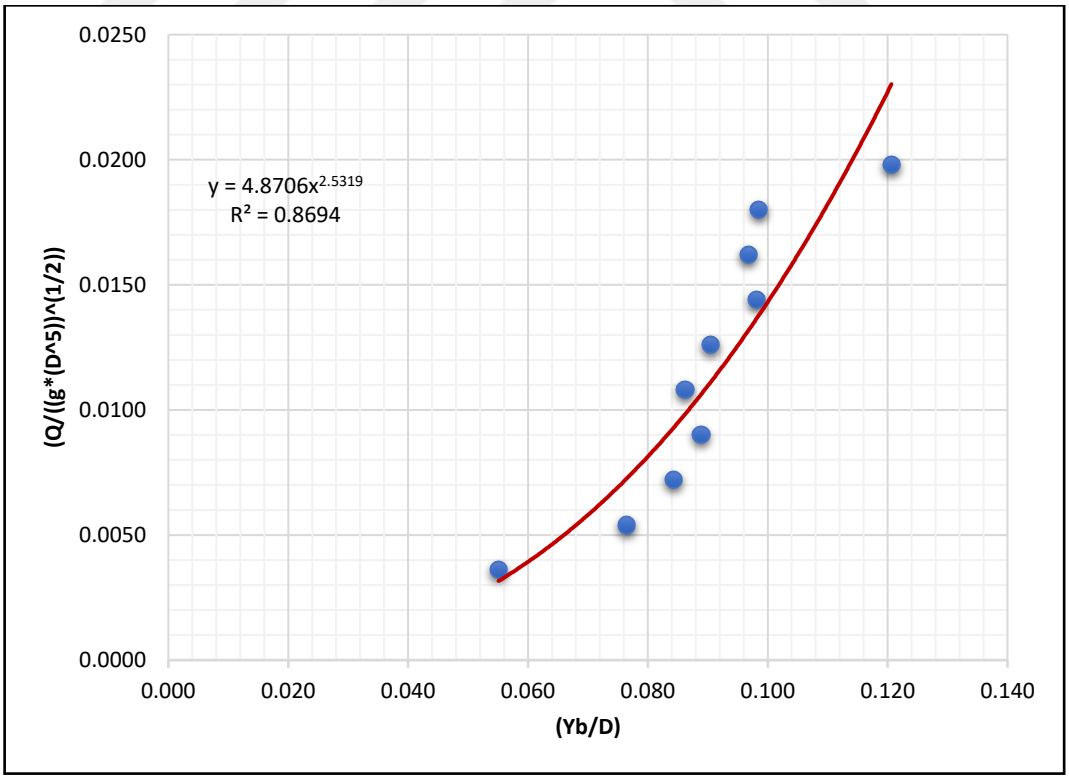

Figure 5.9 The Change of ($\frac{Q}{\sqrt{g\,D^5}}$) with ($\frac{y_b}{D}$) For Rough Bottom Channels (C_1) with Slope (S_2 = 0.01)

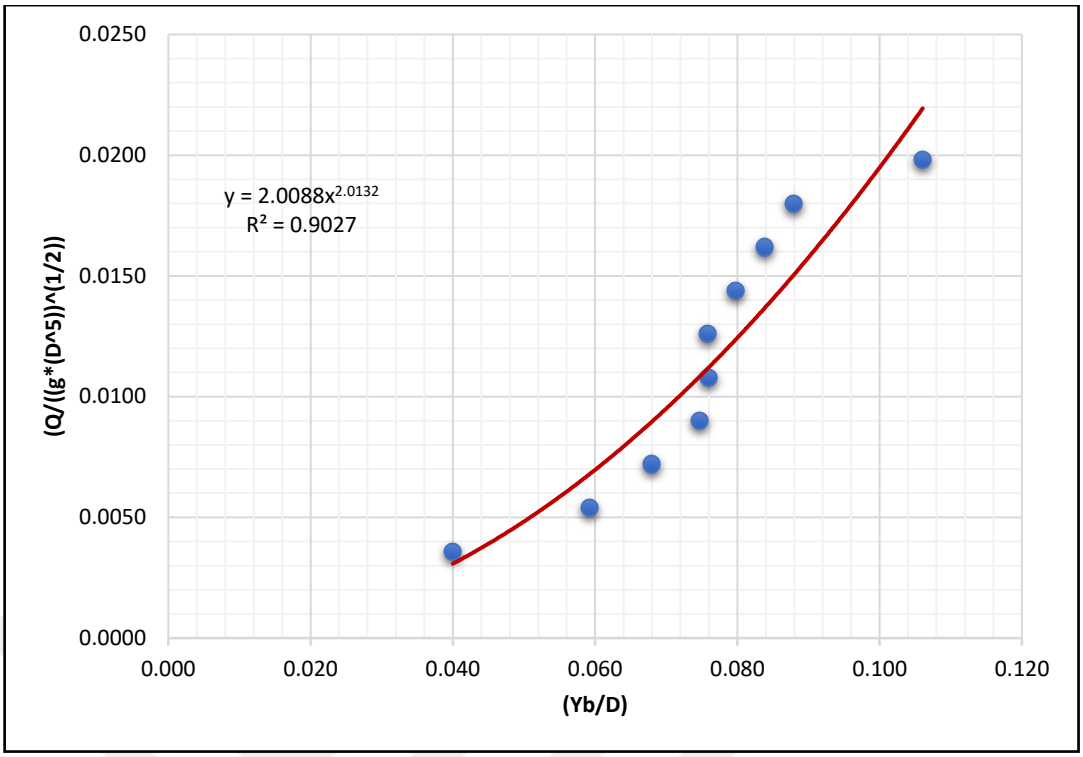

Figure 5.10 The Change of ($\frac{Q}{\sqrt{g\ D^5}}$) with ($\frac{y_b}{D}$) For Rough Bottom Channels (C_1) with Slope (S_3 = 0.015)

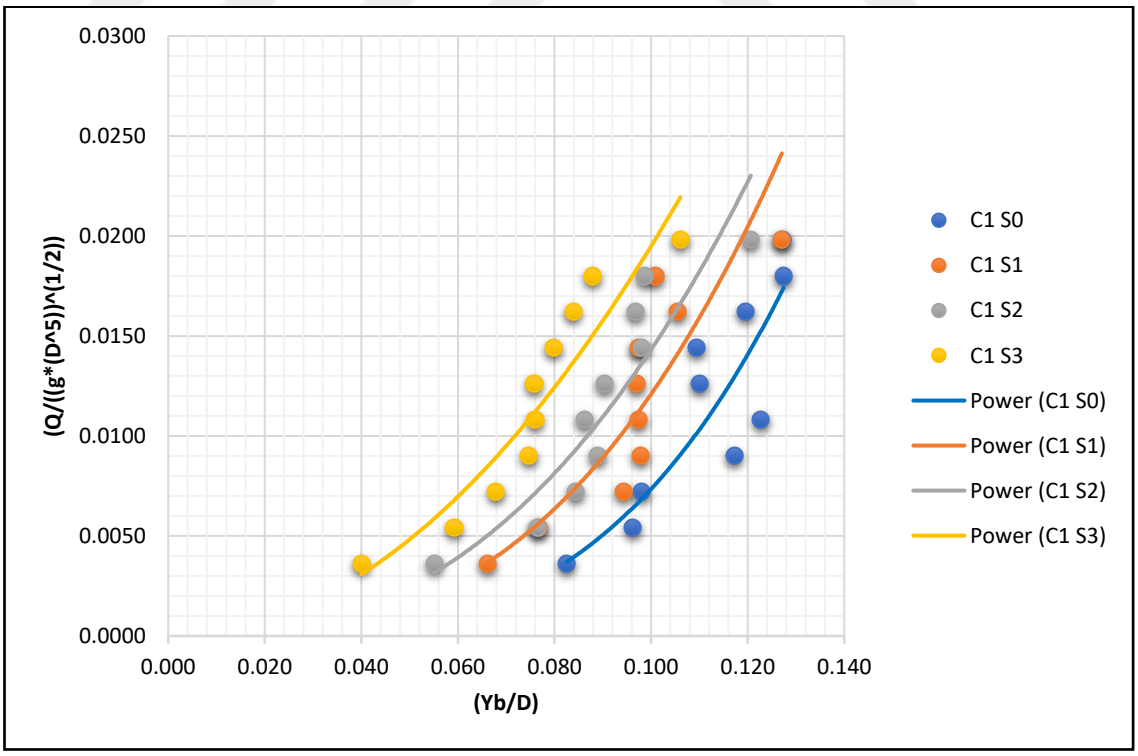

Figure 5.11 The Change of ($\frac{Q}{\sqrt{g\ D^5}}$) with ($\frac{y_b}{D}$) For Rough Bottom Channels (C_1) with Different Slopes

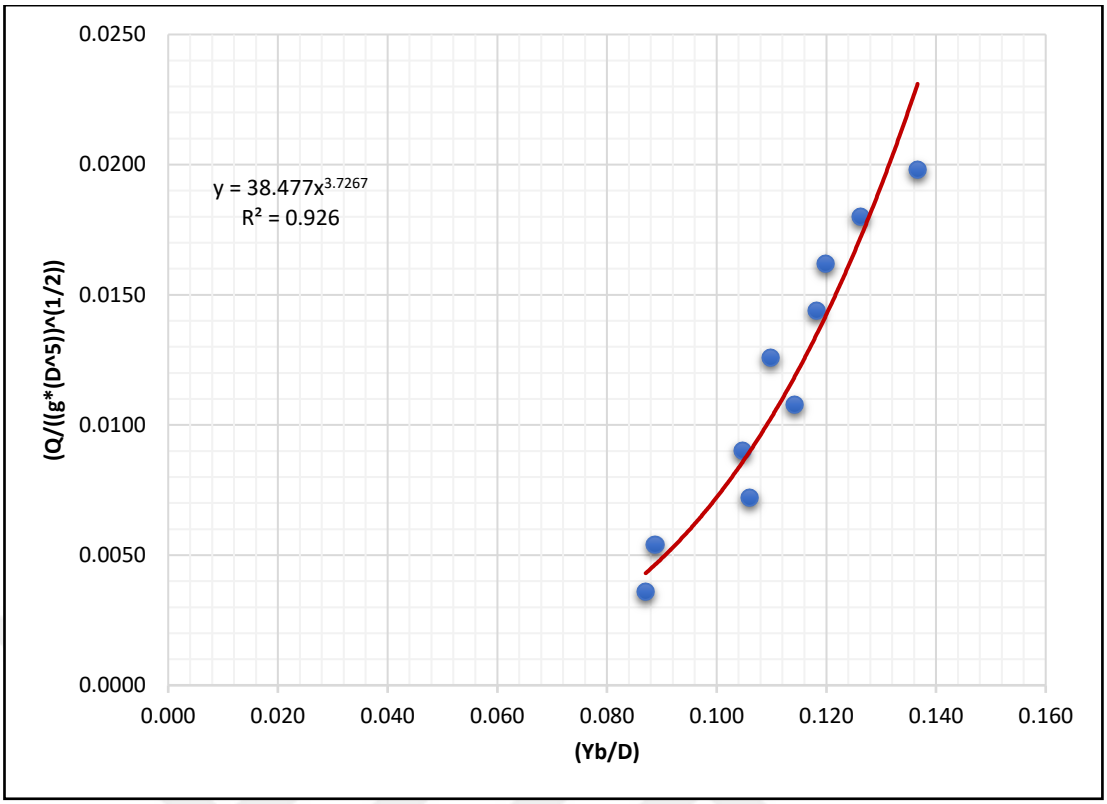

Figure 5.12 The Change of ($\frac{Q}{\sqrt{g\,D^5}}$) with ($\frac{y_b}{D}$) For Rough Bottom Channels (C_2) with Slope ($S_0 = 0$)

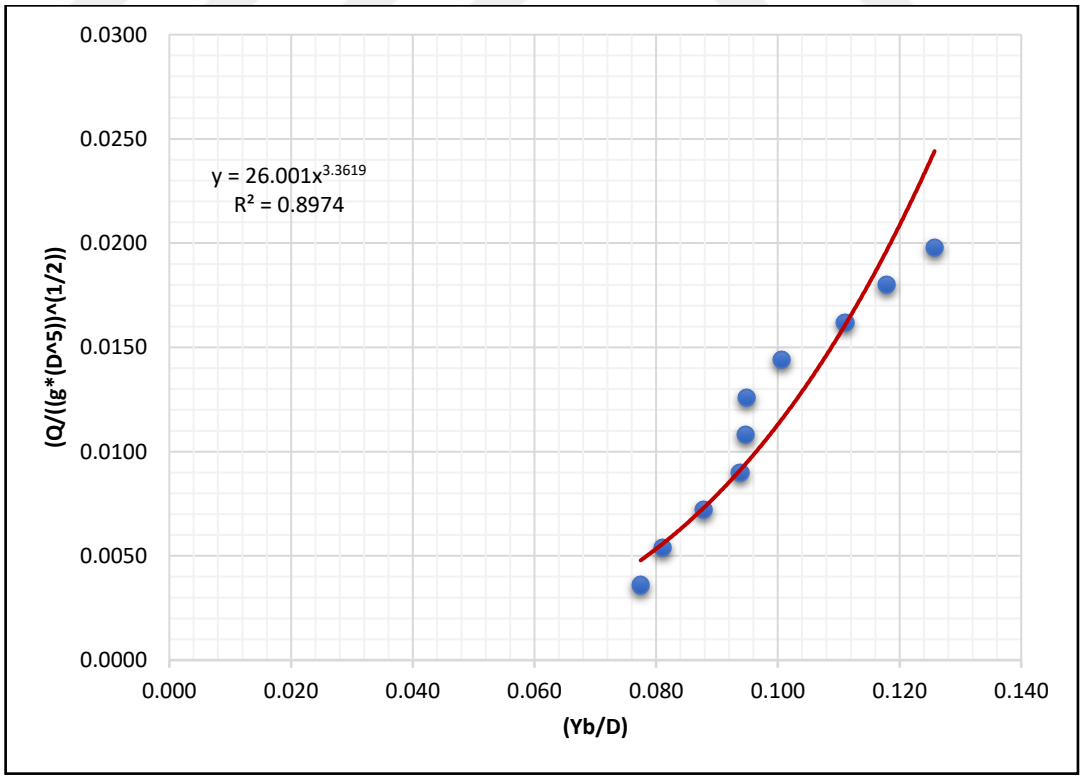

Figure 5.13 The Change of ($\frac{Q}{\sqrt{g\,D^5}}$) with ($\frac{y_b}{D}$) For Rough Bottom Channels (C_2) with Slope ($S_1 = 0.005$)

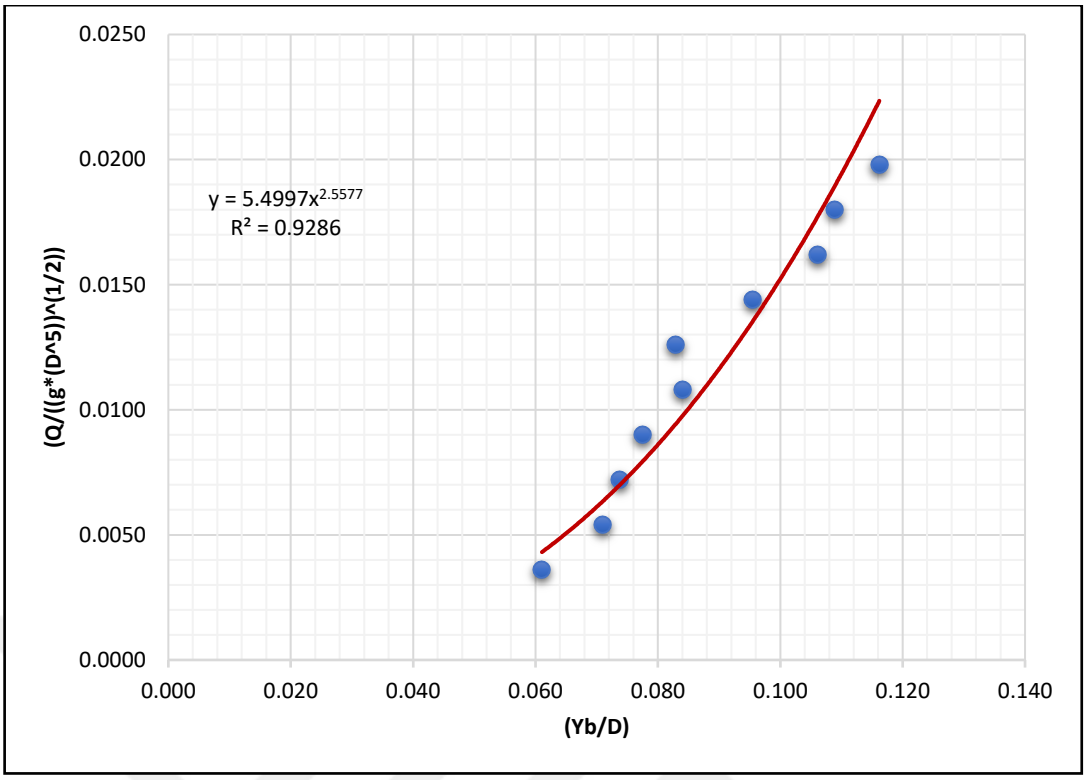

Figure 5.14 The Change of ($\frac{Q}{\sqrt{g\ D^5}}$) with ($\frac{y_b}{D}$) For Rough Bottom Channels (C_2) with Slope (S_2 = 0.01)

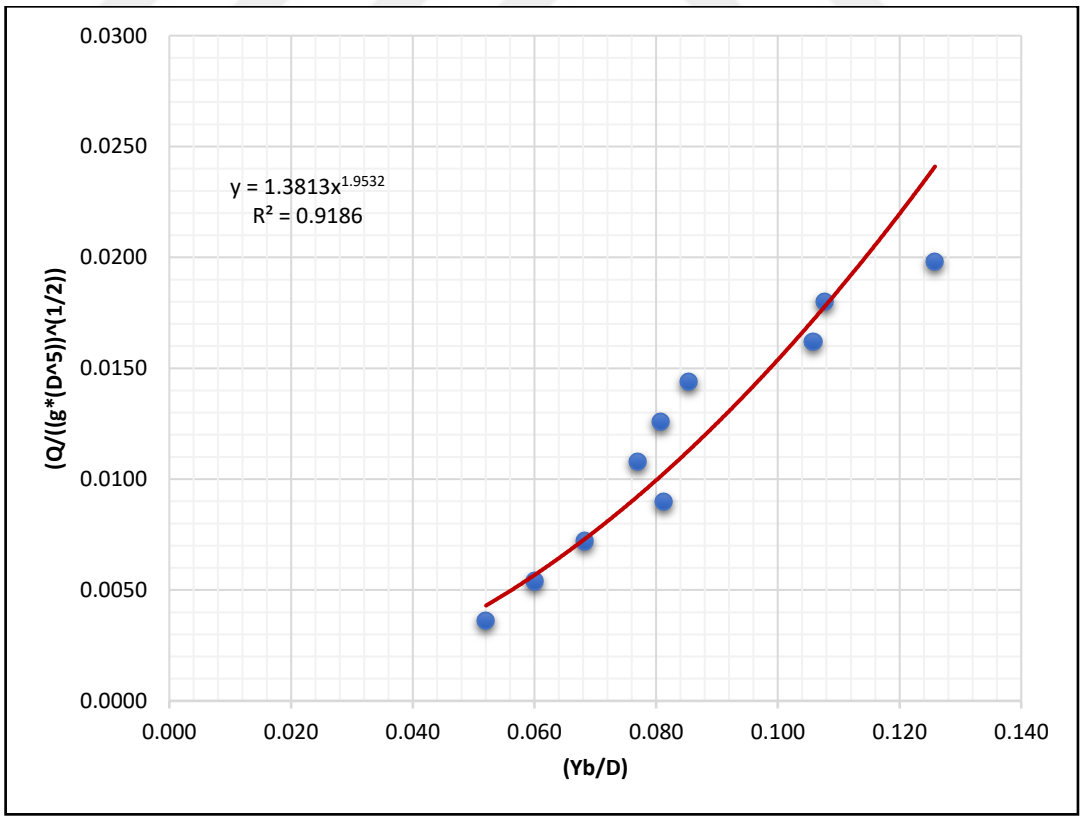

Figure 5.15 The Change of ($\frac{Q}{\sqrt{g\ D^5}}$) with ($\frac{y_b}{D}$) For Rough Bottom Channels (C_2) with Slope (S_3 = 0.015)

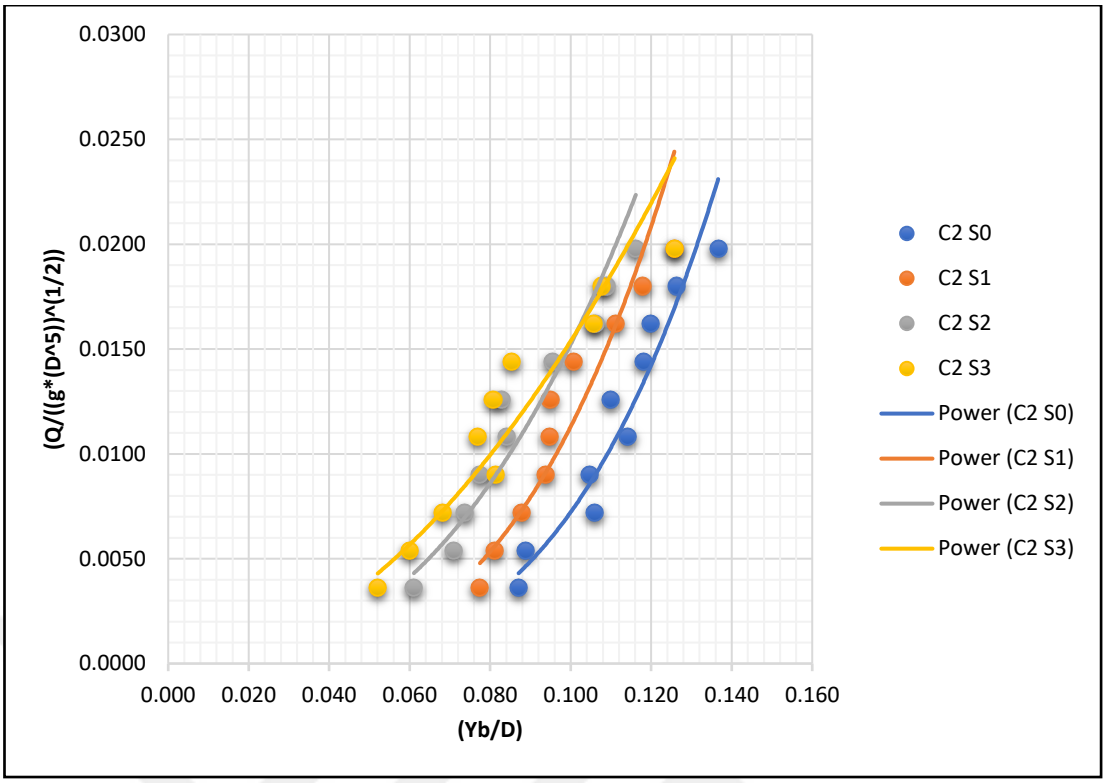

Figure 5.16 The Change of ($\frac{Q}{\sqrt{g\ D^5}}$) with ($\frac{y_b}{D}$) For Rough Bottom Channels (C_2) with Different Slopes

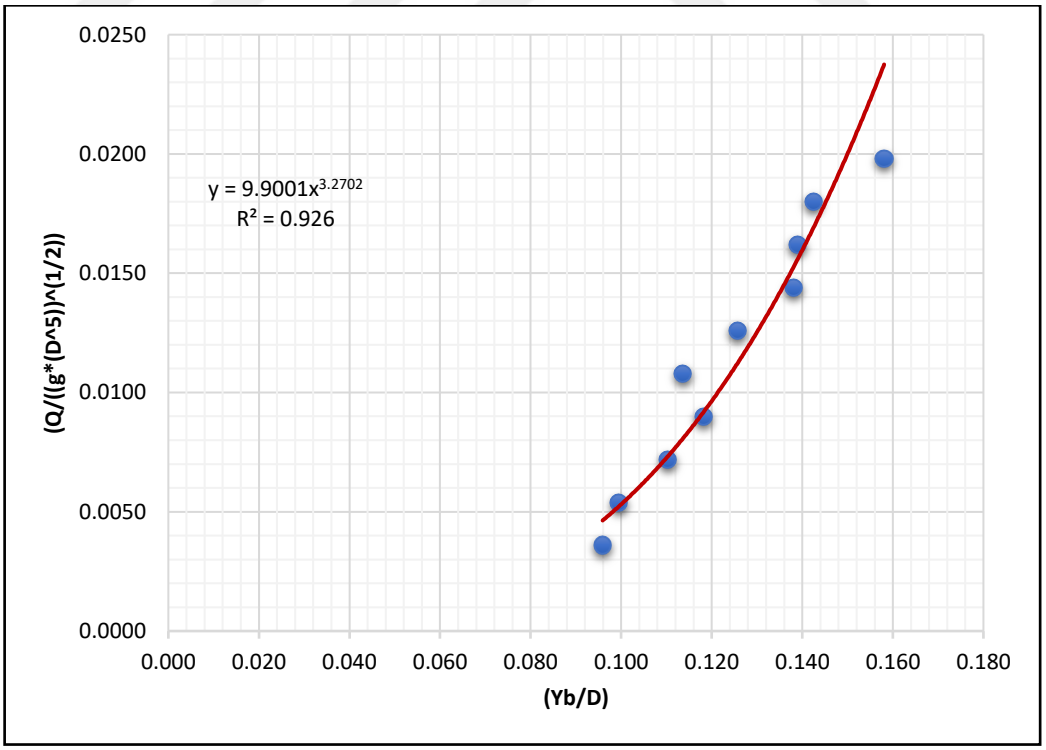

Figure 5.17 The Change of ($\frac{Q}{\sqrt{g\ D^5}}$) with ($\frac{y_b}{D}$) For Rough Bottom Channels (C_3) with Slope ($S_0 = 0$)

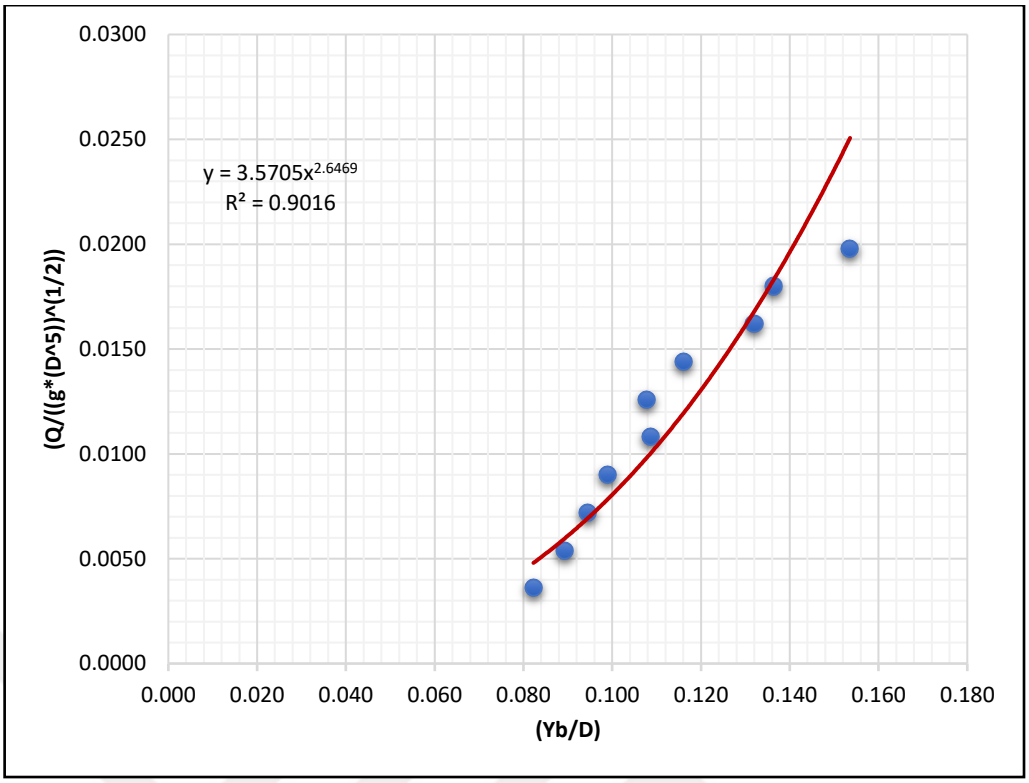

Figure 5.18 The Change of ($\frac{Q}{\sqrt{g\,D^5}}$) with ($\frac{y_b}{D}$) For Rough Bottom Channels (C_3) with Slope (S_1 = 0.005)

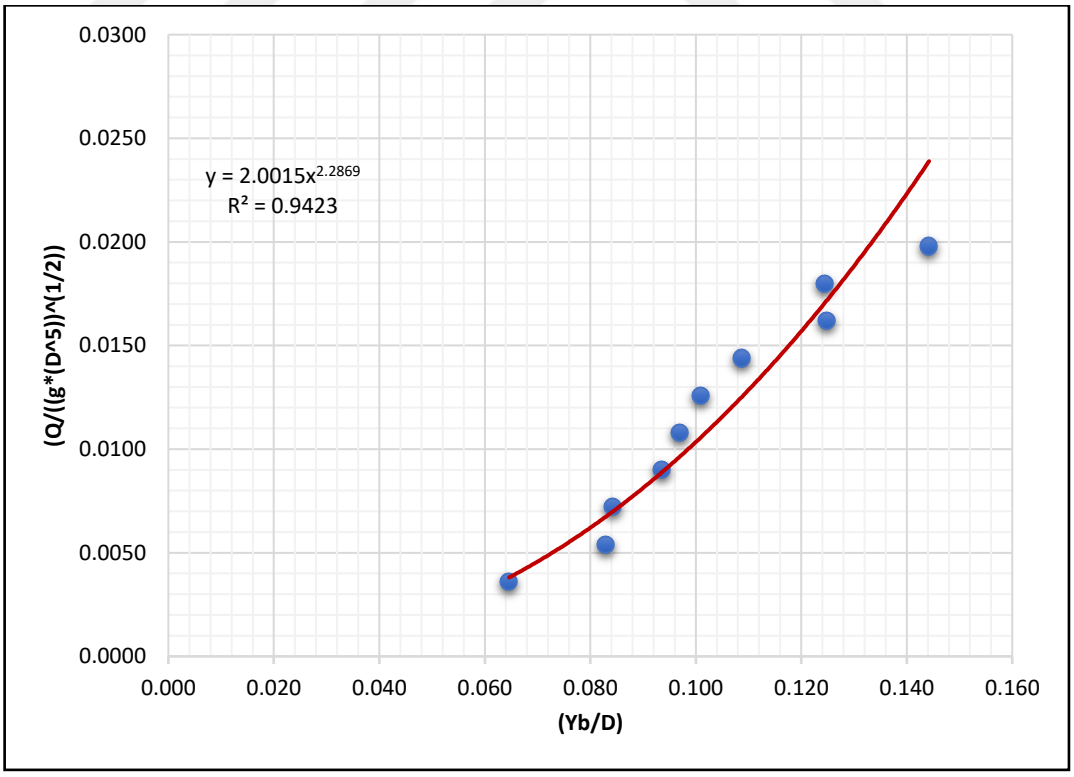

Figure 5.19 The Change of ($\frac{Q}{\sqrt{g\,D^5}}$) with ($\frac{y_b}{D}$) For Rough Bottom Channels (C_3) with Slope (S_2 = 0.01)

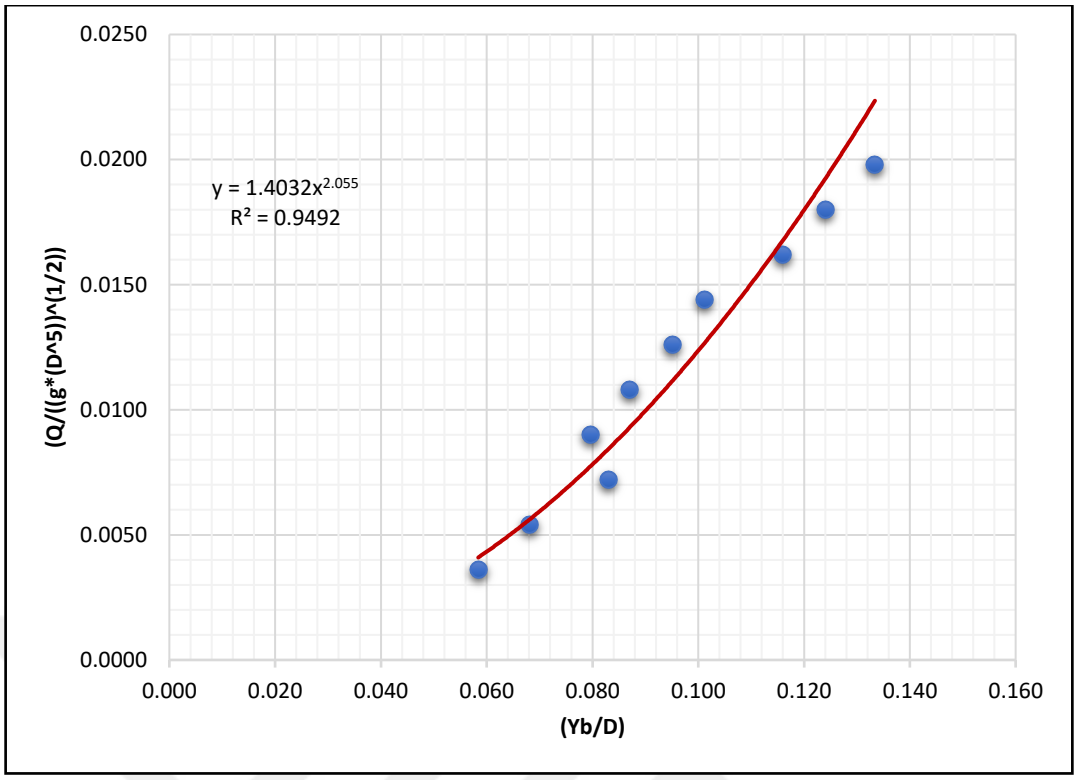

Figure 5.20 The Change of ($\frac{Q}{\sqrt{g\,D^5}}$) with ($\frac{y_b}{D}$) For Rough Bottom Channels (C_3) with Slope (S_3 = 0.015)

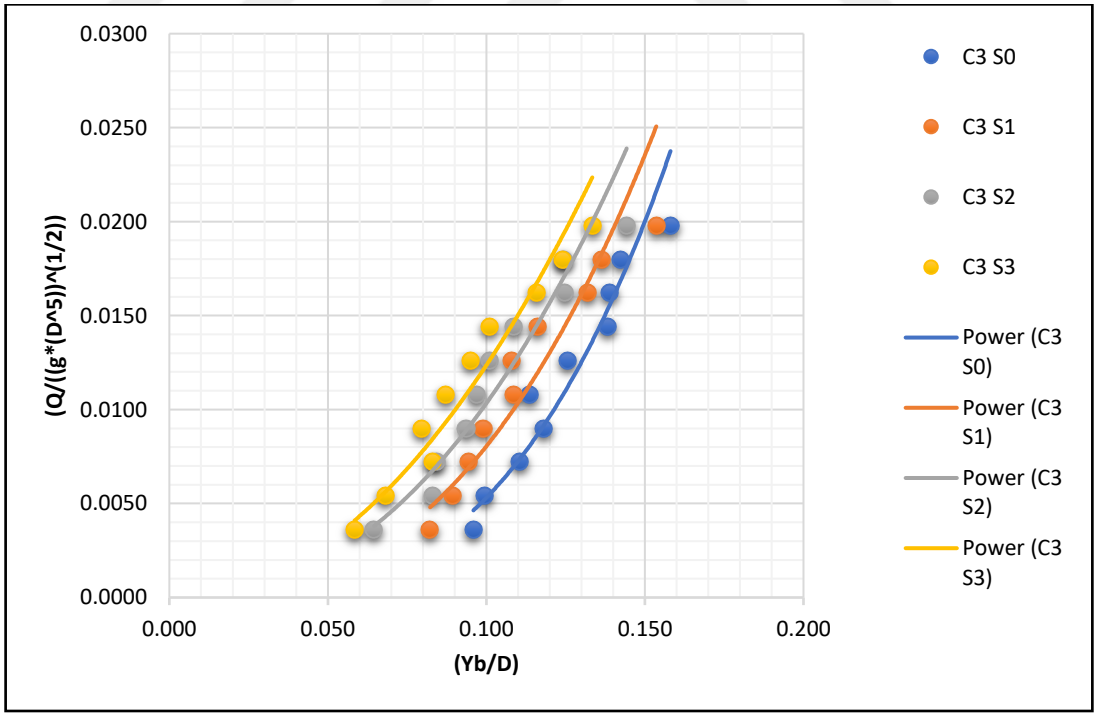

Figure 5.21 The Change of ($\frac{Q}{\sqrt{g\,D^5}}$) with ($\frac{y_b}{D}$) For Rough Bottom Channels (C_3) with Different Slopes

Table 5.2 The Constants (a_1) and (b_1) and Determination Coefficient (R^2) Values for Soft and Rough Bottom Channels with different Slopes

Item	a_1	b_1	Equations	R^2
C_0 S_0	1.4975	1.7977	(5.5)	0.9909
C_0 S_1	1.2295	1.6889	(5.6)	0.9804
C_0 S_2	0.7229	1.4535	(5.7)	0.9846
C_0 S_3	0.8588	1.4913	(5.8)	0.9734
C_1 S_0	26.651	3.5595	(5.9)	0.8232
C_1 S_1	9.2213	2.8822	(5.10)	0.8346
C_1 S_2	4.8706	2.5319	(5.11)	0.8694
C_1 S_3	2.0088	2.0132	(5.12)	0.9027
C_2 S_0	38.477	3.7267	(5.13)	0.926
C_2 S_1	26.001	3.3619	(5.14)	0.8974
C_2 S_2	5.4997	2.5577	(5.15)	0.9286
C_2 S_3	1.3813	1.9532	(5.16)	0.9186
C_3 S_0	9.9001	3.2702	(5.17)	0.926
C_3 S_1	3.5705	2.6469	(5.18)	0.9016
C_3 S_2	2.0015	2.2869	(5.19)	0.9423
C_3 S3	1.4032	2.055	(5.20)	0.9492

5.1.3 (y_b/D) Change with (y_c/D)

The change of brink depth ratio (y_b/D) with the critical depth ratio (y_c/D) was studied for soft bottom channels (C_0) and coarse (C_1, C_2, C_3) and for different slopes (0, 1/200, 2/200, 3/200). the laboratory data were plotted for all bottom slopes in figures (5.22, 5.23, 5.24 and 5.25). In these figures, a better line between (y_b/D) and (y_c/D) was found to form simple linear equations with the following formula:

$$(\frac{y_b}{D}) = a_2(\frac{y_c}{D}) \quad (5.21)$$

Where (a_2) = constant.

The value of the constant (a_2) and the corresponding values of the determination coefficient (R^2) and the groups of Froude number (F_r) of upstream flow had been found. where:

$$F_r = {V}/{\sqrt{gD_h}} \quad (5.22)$$

Where: V: the flow velocity, g: gravity acceleration, D_h: the hydraulic depth = (A/T), A: the flow cross sectional area, T: the top width of channel flow.

For semicircular channels:

$$T = 2\,r\,sin\theta \quad (5.23)$$

r: channel radius (m)

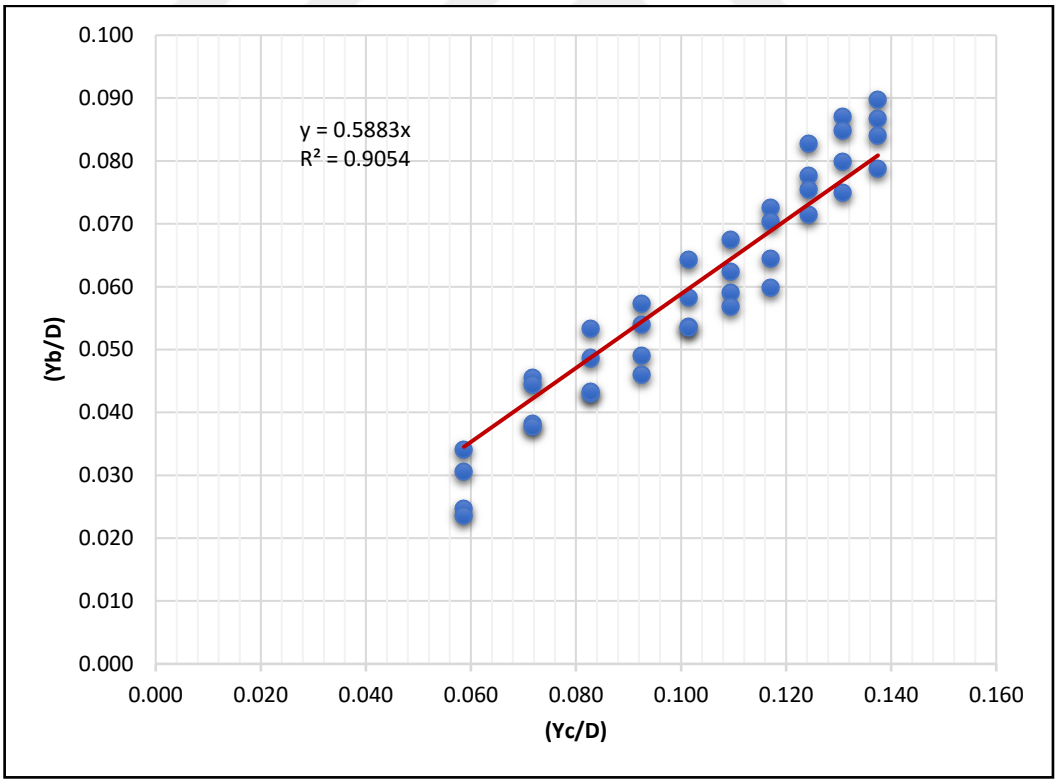

Figure 5.22 The Change of (y_b/D) With (y_c/D) For Soft Bottom Channels (C_0) with Different Slopes

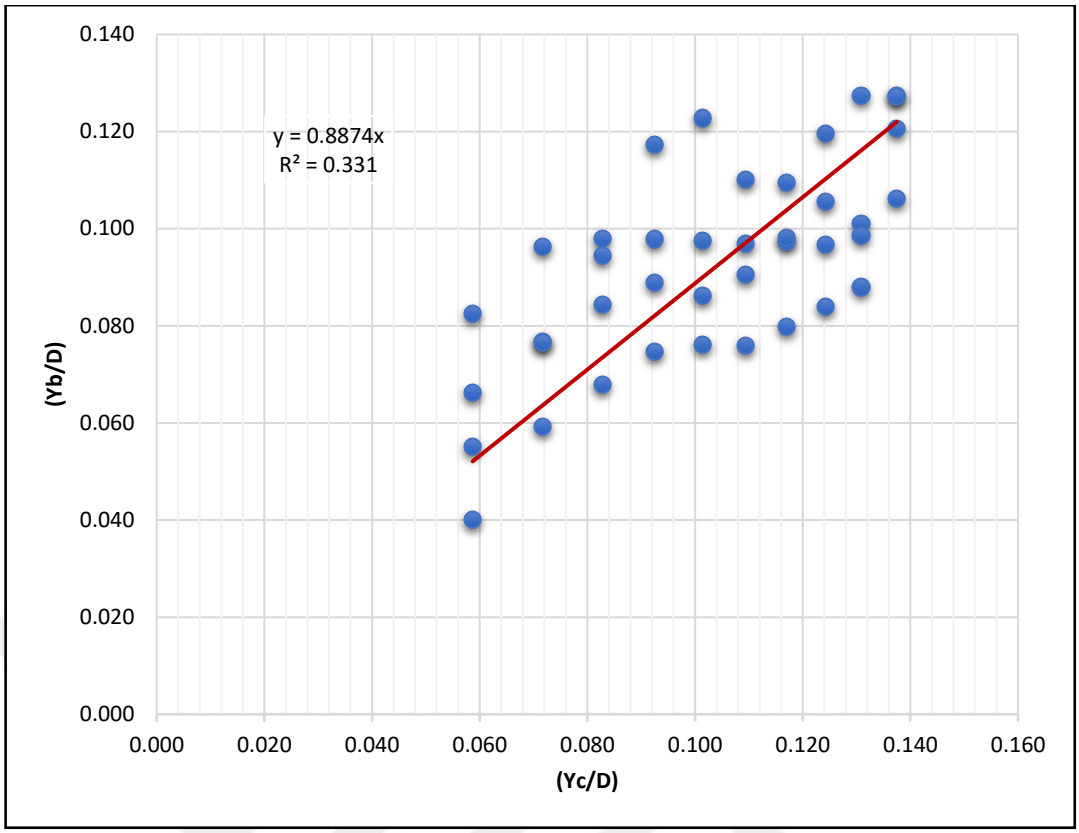

Figure 5.23 The Change of (y_b/D) With (y_c/D) For Rough Bottom Channels (C_1) with Different Slopes

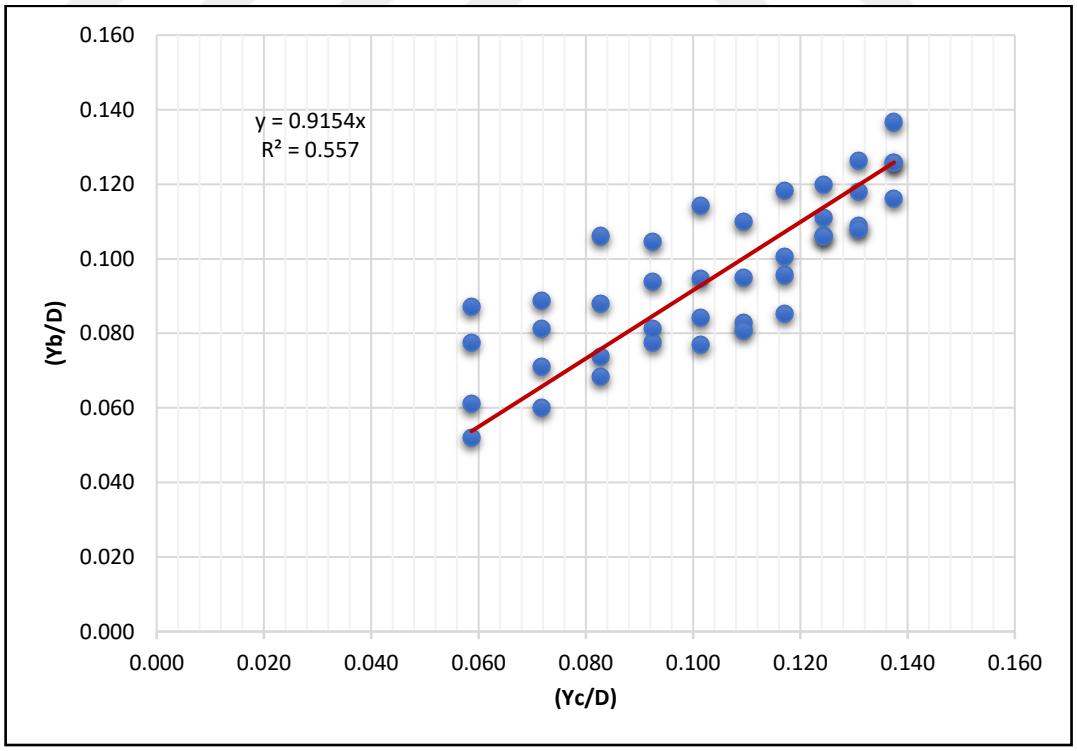

Figure 5.24 The Change of (y_b/D) With (y_c/D) For Rough Bottom Channels (C_2) with Different Slopes

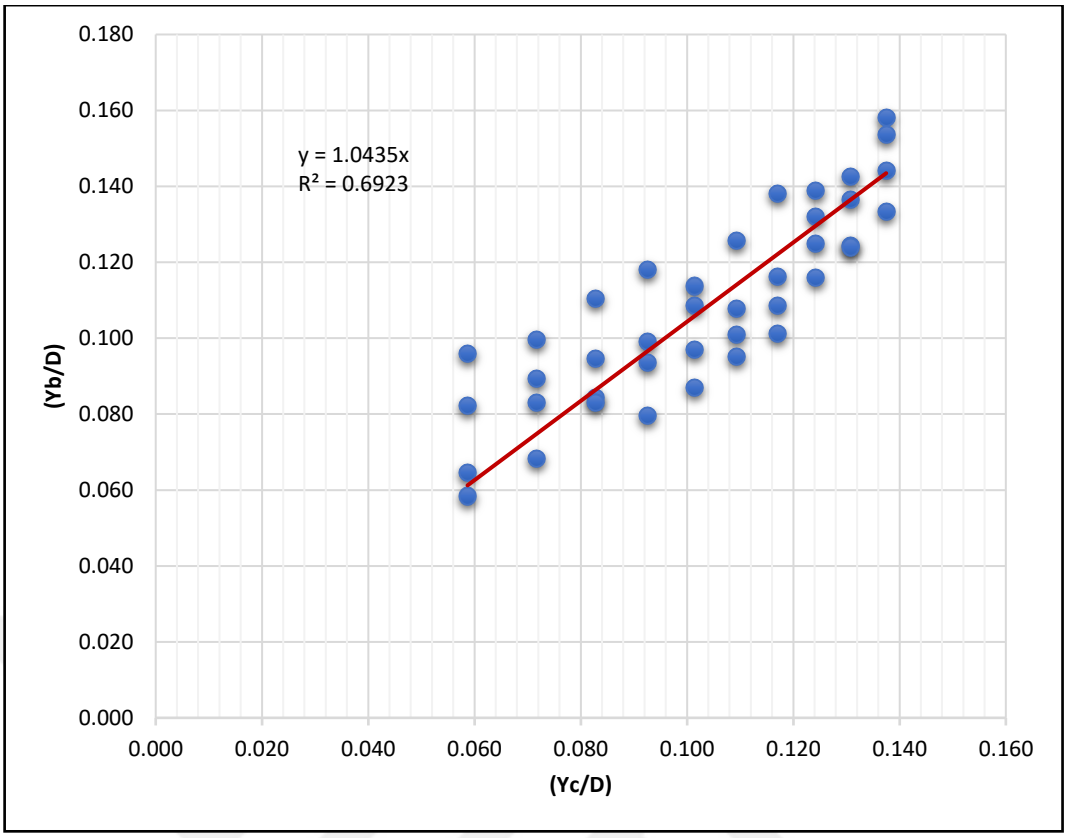

Figure 5.25 The Change of (y_b/D) With (y_c/D) For Rough Bottom Channels (C_3) with Different Slopes

The information's of these equations had been organized in table (5.3). It was found in these figures that the values of (y_b/D) are increase with the increase of (y_c/D) values and the best line between them represent with a linear relationship with a high coefficient of correlation. The slope of each line gives the values of the final depth ratio. It is also observed through these figures that the final depth ratio increases with increasing the slope of the bottom. The average value of (y_b/y_c) is equal to (0.881) for semicircular channels with free overfall and for subcritical flow state. The average value of (y_b/y_c) for semicircular channels with soft bottom is equal to (0.574) with determination coefficient (R^2) equal to (0.9054).

Because the section used in this study has not been used previously in previous studies, so there are no studies to compare the results obtained from this study with the previous results except the studies of (Subhasish Dey, D. Nagesh Kumar and D. Ram Singh,2002), (Subhasish Dey,2003), (R.V. Raikar, D. Nagesh Kumar, Subhasish Dey,2004), (Z. Ahmad,2004) and (Mahesh Pal, Arun Goel,2005) on inverted semicircular channels, where their studies showed that the value of the ratio (y_b / y_c) is equal to (0.695), (0.705), (0.705), (0.713) and (0.704) respectively, for inverted

semicircular channels with free overfall. Although the status of the section in previous studies is different but the results of the current study appear close to the results of these studies and the reason of this difference may be due to the dimensions of the channels used in the experiments, in addition to the materials used in the bottom roughness and the slopes and the state of experiments.

Table 5.3 The Constant (a_2) and Determination Coefficient (R^2) and Froude No. Groups Values for Soft and Rough Bottom Channels with different Slopes

Item	$a_2 = (y_b/y_c)$	Equations	R^2	Froude No. groups
C_0	0.574	(5.24)	0.9054	0.80 – 2.22
C_1	0.928	(5.25)	0.331	0.23 – 1.02
C_2	0.951	(5.26)	0.557	0.19 – 0.68
C_3	1.073	(5.27)	0.6923	0.13 – 0.50
Average =	0.881			

5.1.4 (y_b/y_c) Change with Channel Bed Slope

As we noticed from table (5.3) that the end depth ratio (y_b/y_c) varies with the channel bed slope (S). The values of (y_b/y_c) are taken from the best fit lines of the Figs. (5.22, 5.23, 5.24 and 5.25). the average values of (y_b/y_c) are plotted with bed slopes values for channels (C_0, C_1, C_2 and C_3) for constant roughness channels with different slope as shown in Fig. (5.26). The obtained results can be defined by a simple linear equation of the following form with high coefficient of determination ($R^2 = 0.8358$) as:

$$\frac{y_b}{y_c} = 0.6536 + 30.373\, S \qquad (5.28)$$

Equation (5.28) and Fig. (5.26) show that the average ratio (y_b/y_c) increases with increasing the channel bed slope. Also, the variation of the (EDR) with the slope had been studied for constant slope channels with different roughness, the results had been plotted as in Fig. (5.27). The obtained results can be defined by a simple linear equation of the following form with high coefficient of determination ($R^2 = 0.9911$) as:

$$\frac{y_b}{y_c} = 1.0191 - 18.352\,S \qquad (5.29)$$

Equation (5.29) and Fig. (5.27) show that the average ratio (y_b/y_c) decreases with increasing the channel bed slope.

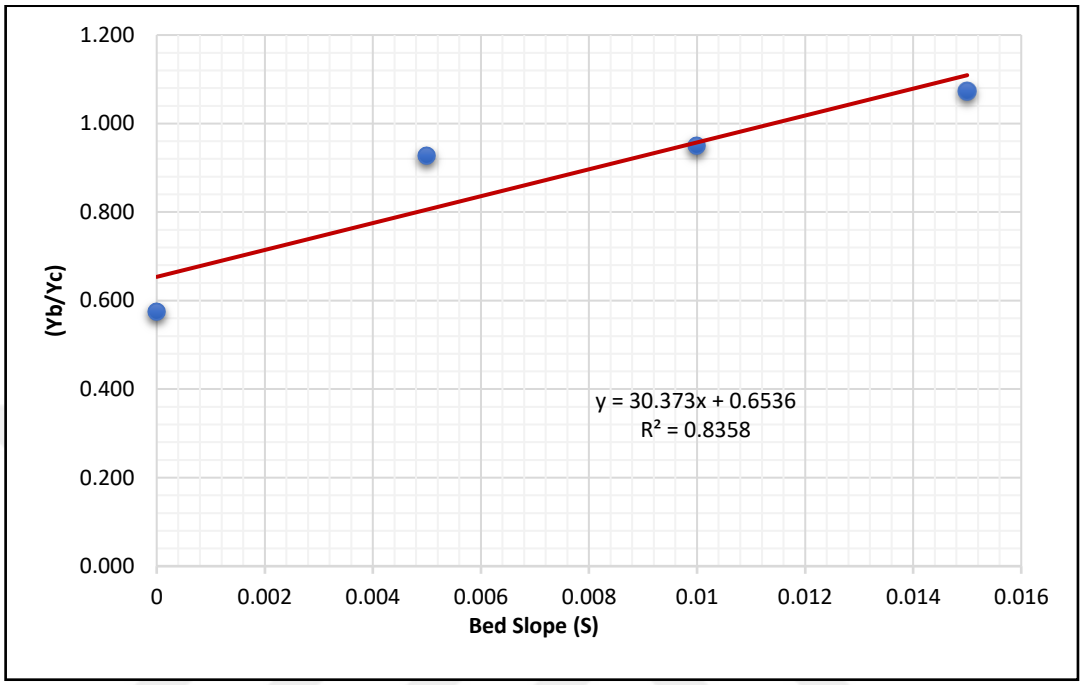

Figure 5.26 The Change of (y_b/y_c) With channel bed slope (S) (Constant Roughness and Different Slope)

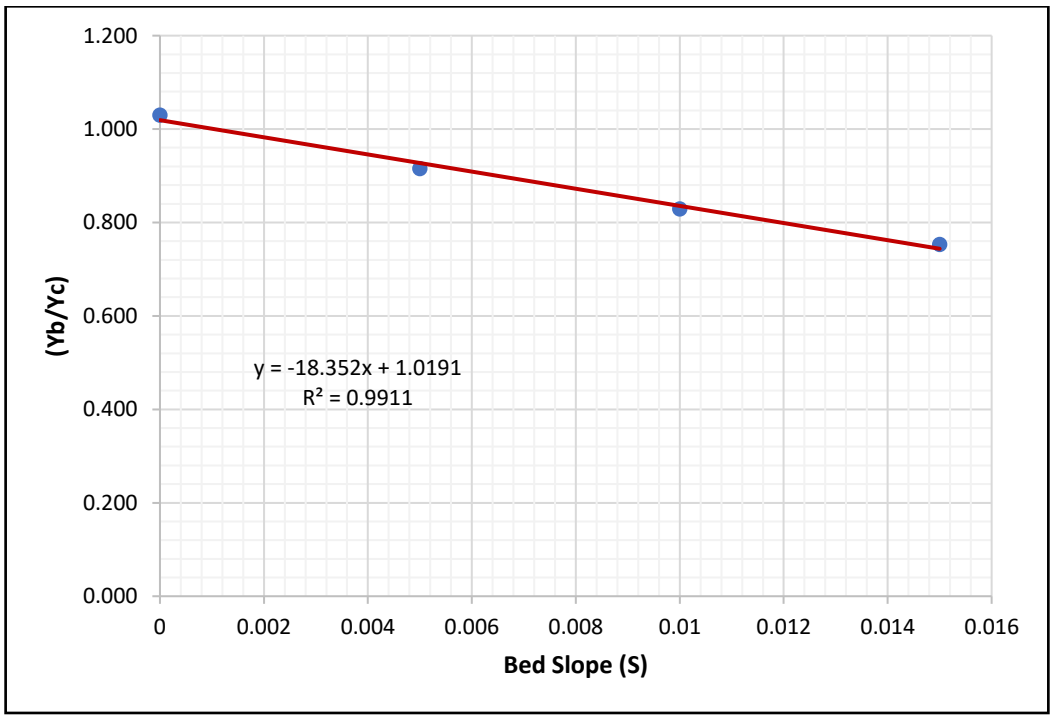

Figure 5.27 The Change of (y_b/y_c) With channel bed slope (S) (Constant Slope and Different Roughness)

5.1.5 Variation of ($Q/\sqrt{g\ D^5}$) with ($\frac{y_b}{D}$) and (S) and (n)

Equation (3.17) includes the four variables, and it is clear that there is a functional relationship between ($Q/\sqrt{g\ D^5}$), ($\frac{y_b}{D}$), (S) and (n) for the semicircular channels with free overfall. In order to determine the relationship accurately, the statistical analysis program (SPSS 25) was used to analyze the correlation between the data and to determine the type and form of the equation for each case. The data were divided into three cases:

Case (1): (S =0) and (n = 0) smooth bed:

For the horizontal and smooth bed semicircular channels with (S = 0) and (n = 0), all laboratory data for this case were used and entered into the statistical analysis program (SPSS 25) to conduct the correlation test and determine the general equation that links these variables. The relationship which obtained for this condition was in the form of power equation as follows:

$$\left(\frac{Q}{\sqrt{g\ D^5}}\right) = 1.497\ \left(\frac{y_b}{D}\right)^{1.798} \tag{5.30}$$

Equation (5.30) was obtained with determination coefficient (R^2 = 0.991) and with standard error (0.056). The accuracy of the equation was verified in discharge calculating by entering the laboratory data and calculate the expected or predicted discharge, where the discharge can be calculated from:

$$Q = 1.497\ g^{0.5}\ y_b^{1.798}\ D^{0.702} \tag{5.31}$$

and then it was drawn with the discharge measured in the laboratory. Fig. (5.28) show excellent matching between the measured and predicted discharge values.

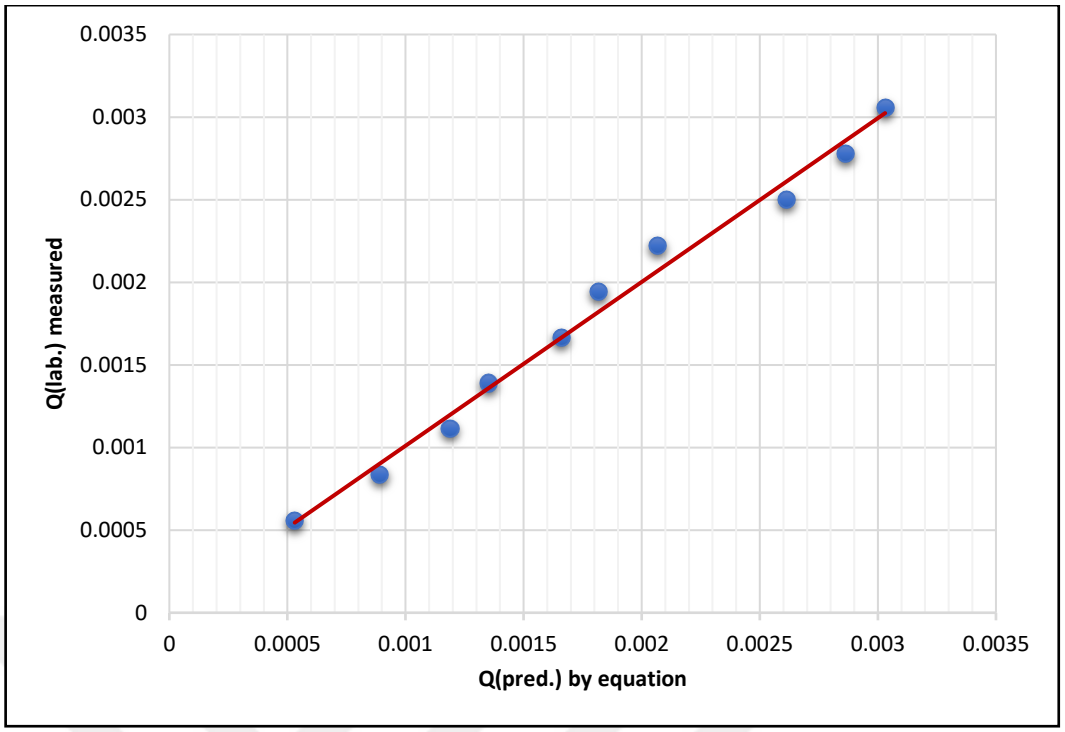

Figure 5.28 The Observed discharge with The Predicted Discharge for smooth bed channels (S=0 and n=0)

Case (2): (S = 0) and (n = 0) rough bed:

For the horizontal and rough bed semicircular channels with (S = 0) and (n = 0), all laboratory data for this case were used and entered into the statistical analysis program (SPSS 25) to conduct the correlation test and determine the general equation that links these variables. The relationship which obtained for this condition was in the form of power equation as follows:

$$\left(\frac{Q}{\sqrt{g\,D^5}}\right) = 8.660\ \left(\frac{y_b}{D}\right)^{3.101} \qquad (5.32)$$

Equation (5.32) was obtained with determination coefficient (R^2 = 0.788) and with standard error (0.250). The accuracy of the equation was verified in discharge calculating by entering the laboratory data and calculate the expected or predicted discharge, where the discharge can be calculated from:

$$Q = 8.660\ g^{0.5}\ y_b^{3.101}\ D^{-0.601} \qquad (5.33)$$

and then it was drawn with the discharge measured in the laboratory. Fig. (5.29) show good matching between the measured and predicted discharge values.

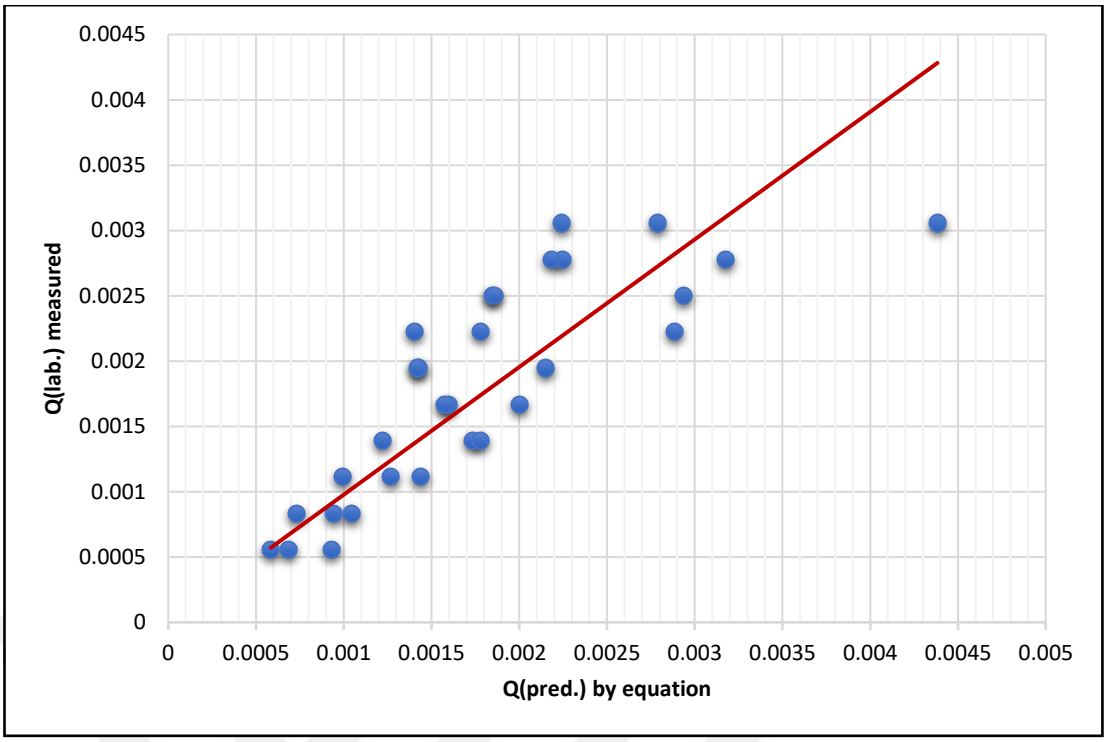

Figure 5.29 The Observed discharge with The Predicted Discharge for rough bed channels (S=0 and n=0)

Case (3): (S) and (n) smooth and rough bed:

For smooth and rough semicircular channels with different slopes (S) and different roughness (n), the laboratory data for this case were divided into two parts, (70%) of the results are used and entered into the statistical analysis program (SPSS 25) to conduct the correlation test and determine the general equation that links these variables. The relationship which obtained for this condition was in the form of power equation as follows:

$$\left(\frac{Q}{\sqrt{g\,D^5}}\right) = 0.426\,(\frac{y_b}{D})^{1.723}\,(S)^{0.404}\,(n)^{-0.678} \qquad (5.34)$$

Equation (5.34) was obtained with determination coefficient (R^2 = 0.950). The accuracy of the equation was verified in discharge calculating by entering the (30%) of the laboratory data and calculate the expected or predicted discharge, where the discharge equation is:

$$Q = 0.426\,g^{0.5}\,y_b^{1.723}\,D^{0.777}\,\frac{S^{0.404}}{n^{0.678}} \qquad (5.35)$$

and then it was drawn with the discharge measured in the laboratory. Fig. (5.30) show excellent matching between the measured and predicted discharge values.

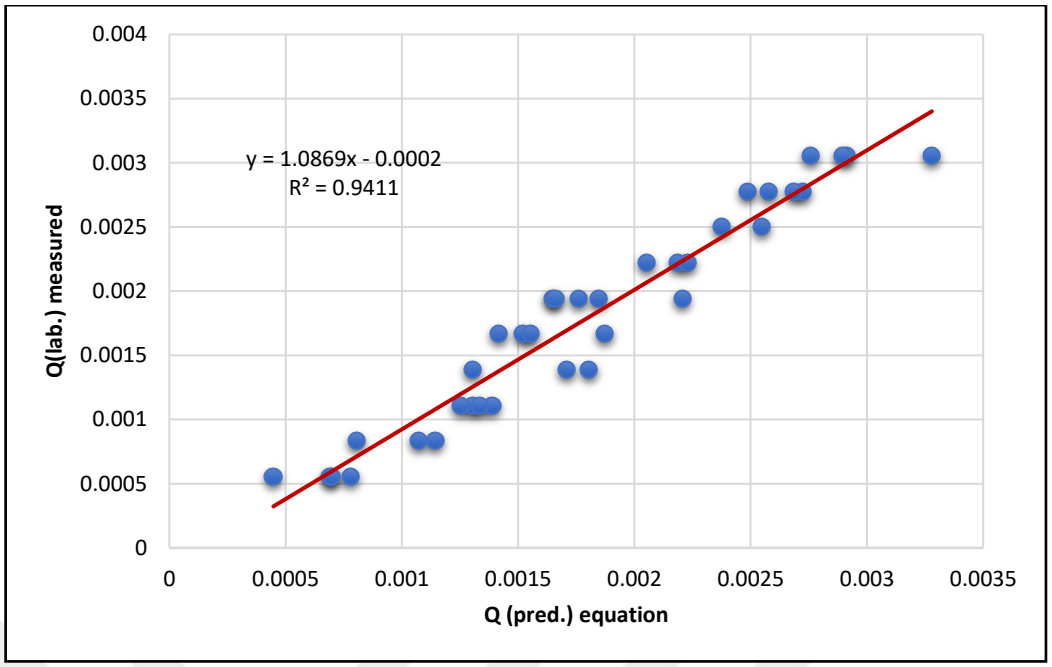

Figure 5.30 The Observed discharge with The Predicted Discharge for smooth and rough bed channels (S and n=0)

5.1.6 Comparison of This Study Results with Previous Studies

In the current study three equations for flow prediction was found with very high correlation coefficients. In order to compare the results obtained from the present study with the results of previous studies to clarify the compatibility of the extracted relationship between the depth of the edge and the discharge scientifically and since most of the previous studies dealt with the hydraulic characteristics of flow over free overfall of rectangular, triangular and trapezoidal channels but we could not perform the comparison because the section used in this study has not been conducted laboratory tests and scientific studies on it and this study is the first in this area with regard to semicircular channels.

The results of the current study were compared with previous studies made by researchers and scientists on different channels cross sections such as researchers (Subhasish Dey, D. Nagesh Kumar and D. Ram Singh,2002), (Subhasish Dey,2003), (R.V. Raikar, D. Nagesh Kumar, Subhasish Dey,2004) and (Z. Ahmed,2004) as in table (5.4).

Table 5.4 The Flow Equations Comparison of Different Channels Cross Sections

No.	Cross Section	Researcher	EDR	Discharge Equation	Status
1	Rectangular	Rouse	0.715	$1.654\ g^{0.5}\ b\ y_b^{1.5}$	C
		Rajaratnam & Muralidhar	0.715	$1.654\ g^{0.5}\ b\ y_b^{1.5}$	C
			0.705	$1.6893\ g^{0.5}\ b\ y_b^{1.5}$	U
		Hager	0.696	$1.7222\ g^{0.5}\ b\ y_b^{1.5}$	U
		Murty	0.705	$1.6893\ g^{0.5}\ b\ y_b^{1.5}$	U
		Anderson	0.694	$1.7297\ g^{0.5}\ b\ y_b^{1.5}$	U
2	Triangular	Rajaratnam & Muralidhar	0.795	$1.2548\ g^{0.5}\ m\ y_b^{2.5}$	U
		Ali & Sykes	0.798	$1.243\ g^{0.5}\ b\ y_b^{2.5}$	U
		Murty	0.795	$1.2548\ g^{0.5}\ b\ y_b^{2.5}$	U
		Ahmed	0.802	$1.2276\ g^{0.5}\ b\ y_b^{2.5}$	U
		Anderson	0.762	$1.395\ g^{0.5}\ b\ y_b^{2.5}$	U
3	Exponential	Rajaratnam & Muralidhar	0.772	$\frac{1.6779\ g^{0.5}\ c_1\ y_b^{1.5+c_2}}{(1+c_2)^{1.5}}$	U
		Ali & Sykes	0.747	$\frac{1.7921\ g^{0.5}\ c_1\ y_b^{1.5+c_2}}{(1+c_2)^{1.5}}$	U
		Murty	0.758	$\frac{1.7405\ g^{0.5}\ c_1\ y_b^{1.5+c_2}}{(1+c_2)^{1.5}}$	U
		Anderson	0.735	$\frac{1.8511\ g^{0.5}\ c_1\ y_b^{1.5+c_2}}{(1+c_2)^{1.5}}$	U

Table 5.4.1 The Flow Equations Comparison of Different Channels Cross Sections

No.	Cross Section	Researcher	EDR	Discharge Equation	Status
4	Inverted Semicircular	Subhasish Dey, D. Nagesh Kumar and D. Ram Singh,2002	0.695	$\frac{Q}{\sqrt{gD^5}} = \frac{1}{8}\frac{(\arcsin\left(2\frac{h_c}{D}\right) + 2(\frac{h_c}{D})\sqrt{1-4(\frac{h_c}{D})^2})^{1.5}}{(1-4(\frac{h_c}{D})^2)^{0.25}}$	
		Subhasish Dey,2003	0.705	$\frac{Q}{\sqrt{gD^5}} = 0.125\frac{\psi^{1.5}(\eta_c)}{(1-4\eta_c^2)^{0.25}}$	
		R.V. Raikar, D. Nagesh Kumar and Subhasish Dey,2004	0.705	Subcritical flow Supercritical flow: $\frac{h_e}{h_c} = 0.589\,(\frac{h_c}{D})^{0.0714}\,S^{-0.217}$ $\hat{Q} = 0.772(\frac{h_e}{D})^{0.874}\,S^{0.303}$	
		Z. Ahmed,2004	0.713	$\frac{Q}{\sqrt{gD^5}} = \frac{(Sin^{-1}\left(2.8\frac{y_e}{D}\right) + 2.8\frac{y_e}{D}\sqrt{1-8(\frac{y_e}{D})})^{3/2}}{8(1-8\,(\frac{y_e}{D})^2)^{1/4}}$	
		M.K. Beirami, S.V. Nabavi and M.R. Chamani,2006	0.70	Establishing a figure to estimate the discharge according to $(\frac{y_b}{D})$	
		Mahesh Pal, Arun Goel,2005	0.704		

Table 5.4.2 The Flow Equations Comparison of Different Channels Cross Sections

No.	Cross Section	Researcher	EDR	Discharge Equation	Status
5	Semi Circular	Present Study	0.881 0.574	Semicircular channels with subcritical flow Semicircular channels with subcritical flow and smooth bed $\left(\frac{Q}{\sqrt{g\ D^5}}\right) = 1.497\ (\frac{y_b}{D})^{1.798}$ $\left(\frac{Q}{\sqrt{g\ D^5}}\right) = 8.660\ (\frac{y_b}{D})^{3.101}$ $\left(\frac{Q}{\sqrt{g\ D^5}}\right) = 0.426\ (\frac{y_b}{D})^{1.723}\ (S)^{0.404}\ (n)^{-0.678}$	C

Where: U: Unconfined, and C: Confined

Through this study it is possible to estimate the discharge of the semicircular channels by knowing the water depth at the edge of the free overfall (y_b) and the longitudinal channel slope (S) and channel diameter (D)

CHAPTER 6

CONCLUSIONS AND RECOMMENDATIONS

6.1 CONCLUSIONS

After the experiments were completed in the laboratory and the values of the main variables were stabilized. The variables affecting the flow were studied through the analytical relations using the statistical analysis program SPSS and the graphs according to their equations were drawn. The conclusions from the present study can be summarized as follows:

1. Manning Coefficient was calculated for each experiment and the results represented in figure (5.1). The highest value of Manning coefficient was found in the size model (6.33) mm and it is equal to (0.045866), which is the maximum size used for roughness. This gives us a greater understanding of the importance of the size of the granules in the water stream. The larger the grain, the greater the roughness of the bottom and thus increase friction with the bottom of the water stream, which reduces the flow speed.

2. The relationship between the flow Froude number in term of final depth (F_{rb}) which represented in the non-dimensional factor ($\frac{Q}{\sqrt{g\ D^5}}$) and the final depth ratio (y_b/D) were studied for smooth and rough bed and for different bed slopes (0, 0.005, 0.01 and 0.015) and different roughness models. The data for both variables were represented in statistical figures for each individual experiment with specific slope and specific roughness. The relationship between the two variables was a simple power equation with a high correlation coefficient. The value of Froude number (Fr_b) increased with the increase in (y_b/D) values for different slopes and roughness. The bed slope and roughness had no effect on the relationship between the two variables in subcritical flow state as in table (5.2) and figures (5.2 to 5.21) where it still power equation.

3. The relationship of the brink depth ratio (y_b/D) with the critical depth ratio (y_c/D) was studied for each experiment according to the roughness and slope of each model, Data were represented in statistical figures and the relationship between the two variables was determined. The result was that both variables were associated with a simple linear relationship and with high correlation coefficient. As in table (5.3) and figures (5.22 to 5.25). the values of (y_b) increased with increasing the (y_c) values.

4. The end depth ratio (EDR) relationship with slope change were studied for different roughness. The results showed that the (y_b/y_c) ratio increased with slope increasing for different slopes and constant roughness channels as in figure (5.26) and the relationship is represented by simple linear equation. Whereas this ratio reduces with the slope increasing for constant slope and different roughness channels as in figure (5.27) and the relationship was represented by simple linear equation.

5. The (EDR) value for semicircular channels with free overfall was equal to (0.881) for subcritical flow state. The (EDR) value for semicircular channels with smooth bed was (0.574) with correlation coefficient equal to (R^2 = 0.9054).

6. The combined effect of ($Q/\sqrt{g\ D^5}$) with ($\frac{y_b}{D}$) and (S) and (n) were studied for smooth and rough beds with different bed slopes. Three equations for flow in semicircular channels were concluded for subcritical flow state, the first one for horizontal and smooth bed semicircular channels, The second one for horizontal and rough bed semicircular channels, The third one for smooth and rough bed and different slope semicircular channels.

6.2 RECOMMENDATIONS

Based on previous studies of different sections and through the experience gained from this study, future studies require the following improvements:

1. In this study, the channels with the semicircular cross-section were studied. It is recommended to study different types of sections such as (rectangle, trapezoidal, triangular, elliptical, and exponential) and by using the same factors of slope, roughness and discharge.
2. In this study, sand granules were used as roughness elements, it is recommended to use more gradients and compare their effect relative to the studied gradients.
3. The interest of using semicircular channels of different sizes, larger and smaller using the same gradients and slopes and comparing the results obtained with the results to be obtained in addition to studying the effect of size on the final results.
4. Study the effect of roughness distribution on the flow equation.
5. The interest of examining the channels with steep slopes, which produces high values for the Froude number, and indicate the effect of high values of this variable on the expressions obtained.

REFERENCES

[1] A. Osman. (2006). Open Channel Hydraulics, First Edition,Canada.

[2] Ti, Ş, C Ersen Firat, and A Metin Ger. (2008). Use of Brink Depth in Discharge Measurement, *Journal of Irrigation and Drainage Engineering*, **134**(1).

[3] Chamani, M R, and M K Beirami.(2002). Flow Characteristics at Drops, *Journal of Hydraulic Engineering,* **128**(8).

[4] Dey, Subhasish, B. Ravi Kumar. (2002). Hydraulics of Free Overdall in Triangular Shaped Channels, **27**(3):353–363.India.

[5] Dey, Subhasish. (2003). Free Overfall in Inverted Semicircular Channels, *Journal of Hydraulic Engineering*, **129**(6).

[6] Nabavi, Seyed Vahid. (2015). Flow Measurement in Rectangular Channels, *Bulletin of Environment, Pharmacology and Life Sciences Bull. Env.Pharmacol. Life Sci*., **4**(1) : 457-467.

[7] Pal, Mahesh, and Arun Goel. (2005). Prediction of the End-Depth Ratio and Discharge in Semi-Circular and Circular Shaped Channels Using Support Vector Machines, **17**.

[8] Ferro1, Vito. (1999). Theoretical End-Depth-Discharge Relationship for Free Overfall, *Journal of Irrigation and Drainage Engineering*, **125**(1) : 40–44.

[9] Hatzigiannakis, Evangelos. (1995). General End-Depth-Discharge Relationship at Free Overfall in Trapezoidal Channel, *Journal of Irrigation and Drainage Engineering*, **121**(2).

[10] Keller, By Robert J, and Soon S Fong. (1989). Flow Measurement with Trapezoidal Free Overfall, *Journal of Irrigation and Drainage Engineering*, **115**(1).

[11] Beirami, M K, S V Nabavi, and M R Chamani. (2006). Free Overfall in Channels with Different Cross Sections and sub-critical Flow, *Iranian Journal of Science & Technology*, Transaction B, Engineering, **30**(B1).

[12] Alastair C. Davis, l Brian G. S. Ellett, 2 and Richard P. Jacob3. (1998). Flow Measurement in Sloping Channels with Rectangular free overfall, *Journal of Hydraulic Engineering*, **124**(7).

[13] Ramamurthy, A S, Junying Qu, and Diep Vo.(2006). VOF Model for Simulation of a Free Overfall in Trapezoidal Channels, *Journal of Irrigation and Drainage Engineering*, **132**(4).

[14] George Terzidis3 and Litsa Anastasiadou-Partheniou4. (1989). Flow Measurements with Trapezoidal Free Overfall, *Soil Sci. and Agric. Engrg. Aristotle Univ. of Thessaloniki*, Greece (1) : 860–62.

[15] Vito Ferro1. (1992). Flow Measurement with Rectangular Free Overfall, *Journal of Irrigation and Drainage Engineering*, **118**(6).

[16] R. D. Gupta, M. Jamil and M. Mohsin. (1993). Discharge Prediction in Smooth Trapezoidal Free Overfall (Positive, Zero and Negative Slopes), *Journal of Irrigation and Drainage Engineering*, **119**(2).

[17] Nabavi, Seyed Vahid. (2008). End Depth as Measuring Device in Inverted Semicircular Channels, *3rd IASME / WSEAS Int. Conf. on Water Resources*, Hydraulics & Hydrology (WHH '08), University of Cambridge, UK.

[18] Ahmad, Z. (2003). Quasi-Theoretical End-Depth-Discharge Relationship for Rectangular Channels, *Journal of Irrigation and Drainage Engineering*, **129**(2): 138–41.

[19] Rashwan, I. M. H., and M. I. Idress. (2012). Brink as a Device for Measurement Discharge for Partially Filled Circular Channel, *Ain Shams Engineering Journal*, **4**(2):133-141, Egypt.

[20] Ahmad, Z. (2005). Flow Measurement Using Free Overfall in Inverted Semi-Circular Channel, **16** : 21–26.India.

[21] Dey, Subhasish. (2005). End Depth in U-Shaped Channels: A Simplified Approach, *Journal of Hydraulic Engineering***, 131**(6).

[22] Deyl, By Subhasish. (1998). End Depth in Circular Channels, *Journal of Hydraulic Engineering***, 124**(8).

[23] Dey1, Subhasish. (2001). EDR in Circular Channels, *Journal of Irrigation and Drainage Engineering*, **127**(2): 110–12.

[24] Guo, Yakun, Lixiang Zhang, Yongming Shen, and Jisheng Zhang. 2008. Modeling Study of Free Overfall in a Rectangular Channel with Strip Roughness, *Journal of Hydraulic Engineering*, **134**(5).

[25] Swetapadma, Sonali, Prof. S. K. Mittal, and Prof. M. K. Choudhary. (2014). Brink Depth at Free Overfall – A Review, *International Journal of Engineering Research***, 3**: 594-601.

[26] Noori, Bahzad M A, and Safa S Ibrahim. (2016). Effect of Bed and Side Slopes on Flow Measurements in Trapezoidal Free Overfall Channels, *Arab J Sci Eng.*, **41**: 4187– 4194.

[27] Vatankhah, Ali R. (2012). Direct Solution for Discharge in Generalized Trapezoidal Free Overfall, Flow Measurement and Instrumentation, **29**.

[28] Raikar, R V, D Nagesh Kumar, and Subhasish Dey.(2004). End Depth Computation in Inverted Semicircular Channels Using ANNs, **15**.

[29] Chow, Ven Te.(1959). Open Channel Hydraulics. *McGraw-Hill Book Company*, USA.

[30] Soediono, Budi.(1989). Dimensinal Analysis, *Journal of Chemical Information and Modeling*, **53**(1).

[31] Yoon, Hyunse. (2014). Dimensional Analysis.Assistant Research Scientist IIHR-Hydroscience & Engineering,

[32] Office, Corporate, and Road No., Unit & Dimension, (1), IPIA, Kota (Raj.).

[33] Henry L. Langhaar, John Wiley & Sons. (2007). A Transalation of Dimensional Analysis and Theory of Models, *INC Book by Jalal Haj Abed*.

[34] Mason, Robert D., and William G: Marchal' Douglas A. (1999). Statistical Techniques in Business and Economics, *The Irwin/McGraw-Hill Series Operations and Decision Sciences*, international edition: 791, USA.

[35] Montgomery, Dc. (2009). Introduction to Statistical Quality Control, *John Wiley & Sons Inc*, 6th Edition:754, USA.

[36] H. Schlichting. (1937). Experimental Investigation of the Problem Surface Roughness, *National Advisory Committee for Aeronautics*, **VII**(1), Washington.

[37] P. I. Gordienko. (2010). The Influence Of Channel Roughness And Flow States On Hydraulic Resistances Of Turbulent Flow, *Journal of Hydraulic Research*,

5(4): 249-261.

[38] Dey, Subhasish. (2000). End depth in steeply sloping rough rectangular channels, Sadhana, **25**(1): 1-10, India.

Appendix (A)

Derivations:

A.1 The Momentum Equation

Rate of momentum transfer = $\rho \int_A v^2 \, dA$ **(A.1)**

We often express the momentum transfer rate in terms of the average cross-sectional velocity (V), as:

Rate of momentum transfer = $\beta \rho V^2 A = \beta \rho Q V$ **(A.2)**

Where (β) momentum coefficient (or momentum correction coefficient) introduced to account for the non-uniform velocity distribution within the channel section. For regular channels (β) is often set equal to 1.0 for simplicity and because it varies from (1.01) to (1.12) in straight channels (Chow 1959).

The difference in pressure force is equal to the rate of change of the momentum between the end and the far upstream sections. Strictly, this simplification refers to the case of one-dimensional flow through a horizontal channel of negligible frictional resistance.

$$\boldsymbol{Q\rho(V_b - V_c) = F_c - F_b} \quad \textbf{(A.3)}$$

Where:

ρ: the mass density of fluid, Q = the mean discharge, V = the mean velocity, F = the pressure forces, b and c refer to the end place and critical section respectively.

Substituting ($F_c = \gamma(A\bar{y})_c$) and ($F_b = K\gamma(A\bar{y})_b$) by using ($V = {}^{Q}/_{A}$) and (γ = ρg) in equation (A.3) and re-arrange it we obtain:

$$Q\rho(V_b - V_c) = \gamma(A\bar{y})_c - K\gamma(A\bar{y})_b$$

$$Q\rho\left(\frac{Q}{A_b} - \frac{Q}{A_c}\right) = \gamma(A\bar{y})_c - K\gamma(A\bar{y})_b$$

$$\frac{\gamma Q^2}{g}\left(\frac{1}{A_b} - \frac{1}{A_c}\right) = \gamma(A\bar{y})_c - K\gamma(A\bar{y})_b$$

$$\frac{Q^2}{g}\left[\frac{1}{A_b}-\frac{1}{A_c}\right]=(A\bar{y})_c-K(A\bar{y})_b \quad \textbf{(A.4)}$$

Where:

K: the pressure coefficient, γ: the specific weight of fluid, A: the cross-sectional area of flow, ȳ: the depth from flow surface to the centroid of cross-sectional area.

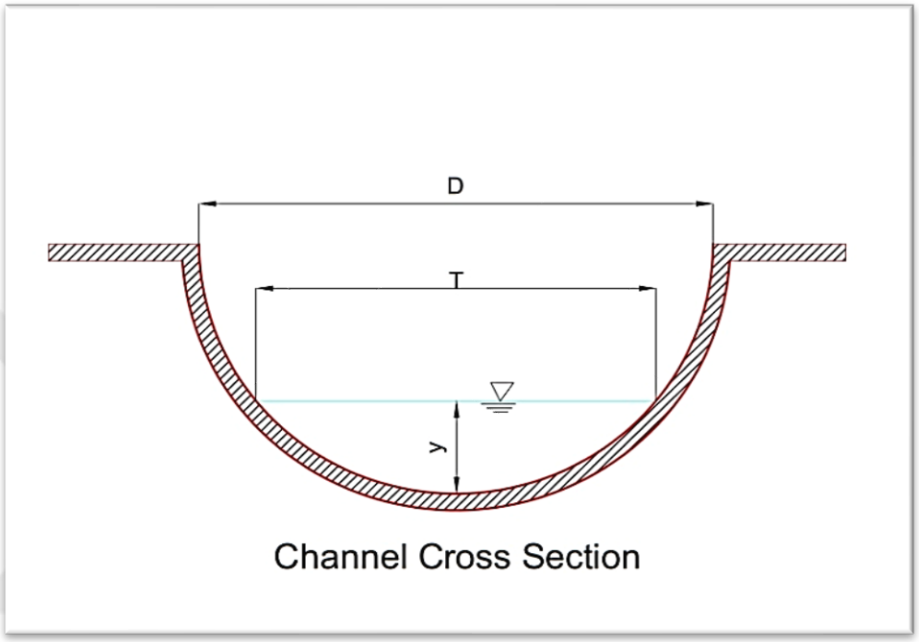

The relationship between discharge and critical depth can be written as:

$$\frac{Q^2}{g}=\frac{A_c^3}{T_c} \quad \textbf{(A.5)}$$

T_c: the top width of water, g: the gravity acceleration.

Substituting equation (A.5) in equation (A.4) and re-arrange it we conclude:

$$\frac{A_c^3}{T_c}\left[\frac{1}{A_b}-\frac{1}{A_c}\right]=(A\bar{y})_c-K(A\bar{y})_b$$

$$\frac{A_c}{T_c}\left[\frac{A_c^2}{A_b}-A_c\right]=(A\bar{y})_c-K(A\bar{y})_b$$

$$K=\frac{A_c}{A_b\bar{y_b}}*\left[\bar{y_c}-\frac{A_c}{T_c}\left[\frac{A_c}{A_b}-1\right]\right] \quad \textbf{(A.6)}$$

Where:

$$A_b = \pi r^2 \frac{2\Theta_b}{360} - [(X_b)(H_b)] \quad \text{and} \quad A_c = \pi r^2 \frac{2\Theta_c}{360} - [(X_c)(H_c)]$$

$$\bar{y} = \frac{4r}{3\pi} \quad \text{and} \quad T_c = 2X_c = 2r \sin\Theta_c$$

$$K = \frac{\pi r^2 \frac{2\Theta_c}{360} - [(X_c)(H_c)]}{\pi r^2 \frac{2\Theta_b}{360} - [(X_b)(H_b)]\, y_b^-} * \left[y_c^- - \frac{\pi r^2 \frac{2\Theta_c}{360} - [(X_c)(H_c)]}{2r \sin\Theta_c} \left[\frac{\pi r^2 \frac{2\Theta_c}{360} - [(X_c)(H_c)]}{\pi r^2 \frac{2\Theta_b}{360} - [(X_b)(H_b)]} - 1 \right] \right]$$

$$K = \frac{\pi r^2\, \Theta_c - 180\, X_c\ H_c}{[\pi r^2\, \Theta_b - 180\, X_b\ H_b]\, y_b^-} * \left[y_c^- - \frac{\pi r^2\, \Theta_c - 180\, X_c\ H_c}{180} * \frac{1}{2r \sin\Theta_c} \left[\frac{\pi r^2\, \Theta_c - 180\, X_c\ H_c}{\pi r^2\, \Theta_b - 180\, X_b\ H_b} - 1 \right] \right]$$

Let:

$$a_c = \pi r^2\, \Theta_c - 180\, X_c\ H_c$$

$$a_b = \pi r^2\, \Theta_b - 180\, X_b\ H_b \quad \text{Then:}$$

$$K = \frac{a_c}{a_b\, y_b^-} * \left[y_c^- - \left(\frac{a_c}{180} * \frac{1}{T_c} \right) * \left[\frac{a_c}{a_b} - 1 \right] \right] \qquad \textbf{(A.7)}$$

$$\boldsymbol{K = \frac{a_c\, y_c^-}{a_b\, y_b^-} - \left[\frac{a_c^2}{180(a_b y_b^-\, T_c)} * \left(\frac{a_c}{a_b} - 1 \right) \right]} \qquad \textbf{(A.8)}$$

Where:

$y_b^- = \frac{4y_b}{3\pi}$

$y_c^- = \frac{4y_c}{3\pi}$

$T_c = 2\ r\ Sin\ \Theta_c$

$$\Theta_c = \cos^{-1}\left(\frac{H_c}{r}\right) = \cos^{-1}\left(\frac{r - y_c}{r}\right) \quad \text{and} \quad \Theta_b = \cos^{-1}\left(\frac{H_b}{r}\right) = \cos^{-1}\left(\frac{r - y_b}{r}\right)$$

$$X_c = r \sin\Theta_c \qquad \text{and} \quad X_b = r \sin\Theta_b$$

A.2 The Critical Depth Equation

When the flow change from subcritical flow to supercritical flow it should pass through the critical state. The Froude number at this situation is equal to one, and the flow depth (y_n) is transform to be (y_c).so to calculate the channel critical depth we use the Froude number equation as:

$$\boldsymbol{F_r = V \Big/ \sqrt{g D_h}} \qquad \textbf{(A.9)}$$

Where:

V = Q/A

$D_h = A_w/T$, substituting the values of (V) and (D_h) in (F_r) no. equation and put F_r =1 we obtain:

$$1 = V \Big/ \sqrt{gD_h}$$

$$1 = \frac{\frac{Q}{A}}{\sqrt{g\frac{A_w}{T}}}$$

The values of the flow area (A_w) and the water top width (T) equal to:

A_w = area of sector – area of triangle

Where the area of sector is the shaded area in the figure below.

$$A_w = \pi r^2 \frac{2\Theta}{360} - \left[\frac{1}{2}(2X)(H)\right]$$

Cos Θ = H/r, we obtain, H = r Cos Θ

Sin Θ = x/r, we obtain, x = r Sin Θ

At critical state the flow depth will equal to the critical depth:

$y_n = y_c$

y_c = r – H, by substituting the value of (H) we obtain:

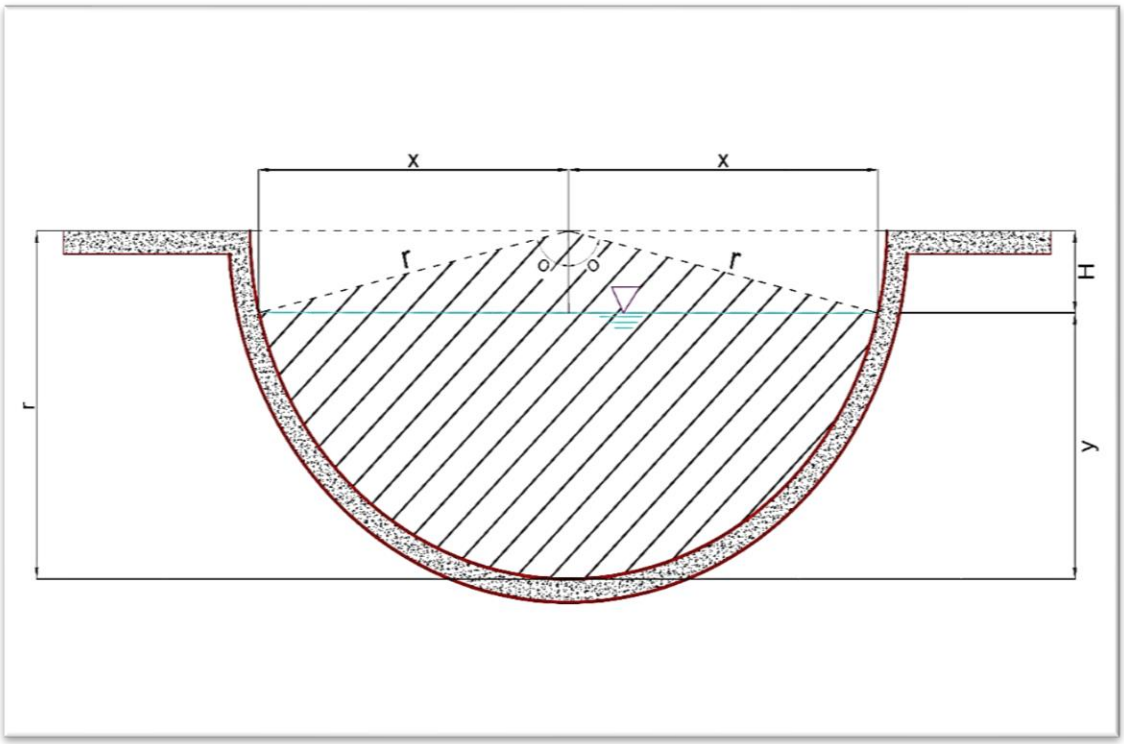

$$\mathbf{y_c = r\ (1- Cos\ \Theta)} \qquad \mathbf{(A.10)}$$

In order to calculate the critical depth, we need to find the angle (Θ) which give (F_r) no. equal to (1), so by substituting the values of (V), (D_h), (A_w) and (T) in terms of (Θ) we obtain:

$$A_w = \pi r^2 \frac{2\Theta}{360} - (r^2\ Sin\ \Theta\ Cos\ \Theta)$$

T = 2 r Sin Θ

$$1 = \frac{\frac{Q}{\pi r^2 \frac{2\Theta}{360} - (r^2\ Sin\ \Theta\ Cos\ \Theta)}}{\sqrt{9.81\left(\frac{\pi r^2 \frac{2\Theta}{360} - (r^2\ Sin\ \Theta\ Cos\ \Theta)}{2r\ Sin\ \Theta}\right)}}$$

$$\mathbf{1} = \frac{\frac{Q}{r^2\ (0.0174\ \Theta - Sin\ \Theta\ Cos\ \Theta)}}{\sqrt{4.905\left(\frac{r(0.0174\ \Theta - Sin\ \Theta\ Cos\ \Theta)}{Sin\ \Theta}\right)}} \qquad \mathbf{(A.11)}$$

By using trial and error, equation (A.11) give the value of (Θ) which corresponds the critical state and give the critical depth of water for each experiment.

Appendix (B)
The Laboratory Data for The Current Study

Table (B.1): Data recorded during laboratory work

No.	Roughness Hight(mm)	Channel Slope	Discharge (m^3/hr)	Normal Depth ($y_{n\ equ.}$) (mm)	Critical Depth (y_c) (mm)	Brink Depth ($y_{b\ equ.}$) (mm)
1	Smooth	0	2	19.41	17.60	10.22
2	Smooth	0	3	21.97	21.52	13.65
3	Smooth	0	4	23.88	24.83	16.01
4	Smooth	0	5	25.46	27.76	17.2
5	Smooth	0	6	28.69	30.43	19.27
6	Smooth	0	7	29.26	32.82	20.26
7	Smooth	0	8	31.83	35.13	21.76
8	Smooth	0	9	35.16	37.29	24.8
9	Smooth	0	10	37.1	39.26	26.09
10	Smooth	0	11	39.37	41.24	26.93
11	Smooth	1/200	2	16.5	17.60	9.15
12	Smooth	1/200	3	19.08	21.52	13.34
13	Smooth	1/200	4	21.43	24.83	14.59
14	Smooth	1/200	5	24.39	27.76	16.2
15	Smooth	1/200	6	26.94	30.43	17.47
16	Smooth	1/200	7	27.38	32.82	18.73
17	Smooth	1/200	8	29.3	35.13	21.11

No.	Roughness Hight(mm)	Channel Slope	Discharge (m^3/hr)	Normal Depth ($y_{n\ equ.}$) (mm)	Critical Depth (y_c) (mm)	Brink Depth ($y_{b\ equ.}$) (mm)
18	Smooth	1/200	9	33.36	37.29	23.3
19	Smooth	1/200	10	34.87	39.26	25.46
20	Smooth	1/200	11	36.5	41.24	26.02
21	Smooth	2/200	2	12.66	17.60	7.42
22	Smooth	2/200	3	14.71	21.52	11.45
23	Smooth	2/200	4	17.59	24.83	12.91
24	Smooth	2/200	5	21.59	27.76	14.73
25	Smooth	2/200	6	23	30.43	16.09
26	Smooth	2/200	7	25.3	32.82	17.72
27	Smooth	2/200	8	26.64	35.13	19.34
28	Smooth	2/200	9	31.53	37.29	22.6
29	Smooth	2/200	10	32.88	39.26	23.96
30	Smooth	2/200	11	34.82	41.24	25.21
31	Smooth	3/200	2	12.37	17.60	7.08
32	Smooth	3/200	3	14.25	21.52	11.31
33	Smooth	3/200	4	16.64	24.83	13
34	Smooth	3/200	5	19.84	27.76	13.79
35	Smooth	3/200	6	22.22	30.43	16.06
36	Smooth	3/200	7	23.81	32.82	17.04
37	Smooth	3/200	8	24.82	35.13	17.96
38	Smooth	3/200	9	29.09	37.29	21.43
39	Smooth	3/200	10	29.93	39.26	22.5
40	Smooth	3/200	11	32.84	41.24	23.62

No.	Roughness Hight(mm)	Channel Slope	Discharge (m^3/hr)	Normal Depth (yn equ.) (mm)	Critical Depth (yc) (mm)	Brink Depth (yb equ.) (mm)
41	2	0	2	36.77	17.60	24.76
42	2	0	3	39.89	21.52	28.89
43	2	0	4	41.09	24.83	29.40
44	2	0	5	46.22	27.76	35.18
45	2	0	6	48.93	30.43	36.84
46	2	0	7	44.36	32.82	33.01
47	2	0	8	44.02	35.13	32.85
48	2	0	9	49.24	37.29	35.89
49	2	0	10	50.87	39.26	38.23
50	2	0	11	50.34	41.24	38.19
51	2	1/200	2	30.85	17.60	19.85
52	2	1/200	3	32.63	21.52	23.04
53	2	1/200	4	39.15	24.83	28.31
54	2	1/200	5	40.70	27.76	29.36
55	2	1/200	6	40.07	30.43	29.23
56	2	1/200	7	40.92	32.82	29.08
57	2	1/200	8	41.38	35.13	29.20
58	2	1/200	9	44.57	37.29	31.66
59	2	1/200	10	42.37	39.26	30.29
60	2	1/200	11	50.57	41.24	38.13
61	2	2/200	2	28.01	17.60	16.53
62	2	2/200	3	32.35	21.52	22.95
63	2	2/200	4	34.94	24.83	25.32

No.	Roughness Hight(mm)	Channel Slope	Discharge (m^3/hr)	Normal Depth ($y_{n\ equ.}$) (mm)	Critical Depth (y_c) (mm)	Brink Depth ($y_{b\ equ.}$) (mm)
64	2	2/200	5	35.91	27.76	26.67
65	2	2/200	6	34.73	30.43	25.87
66	2	2/200	7	37.43	32.82	27.15
67	2	2/200	8	40.20	35.13	29.44
68	2	2/200	9	41.53	37.29	29.03
69	2	2/200	10	41.00	39.26	29.58
70	2	2/200	11	48.44	41.24	36.20
71	2	3/200	2	22.91	17.60	12.00
72	2	3/200	3	27.22	21.52	17.77
73	2	3/200	4	29.81	24.83	20.38
74	2	3/200	5	32.44	27.76	22.42
75	2	3/200	6	32.15	30.43	22.80
76	2	3/200	7	32.91	32.82	22.75
77	2	3/200	8	34.64	35.13	23.94
78	2	3/200	9	36.65	37.29	25.17
79	2	3/200	10	39.09	39.26	26.38
80	2	3/200	11	44.09	41.24	31.82
81	4.75	0	2	40.56	17.60	26.12
82	4.75	0	3	42.68	21.52	26.64
83	4.75	0	4	47.12	24.83	31.81
84	4.75	0	5	47.45	27.76	31.40
85	4.75	0	6	51.34	30.43	34.26
86	4.75	0	7	51.68	32.82	32.97
87	4.75	0	8	54.64	35.13	35.48

No.	Roughness Hight(mm)	Channel Slope	Discharge (m^3/hr)	Normal Depth ($y_{n\ equ.}$) (mm)	Critical Depth (y_c) (mm)	Brink Depth ($y_{b\ equ.}$) (mm)
88	4.75	0	9	55.05	37.29	35.96
89	4.75	0	10	57.54	39.26	37.89
90	4.75	0	11	59.34	41.24	40.99
91	4.75	1/200	2	34.31	17.60	23.24
92	4.75	1/200	3	38.13	21.52	24.34
93	4.75	1/200	4	40.63	24.83	26.35
94	4.75	1/200	5	42.99	27.76	28.15
95	4.75	1/200	6	45.66	30.43	28.42
96	4.75	1/200	7	47.29	32.82	28.47
97	4.75	1/200	8	49.04	35.13	30.19
98	4.75	1/200	9	52.25	37.29	33.33
99	4.75	1/200	10	54.77	39.26	35.38
100	4.75	1/200	11	56.20	41.24	37.73
101	4.75	2/200	2	28.58	17.60	18.32
102	4.75	2/200	3	34.11	21.52	21.28
103	4.75	2/200	4	35.97	24.83	22.12
104	4.75	2/200	5	38.20	27.76	23.25
105	4.75	2/200	6	41.41	30.43	25.24
106	4.75	2/200	7	43.20	32.82	24.87
107	4.75	2/200	8	47.03	35.13	28.67
108	4.75	2/200	9	50.15	37.29	31.84
109	4.75	2/200	10	51.66	39.26	32.69
110	4.75	2/200	11	52.16	41.24	34.86
111	4.75	3/200	2	25.67	17.60	15.62

No.	Roughness Hight(mm)	Channel Slope	Discharge (m^3/hr)	Normal Depth ($y_{n\ equ.}$) (mm)	Critical Depth (y_c) (mm)	Brink Depth ($y_{b\ equ.}$) (mm)
112	4.75	3/200	3	31.34	21.52	18.00
113	4.75	3/200	4	33.92	24.83	20.48
114	4.75	3/200	5	38.40	27.76	24.39
115	4.75	3/200	6	38.62	30.43	23.08
116	4.75	3/200	7	40.64	32.82	24.24
117	4.75	3/200	8	42.59	35.13	25.60
118	4.75	3/200	9	49.51	37.29	31.74
119	4.75	3/200	10	49.90	39.26	32.32
120	4.75	3/200	11	54.28	41.24	37.75
121	6.33	0	2	48.61	17.60	28.77
122	6.33	0	3	51.03	21.52	29.86
123	6.33	0	4	53.39	24.83	33.12
124	6.33	0	5	54.33	27.76	35.46
125	6.33	0	6	53.09	30.43	34.11
126	6.33	0	7	57.10	32.82	37.71
127	6.33	0	8	60.38	35.13	41.45
128	6.33	0	9	63.12	37.29	41.68
129	6.33	0	10	64.65	39.26	42.76
130	6.33	0	11	67.83	41.24	47.42
131	6.33	1/200	2	37.35	17.60	24.68
132	6.33	1/200	3	42.56	21.52	26.81
133	6.33	1/200	4	43.67	24.83	28.37
134	6.33	1/200	5	48.95	27.76	29.70
135	6.33	1/200	6	52.80	30.43	32.59

No.	Roughness Hight(mm)	Channel Slope	Discharge (m^3/hr)	Normal Depth ($y_{n\ equ.}$) (mm)	Critical Depth (y_c) (mm)	Brink Depth ($y_{b\ equ.}$) (mm)
136	6.33	1/200	7	53.86	32.82	32.36
137	6.33	1/200	8	55.36	35.13	34.83
138	6.33	1/200	9	61.64	37.29	39.61
139	6.33	1/200	10	64.05	39.26	40.93
140	6.33	1/200	11	66.66	41.24	46.08
141	6.33	2/200	2	30.77	17.60	19.38
142	6.33	2/200	3	38.76	21.52	24.89
143	6.33	2/200	4	38.09	24.83	25.28
144	6.33	2/200	5	44.64	27.76	28.09
145	6.33	2/200	6	48.58	30.43	29.09
146	6.33	2/200	7	49.92	32.82	30.29
147	6.33	2/200	8	51.82	35.13	32.59
148	6.33	2/200	9	58.36	37.29	37.46
149	6.33	2/200	10	58.68	39.26	37.32
150	6.33	2/200	11	62.44	41.24	43.27
151	6.33	3/200	2	28.20	17.60	17.52
152	6.33	3/200	3	34.92	21.52	20.45
153	6.33	3/200	4	37.42	24.83	24.91
154	6.33	3/200	5	40.36	27.76	23.88
155	6.33	3/200	6	45.45	30.43	26.11
156	6.33	3/200	7	47.60	32.82	28.53
157	6.33	3/200	8	49.38	35.13	30.35
158	6.33	3/200	9	55.36	37.29	34.79

No.	Roughness Hight(mm)	Channel Slope	Discharge (m^3/hr)	Normal Depth ($y_{n\ equ.}$) (mm)	Critical Depth (y_c) (mm)	Brink Depth ($y_{b\ equ.}$) (mm)
159	6.33	3/200	10	58.13	39.26	37.20
160	6.33	3/200	11	60.44	41.24	40.02